

ORNL/TM-10233

3 4456 0382548 5

**OAK RIDGE  
NATIONAL  
LABORATORY**

**MARTIN MARIETTA**

**Calculation of the Inventory and  
Near-Field Release Rates of Radioactivity  
from Neutron-Activated Metal Parts  
Discharged from the High Flux Isotope  
Reactor and Emplaced in Solid Waste  
Storage Area 6 at Oak Ridge National  
Laboratory**

A. D. Kelmers  
J. R. Hightower

OAK RIDGE NATIONAL LABORATORY  
CENTRAL RESEARCH LIBRARY  
CIRCULATION SECTION  
4500H ROOM 175  
**LIBRARY LOAN COPY**  
DO NOT TRANSFER TO ANOTHER PERSON  
If you wish someone else to see this  
report, send in name with report and  
the library will arrange a loan.  
ORNL/TM-10233

OPERATED BY  
MARTIN MARIETTA ENERGY SYSTEMS, INC.  
FOR THE UNITED STATES  
DEPARTMENT OF ENERGY

Printed in the United States of America. Available from  
National Technical Information Service  
U.S. Department of Commerce  
5285 Port Royal Road, Springfield, Virginia 22161  
NTIS price codes—Printed Copy: A07 Microfiche A01

This report was prepared as an account of work sponsored by an agency of the United States Government. Neither the United States Government nor any agency thereof, nor any of their employees, makes any warranty, express or implied, or assumes any legal liability or responsibility for the accuracy, completeness, or usefulness of any information, apparatus, product, or process disclosed, or represents that its use would not infringe privately owned rights. Reference herein to any specific commercial product, process, or service by trade name, trademark, manufacturer, or otherwise, does not necessarily constitute or imply its endorsement, recommendation, or favoring by the United States Government or any agency thereof. The views and opinions of authors expressed herein do not necessarily state or reflect those of the United States Government or any agency thereof.

Chemical Technology Division

CALCULATION OF THE INVENTORY AND NEAR-FIELD RELEASE RATES  
OF RADIOACTIVITY FROM NEUTRON-ACTIVATED METAL PARTS  
DISCHARGED FROM THE HIGH FLUX ISOTOPE REACTOR AND  
EMPLACED IN SOLID WASTE STORAGE AREA 6 AT  
OAK RIDGE NATIONAL LABORATORY

A. D. Kelmers  
J. R. Hightower

**NOTICE** This document contains information of a preliminary nature.  
It is subject to revision or correction and therefore does not represent a  
final report.

Manuscript Completed: November 1986  
Date of Issue: May 1987

Prepared by the  
OAK RIDGE NATIONAL LABORATORY  
Oak Ridge, Tennessee 37831  
operated by  
MARTIN MARIETTA ENERGY SYSTEMS, INC.  
for the  
U.S. DEPARTMENT OF ENERGY  
under contract DE-AC05-84OR21400





CONTENTS

	<u>Page</u>
ABSTRACT . . . . .	1
1. EXECUTIVE SUMMARY. . . . .	2
1.1 REPORT PURPOSE AND SCOPE. . . . .	2
1.2 DESCRIPTION OF HFIR PARTS EMPLACED IN SWSA-6. . . . .	2
1.3 CALCULATED RADIONUCLIDE INVENTORY AS OF JUNE 1, 1986. . . . .	3
1.4 RELEASE RATES OF EUROPIUM RADIONUCLIDES FROM CONTROL PLATES AND CYLINDERS. . . . .	5
1.5 RELEASE RATES OF IRON, COBALT, AND NICKEL RADIONUCLIDES FROM STAINLESS STEEL AND COBALT ALLOY WASTES. . . . .	7
1.6 RELEASE RATES OF BERYLLIUM, CALCIUM, AND IRON FROM REFLECTORS. . . . .	8
1.7 SUGGESTED RESEARCH/DEVELOPMENT NEEDS TO IMPROVE CALCULATED RELEASE RATES OF EUROPIUM RADIONUCLIDES. . . . .	8
1.7.1 Currently Emplaced Wastes. . . . .	9
1.7.2 Future Waste Disposal or Storage Options . . . . .	11
2. INTRODUCTION	
2.1 APPROACH TO MODELING RADIOACTIVITY RELEASE RATES. . . . .	13
2.1.1 General Description. . . . .	13
2.1.2 Stainless Steel and Cobalt Alloy Parts . . . . .	17
2.1.3 Control Cylinder and Plates. . . . .	18
2.1.4 Reflectors . . . . .	19
2.2 CONTRIBUTION OF HFIR WASTES TO THE RADIOACTIVITY INVENTORY AT SWSA-6 . . . . .	19
2.3 DESCRIPTION OF HFIR WASTES AND EMPLACEMENT TECHNIQUE AT SWSA-6. . . . .	20
2.4 NEAR-FIELD GEOCHEMICAL CONDITIONS AT SWSA-6 . . . . .	22
2.4.1 Soil/Groundwater System Acidity. . . . .	23
2.4.2 Redox Condition. . . . .	24
2.4.3 Groundwater Chemistry. . . . .	24
2.4.4 Soil Mineralogy. . . . .	25
2.4.5 Groundwater Flux . . . . .	25
2.5 RADIOLYSIS. . . . .	26

## CONTENTS (continued)

	<u>Page</u>
3. STAINLESS STEEL AND COBALT ALLOY PARTS . . . . .	27
3.1 DESCRIPTION OF PARTS EMPLACED IN SWSA-6 . . . . .	27
3.2 CALCULATION OF RADIOACTIVITY RELEASE RATES. . . . .	30
3.2.1 Waste Leachate Chemistry . . . . .	30
3.2.2 Time of Radioactivity Release. . . . .	32
3.2.3 Corrosion of Metal Parts . . . . .	32
3.2.3.1 Stainless Steel . . . . .	32
3.2.3.2 Cobalt Alloy. . . . .	34
3.2.4 Radionuclide Solubility. . . . .	34
3.2.5 Geometry/Surface Area of Parts . . . . .	38
3.2.6 Radionuclide Release Rates . . . . .	39
3.3 CONCLUSIONS AND RECOMMENDATIONS . . . . .	42
3.3.1 Predicted Performance of Emplaced Parts. . . . .	42
3.3.2 Additional Research/Development Needs. . . . .	43
4. CONTROL CYLINDERS AND PLATES . . . . .	44
4.1 CONTROL CYLINDER AND PLATES EMPLACED IN SWSA-6. . . . .	44
4.1.1 Description of Control Cylinders and Radionuclides Formed . . . . .	44
4.1.2 Emplacement in SWSA-6. . . . .	45
4.2 CALCULATION OF THE RADIONUCLIDE INVENTORY . . . . .	46
4.3 WASTE LEACHATE CHEMISTRY AND PARAMETERS USED IN CALCULATIONS. . . . .	52
4.3.1 Auger-Hole Liner Corrosion . . . . .	52
4.3.2 Aluminum Cladding Corrosion. . . . .	52
4.3.3 Rate of Reaction of Cermet with Groundwater. . . . .	55
4.3.4 Time of Initial Radioactivity Release. . . . .	56
4.3.5 Radionuclide Solubility. . . . .	57
4.3.6 Radionuclide Diffusivity . . . . .	63
4.4 MODELS FOR ESTIMATING RELEASE OF EUROPIUM RADIONUCLIDES . .	63
4.4.1 Diffusion-Limited Release Model. . . . .	64
4.4.2 Saturation-Limited Release Model . . . . .	67
4.5 RELEASE RATES OF EUROPIUM RADIONUCLIDES . . . . .	67
4.5.1 Mixed Release Rate-Limiting Modes. . . . .	67
4.5.2 Single Release Rate-Limiting Mode. . . . .	68

## CONTENTS (continued)

	<u>Page</u>
4.6 CONCLUSIONS AND RECOMMENDATIONS . . . . .	72
4.6.1 Predicted Performance of Emplaced Cylinder and Plates . . . . .	72
4.6.2 Additional Research/Development Needed . . . . .	79
5. REFLECTORS . . . . .	80
5.1 DESCRIPTION OF REFLECTORS EMPLACED IN SWSA-6. . . . .	80
5.2 CALCULATION OF RADIOACTIVITY RELEASE RATES. . . . .	81
5.2.1 Inventory of Reflector Components in SWSA-6. . . . .	81
5.2.2 Waste Leachate Chemistry . . . . .	81
5.2.3 Time of Radioactivity Release. . . . .	83
5.2.4 Radionuclide Solubility. . . . .	83
5.2.5 Radionuclide Diffusivity . . . . .	87
5.2.6 Corrosion of Beryllium Metal . . . . .	88
5.2.7 Geometry/Surface Area of Emplaced Reflectors . . . . .	90
5.2.8 Radionuclide Release Rates . . . . .	90
5.3 CONCLUSIONS AND RECOMMENDATIONS . . . . .	93
5.3.1 Predicted Performance of Emplaced Reflectors . . . . .	93
5.3.2 Additional Research/Development Needed . . . . .	93
6. ACKNOWLEDGMENTS. . . . .	94
7. REFERENCES . . . . .	95
APPENDIX A. DESCRIPTION OF AUGER-HOLE CONSTRUCTION AND PAST HFIR WASTE EMPLACEMENT PRACTICE. . . . .	101
APPENDIX B. DERIVATION OF RELEASE RATE FROM LINED AUGER HOLES . . . . .	103
APPENDIX C. DERIVATION OF DIFFUSION RATES IN THE VICINITY OF BERYLLIUM REFLECTORS. . . . .	109

LIST OF FIGURES

	<u>Page</u>
Fig. 3.1. Release rate of cobalt, nickel, and iron radionuclides from HFIR stainless steel and cobalt alloy parts emplaced in SWSA-6	41
Fig. 4.1. Average europium isotope concentration in HFIR control plates as a function of irradiation	50
Fig. 4.2. The influence of pH on the activity of europium in solution (Fig. 14 of Serne and Rai 1976)	60
Fig. 4.3. Conceptual model for diffusion of europium from lined auger holes	66
Fig. 4.4. Mixed-mode release of europium isotopes for the parameters: Eu solubility of $10^{-6}$ mol/L; liner failure at 10 years; cladding failure at 2 years	69
Fig. 4.5. Mixed-mode release rates of europium isotopes for the parameters: Eu solubility of $10^{-4}$ mol/L; liner failure at 10 years; cladding failure at 2 years	70
Fig. 4.6. Mixed-mode release rates of europium isotopes for the parameters: Eu solubility of $10^{-6}$ mol/L; liner failure at 20 years; cladding failure at 4 years	71
Fig. 4.7. Single-mode release rates of europium isotopes for the parameters: Eu solubility of $10^{-6}$ mol/L; liner failure at 10 years; cladding failure at 2 years	73
Fig. 4.8. Single-mode release rates of europium isotopes for the parameters: Eu solubility of $10^{-4}$ mol/L; liner failure at 10 years; cladding failure at 2 years	74
Fig. 4.9. Single-mode release rates of europium isotopes for the parameters: Eu solubility of $10^{-6}$ mol/L; liner failure at 20 years; cladding failure at 4 years	75
Fig. 4.10. Bounding europium release rates: (a) lower bound - single-mode release model; liner fails after 20 years; cladding 4 years; $\text{Eu}^{3+}$ solubility is $10^{-6}$ mol/L; (b) higher bound - mixed-mode release model; liner fails at 10 years; cladding fails at 2 years; Eu solubility is $10^{-4}$ mol/L.	77
Fig. 5.1. Release rates of $^{41}\text{Ca}$ , $^{55}\text{Fe}$ , and $^{10}\text{Be}$ from reflectors at pH 4.4	92
Fig. C.1. Diffusion in the vicinity of beryllium reflector components	110

## LIST OF TABLES

	<u>Page</u>
Table 1.1. SWSA-6 radionuclide inventory of HFIR parts as of June 1, 1986	4
Table 2.1. Approach to modeling near-field radionuclide release rates for HFIR wastes in SWSA-6	14
Table 3.1. Cobalt, nickel, and iron contents of HFIR components	30
Table 3.2. Inventory of HFIR stainless steel and cobalt alloy components emplaced in SWSA-6, as of June 1, 1986	31
Table 4.1. Discharge of control cylinders from the HFIR and disposal in SWSA-6	47
Table 4.2. Calculated europium isotope inventory of control plates and cylinder in SWSA-6 as of June 1, 1986	51
Table 5.1. Discharge from HFIR and inventory of beryllium reflectors emplaced in SWSA-6	82
Table 5.2. Radionuclide release rates from beryllium reflectors as of June 1, 1986	91



CALCULATION OF THE INVENTORY AND NEAR-FIELD RELEASE RATES  
OF RADIOACTIVITY FROM NEUTRON-ACTIVATED METAL PARTS  
DISCHARGED FROM THE HIGH FLUX ISOTOPE REACTOR AND  
EMPLACED IN SOLID WASTE STORAGE AREA 6 AT  
OAK RIDGE NATIONAL LABORATORY

A. D. Kelmers  
J. R. Hightower

ABSTRACT

Reactor components are discharged from the High Flux Isotope Reactor and emplaced in Solid Waste Storage Area 6 at Oak Ridge National Laboratory. The components are radioactive due to neutron activation of various stable isotopes. Emplacement involves disposal in lined and unlined auger holes in soil above the water table. The radionuclide inventory, as of June 1, 1986, of disposed components was calculated. Information on the composition and weight of the components, as well as reasonable assumptions for the neutron flux during use, the time of neutron exposure, and radioactive decay after discharge, were employed in the inventory calculation. The near-field (in the immediate vicinity of the emplaced wastes) release rates of  $^{152}\text{Eu}$ ,  $^{154}\text{Eu}$ , and  $^{155}\text{Eu}$  from control plates and cylinders were calculated for 50 years after emplacement. The release rates of the europium isotopes were uncertain because of the lack of information for a number of the calculational parameters. Two release-rate-limiting models were considered (a saturation-limited model and a diffusion-limited model), and a range of reasonable values were assumed for the time-to-failure of the auger-hole liner and aluminum cladding and europium solubility in SWSA-6 groundwater. The bounding europium radionuclide near-field release rates peaked at about 1.3 Ci/year total for  $^{152,154,155}\text{Eu}$  in 1987 for the lower bound, and at about 420 Ci/year in 1992 for the upper bound. Better input information allowed calculation of the radioactivity releases from the other components with more confidence. The near-field release rates of  $^{55}\text{Fe}$ ,  $^{59}\text{Ni}$ ,  $^{60}\text{Co}$ , and  $^{63}\text{Ni}$  from stainless steel and cobalt alloy components, as well as of  $^{10}\text{Be}$ ,  $^{41}\text{Ca}$ , and  $^{55}\text{Fe}$  from beryllium reflectors, were calculated for the next 100 years, assuming bulk waste corrosion was the release-rate-limiting step. For the stainless steel and cobalt alloy components, the current (1986) total radionuclide release rate was calculated to be about 0.07 Ci/year, which decreases by 2010 to a steady release of about 0.003 Ci/year due primarily to  $^{63}\text{Ni}$ . Under the most conservative assumptions for the reflectors, the current (1986) total radionuclide release rate was calculated to be about  $1.2 \times 10^{-4}$  Ci/year, decreasing by 1992 to a steady release of about  $1.5 \times 10^{-5}$  Ci/year due primarily to  $^{41}\text{Ca}$ . The dominant uncertainties in the calculation of the inventory and release rates, as well as the research and development work would be needed to reduce these uncertainties, are discussed in the report.

## 1. EXECUTIVE SUMMARY

### 1.1 REPORT PURPOSE AND SCOPE

The purpose of the work described in this report was to estimate the near-field radioactivity release rates associated with the high activity low-level wastes currently emplaced in Solid Waste Storage Area 6 (SWSA-6) at Oak Ridge National Laboratory (ORNL). This information would be useful both as a source term in assessing environmental contamination which could be associated with the high activity low-level wastes already emplaced, and in evaluating future modes of disposal or storage of such wastes. Examination of the existing records (Boegly et al. 1985) showed that about 84% of the radioactivity emplaced in SWSA-6 could apparently be accounted for by neutron-activated metal parts discharged from the High Flux Isotope Reactor (HFIR), and the work described in this report was limited to consideration of these HFIR wastes. The radionuclide inventory contained in the HFIR wastes was first calculated, and then realistic or conservative assumptions, as well as existing data, were employed to calculate near-field radionuclide release rates. The dominant uncertainties in the calculations are indicated in the text, and the research and development (R&D) that would be needed to reduce these uncertainties is described.

### 1.2 DESCRIPTION OF HFIR PARTS EMPLACED IN SWSA-6

Three distinctly different types of metal parts are discharged from the HFIR: (1) control cylinders containing control plates composed of a europium oxide-aluminum cermet clad with aluminum; (2) stainless steel ducting, support, and assembly units, as well as cobalt alloy bearings; and (3) beryllium neutron reflectors. During use in the HFIR, these parts received a substantial neutron and thermal exposure. Neutron activation reactions form a number of radioactive isotopes in these parts that require isolation of the discharged parts. The disposal method for all of these parts is similar. The parts are stored in the HFIR pool after discharge from the reactor and, as convenient, are shipped to

SWSA-6. The parts are cut, crushed, or compacted as necessary and placed in a mild steel shipping container with holes in the top and bottom so that the pool water will drain when the can is raised from the pool into the transportation shield. The shipping container with the waste is transported to SWSA-6 and then lowered from the transportation shield into a hole which has been augered in the soil. Available soil is used to back-fill the hole after one to three containers of waste have been placed in a hole. In the case of some of the control plates, a galvanized steel liner was used in the auger hole for worker protection from radiation shine up the hole. Although not designed for the purpose of enhanced waste isolation, the liner does help delay groundwater intrusion to the control plate wastes. Wastes in unlined auger holes have been essentially disposed by a landfill technique since the containers are placed directly in the soil.

### 1.3 CALCULATED RADIONUCLIDE INVENTORY AS OF JUNE 1, 1986

The available SWSA-6 radionuclide inventory information proved to be both inaccurate and incomplete. Therefore, as a first step in calculating release rates, we calculated the radionuclide inventory of the disposed parts as of June 1, 1986 (Table 1.1). The identity and number of parts discharged from the HFIR and shipped to SWSA-6 was obtained from reactor records, and construction information was used to provide the weight and elemental composition of the various parts. Reasonable assumptions as to the neutron flux and exposure time in the reactor were made to allow calculation of the radionuclide inventory. Decay during out-of-reactor time was included in the calculations. The most recent cross sections and half-life values for the respective isotopes were also used in the calculations.

In terms of curies of radioactivity, the  $^{152,154,155}\text{Eu}$  content of the control plates and cylinders dominates the SWSA-6 inventory. The  $^{55}\text{Fe}$ ,  $^{60}\text{Co}$ , and  $^{63}\text{Ni}$  content of the stainless steel and cobalt alloy parts are next in quantity, while much smaller amounts of  $^{10}\text{Be}$ ,  $^{41}\text{Ca}$ , and  $^{55}\text{Fe}$  are present in the reflectors.

Table 1.1. SWSA-6 radionuclide inventory  
of HFIR parts as of June 1, 1986

Radionuclide	Control plates and cylinders (Ci)	Stainless steel and cobalt alloy (Ci)	Neutron reflectors (Ci)
$^{10}\text{Be}$			0.0721
$^{41}\text{Ca}$			0.00592
$^{55}\text{Fe}$		3,372	3.22
$^{59}\text{Ni}$		3.15	
$^{60}\text{Co}$		3,002	
$^{63}\text{Ni}$		353	
$^{152}\text{Eu}$	19,878		
$^{154}\text{Eu}$	21,307		
$^{155}\text{Eu}$	4,420		
Totals	45,605	6,730.15	3.29802

These calculated inventory values for the europium isotopes are much lower than the values in the SWSA-6 data base (see, for example, Table B-3 of Boegly 1984, or Table A.2 of Boegly et al. 1985). This difference stems, in part, from the fact that the standard data base does not take into account radioactive decay after discharge from the reactor. The half-lives of these radionuclides are relatively short, compared to SWSA-6 disposal time, and failure to take credit for the decay which is occurring seems unnecessarily conservative. The calculated quantity of  $^{60}\text{Co}$  also is much lower than the data base value. This situation also may result from the failure to account for radioactive decay in the data base. In addition, the data base value may include disposed cobalt sources not considered in this report. The data base has much lower values for  $^{55}\text{Fe}$  and  $^{63}\text{Ni}$  than we calculated, while  $^{59}\text{Ni}$  is not included in the data base. It seems possible that the presence of these neutron-activated isotopes may not have been considered during compilation of the data base. Our calculated value for  $^{10}\text{Be}$  is much lower than the data base value (Table A.2 of Boegly et al. 1985). We have no good explanation for this difference. The possible presence of small amounts of  $^{41}\text{Ca}$  appears not to have been included in the data base.

#### 1.4 RELEASE RATES OF EUROPIUM RADIONUCLIDES FROM CONTROL PLATES AND CYLINDERS

Of the HFIR wastes emplaced in SWSA-6, the control plates and cylinders may be the most environmentally interesting because (1) the greatest amounts of radioactivity are contained in the europium isotopes (45,605 Ci as of June 1, 1986), and (2) the chemistry and geochemistry of this waste in the soil/groundwater system are the least well understood. No information is available describing the reactions of the europium oxide-aluminum cermet with groundwater or the rate of corrosion of the aluminum cladding by groundwater. Only very limited information is available describing the solubility of europium in groundwater; however, it is apparent that the solubility is very dependent upon the solution pH. Unfortunately, the pH of the SWSA-6 soil/groundwater system in the near-field is also poorly known. Finally, the calculation of release rates is further complicated by the fact that some control plates are in lined auger holes while others are in unlined holes. Where actual data were unavailable, we used reasonable or conservative assumptions in the calculation of the release rates. Because the input data are uncertain, the calculated europium release rates are correspondingly uncertain.

The wastes in unlined auger holes were assumed to be in contact with infiltrating rainwater immediately after emplacement because the shipping can has holes in the top and bottom. These wastes were assumed to be contacted by a volume of groundwater equivalent to the net infiltration rate times the cross-sectional area of the auger holes. The release of europium radionuclides was assumed to begin after failure of the aluminum cladding. The release-rate-limiting step was assumed to be the solubility of europium in the groundwater.

We modeled two possible release scenarios for wastes in the lined auger holes. Release of radionuclides was assumed to begin only after sequential failure of the liner and cladding. In one case, we assumed that the concrete end plugs, and possibly the steel liner, underwent massive failure. For this case, the wastes in the lined auger holes would experience a groundwater-contact situation similar to the wastes

in the unlined auger holes, and the release of radionuclides was similarly modeled. We also modeled a situation where the end plugs would remain intact but the liner would corrode and develop a number of small breaches that would allow groundwater to flood the interior of the liner. For this case, we assumed that the wastes were standing in stagnant groundwater and that diffusion of radionuclides into the boundary layer would be the rate-limiting process.

Radionuclide release rates were calculated assuming the auger hole liner failed at 10 or 20 years, that the aluminum cladding failed after a 2- or 4-year exposure to groundwater, and that the europium solubility was  $1 \times 10^{-4}$  or  $1 \times 10^{-6}$  mol/L. All wastes in unlined auger holes were modeled by the saturation-limited release model, but wastes in the lined auger holes were modeled both by the saturation-limited release model and the diffusion-limited release model. Because of the uncertainties in the input information, we felt that the calculated release rates were most useful in establishing bounding release rate values for the assumed parameters. The lower bound, or least conservative, release rate occurs when all wastes are modeled by the saturation-limited model, the lower europium solubility value, and the longer liner and cladding life values are used. Europium releases begin about 1984 and peak at about 1.3 Ci/year in about 1987. The upper bound (or most conservative) release rate occurs when the wastes in the lined auger holes are modeled by the diffusion-limited model (wastes in the unlined holes are modeled by the saturation-limited model), the higher europium solubility value, and the shorter liner and cladding life values are used. In this case, wastes in the unlined holes begin to release activity about 1982 and peak at about 290 Ci/year at about 1984. A greater release peak of about 420 Ci/year then occurs at about 1992 due to wastes in the lined auger holes. The release rate drops abruptly at about 2015 because all the europium has been leached from the wastes in the lined auger holes.

The europium release rates calculated are near-field releases from the waste to the immediate surroundings in SWSA-6 and are not the release from the site to the environment. Calculation of the mobility of released europium radionuclides through the SWSA-6 soil/groundwater system was

beyond the scope of this task. The substantial uncertainty in input values used to calculate the europium near-field release rates has resulted in several orders-of-magnitude uncertainty. Since these near-field rates constitute the source term for the calculation of environmental releases from the site, it seems desirable to consider improving the input information for the control plates and cylinders (see Sect. 1.7).

#### 1.5 RELEASE RATES OF IRON, COBALT, AND NICKEL RADIONUCLIDES FROM STAINLESS STEEL AND COBALT ALLOY WASTES

The stainless steel and cobalt alloy wastes are considered as a group because they are similar in radionuclide content, exist as corrosion resistant metals, and are all emplaced in unlined auger holes. The radionuclides were assumed to be evenly distributed throughout the respective waste forms. Release was assumed to begin soon after emplacement, and the bulk waste form corrosion was assumed to be the release rate-limiting step. Literature information for the corrosion of similar stainless steel alloys buried in similar soil/groundwater environments was used for the corrosion rate input. A conservative value (highest corrosion rate) was employed. The cobalt alloy bearings were assumed to corrode at the same rate as stainless steel; this also is probably a conservative assumption.

The initial release rate (in 1986) is about 0.07 Ci/year, primarily due to  $^{55}\text{Fe}$  and  $^{60}\text{Co}$ . The rate drops to about 0.003 Ci/year, primarily resulting from  $^{63}\text{Ni}$ , by about 2010 and remains nearly constant after that date because of the long half-life of  $^{63}\text{Ni}$ . These calculated near-field release rates are known with considerably more confidence than those for the europium isotopes because of the more simplified emplacement, data on stainless steel corrosion, and simple release mechanism modeled.

Unless these near-field release rates translate to potentially problematic environmental releases from the site, or the low but continuing release of nickel radionuclides impacts site closure planning, additional or improved information on the stainless steel and cobalt alloy wastes may not be needed.

## 1.6 RELEASE RATES OF BERYLLIUM, CALCIUM, AND IRON FROM REFLECTORS

The reflectors emplaced in SWSA-6 contain only small amounts of radioactivity, primarily  $^{55}\text{Fe}$  formed from contaminant iron assumed to be present in the beryllium. Release was assumed to begin soon after emplacement, and the release-rate-limiting step was assumed to be beryllium corrosion controlled at the possible low SWSA-6 groundwater pH by the availability of dissolved oxygen, or at the possibly high pH by the diffusion of beryllium soluble species through the boundary layer. Due to the lack of literature information on the corrosion rate of beryllium in groundwater, we assumed that it was more rapid than the rate of diffusion of oxygen to the surface; this is a conservative assumption.

For the most acidic SWSA-6 soil/groundwater condition (pH of 4.4), the initial release rate (in 1986) is about  $1.2 \times 10^{-4}$  Ci/year, primarily because of the  $^{55}\text{Fe}$ . The  $^{55}\text{Fe}$  decays relatively rapidly, and after about 1992 a constant release rate is established at about  $1.5 \times 10^{-5}$  Ci/year due to the  $^{41}\text{Ca}$  which may be present as a contaminant in the beryllium. The release rate for  $^{10}\text{Be}$  is still lower; about  $1.8 \times 10^{-6}$  Ci/year. At more alkaline pH conditions all the radionuclide release rates are decreased. At pH 7.7 they are about 3 to 4 orders of magnitude lower.

The near-field release rates of radionuclides from the reflectors appear to be so low that additional or improved input information may not be needed. It could be desirable to run radiochemical analyses of some samples of discharged reflectors to confirm the assumed presence of  $^{41}\text{Ca}$  and  $^{55}\text{Fe}$ .

## 1.7 SUGGESTED RESEARCH/DEVELOPMENT NEEDS TO IMPROVE CALCULATED RELEASE RATES OF EUROPIUM RADIONUCLIDES

Consideration of the R&D effort that could be needed to improve the accuracy of the calculated near-field release rates was limited to the control plate and cylinder wastes. The calculated europium release rates from these wastes are both the greatest and the most uncertain for the HFIR wastes in SWSA-6. The calculated stainless steel and cobalt alloy radionuclide release rates are more accurate because of the better input data on the corrosion rate of the bulk waste form, while the reflectors

contain only small amounts of radioactivity. The information needed with regard to (1) the control cylinder and plate waste already emplaced in SWSA-6, and (2) possible alternative future disposal or storage of these wastes is briefly considered.

#### 1.7.1 Currently Emplaced Wastes

Two major types of uncertainty complicate accurate prediction of the performance of the currently emplaced control plates and cylinders: (1) the lack of information on the corrosion rate of the release barriers, and (2) the absence of data on the reaction of the europium oxide-aluminum cermet with groundwater and the resulting europium saturated solution concentration. Knowledge of the saturated solution concentration is further complicated by the absence of information on the pH of the near-field environment in SWSA-6. If the auger-hole liner and aluminum-cladding release barriers remain intact for times longer than assumed, the europium release peak is delayed and the radionuclide rates decreased because the europium radionuclides are decaying during isolation. If the cermet reacts only slowly with groundwater and/or the europium solubility is lower than assumed, the release rates are also substantially reduced. In particular, the release rate is directly proportional to the solubility value used in the calculations. The following types of activities would be needed to improve the quality of the input information:

1. Auger-hole liner - The auger-hole liner is galvanized road culvert pipe. We were unable to locate any corrosion rate information for this material at ORNL. Contact with manufacturers might develop data. Failing that, long-term corrosion tests in an environment typical of SWSA-6 might be needed.
2. Aluminum cladding - The aluminum cladding receives an appreciable neutron and thermal exposure during use in the HFIR, thus the corrosion rate may be different from that for new material. In any case, the corrosion of aluminum in stagnant water is a catalytic process that may be strongly influenced by specific local conditions. Long-term corrosion tests in an environment similar to that inside the lined auger holes (which may be

different than the geochemical conditions in the overall SWSA-6 site due to isolation by the partially failed liner) would be needed to develop realistic corrosion rate information for waste in lined holes. The tests would likely need to consider pH and radiolysis effects. The geochemical environment in the case of waste in unlined auger holes probably is more similar to the overall SWSA-6 site geochemistry.

3. Reaction of the cermet with groundwater - The europium oxide-aluminum cermet is a unique material, and its chemistry in the presence of water or groundwater has apparently never been studied. Chemical research would be needed to quantify the reaction rate and identify the stable solid phase(s) formed and the solution species. Knowledge of the solids formed is particularly important since the solids determine the solubility (saturated solution concentration) of europium.
4. Europium solubility - Only preliminary measurements of europium solubility as a function of pH or estimates based on lanthanide-group element similitude are available in the literature. The solubility selected is very important in determining the calculated release rates of the europium radionuclides because the rates are linearly proportional to changes in the solubility value. Also, the solubility is strongly dependent upon the groundwater pH since trivalent ions ( $\text{Eu}^{3+}$  is assumed to be the soluble species) hydrolyze extensively at higher pHs. Chemical research would be needed to develop better solubility information. The question of the possible formation of colloidal europium forms should also be addressed.

We recognize that this is a rather daunting list of R&D needs, but without improved information for some of the input values it is difficult to see how the uncertainties in the calculated near-field release rates from the currently emplaced control plate and cylinder wastes can be defensively reduced.

### 1.7.2 Future Waste Disposal or Storage Options

In the consideration of options for the future disposal or storage of discharged control plates and cylinders, enhanced isolation could be an attractive approach. In this case, the wastes would be isolated from contact with groundwater for greater than 10 half-lives of the longest lived radionuclide ( $^{152}\text{Eu}$ , with a half-life of 13.4 years) or for >134 years, to allow nearly complete decay of the radioactivity. Calculating the release of radionuclides (or, more accurately, showing that no radionuclides are released during 134 years) would require only improved information on the stability of the isolation barrier(s). It seems likely that less R&D work might be needed to obtain the necessary information to support modeling this situation than for modeling the soil/groundwater system. Improved corrosion data on the material(s) selected for isolation or storage, or selection of design materials for which adequate data already exist, could be an attractive method of modeling future waste performance.

## 2. INTRODUCTION

This report describes the modeling of near-field radioactivity release rates for some of the high activity low-level wastes emplaced at the Oak Ridge National Laboratory (ORNL) Solid Waste Storage Area 6 (SWSA-6). Low-volume, but high activity wastes discharged from the High Flux Isotope Reactor (HFIR) may account for about 84% of the radioactivity in shipments received at SWSA-6 during recent years (Boegly et al. 1985). We modeled the behavior of these HFIR high activity wastes in the SWSA-6 near-field geologic soil/groundwater system to: (1) explore the modeling methodology, and the supporting data availability, which could be applied to the characterization of low-level disposal sites in the Oak Ridge Reservation; (2) improve the prediction of future performance of the HFIR wastes already emplaced in SWSA-6; and (3) help in the evaluation of alternative disposal/isolation technologies that may be considered for future high activity waste shipments from the HFIR. Modeling was limited to the near-field environment. The near-field is defined to include the

waste form, cladding (if any), auger-hole backfill, auger-hole liner (if any), and intruding groundwater in the immediate vicinity of the waste. A description of auger-hole waste emplacement is given in Appendix A. This near-field release rate would be applicable as a source term for subsequent modeling of the far-field migration of radioactivity through the SWSA-6 site hydrogeologic system. Modeling of far-field radionuclide migration through the site to the environment is a separate activity and would involve other input data and methodology than that employed for the near-field studies described in this report. Therefore, for example, sorption reactions involving radionuclide binding to SWSA-6 soils were not evaluated in this study.

Groundwater intrusion/groundwater migration was the only radioactivity release scenario modeled. The processes or parameters that can lead to, or are involved in, the release of radioactivity from emplaced waste to the far-field environment include: (1) the radionuclide inventory in the emplaced wastes, (2) failure of engineered aspects of the emplacement techniques, (3) the rates of corrosion of cladding and bulk waste forms under the soil/groundwater geochemical environment, (4) the rates of dissolution of the respective radionuclides from the bulk wastes into the intruding groundwater, (5) solubility constraints on the steady-state groundwater concentration of the radionuclides, (6) diffusional constraints on the rate of transport of the respective radionuclides into the boundary layer to the migrating groundwater, and (7) the groundwater flux in the near-field. (In this report, the term "groundwater" is used in the general sense to identify any water in the soil. The HFIR wastes under evaluation are placed in auger holes that are supposed to be well above the water table. Thus, water contacting the wastes is considered to be infiltrating rainwater or meteoric water although it is called groundwater in the text.) Information for all these processes or parameters was not readily available for all the HFIR wastes or for some SWSA-6 geotechnical aspects, and a number of simplifying or limiting assumptions were necessary during modeling of the release rates; these assumptions are described in the body of the report in the sections for the respective wastes.

As a first step in the modeling activity, we compiled all the pertinent published or available information for these HFIR wastes and for the SWSA-6 site. That information is summarized in subsequent sections (Sects. 2.2 through 2.5). The general approach which we took to model radioactivity release rates is described in the following section (Sect. 2.1).

## 2.1 APPROACH TO MODELING RADIOACTIVITY RELEASE RATES

Our approach to modeling the near-field radioactivity release rates for the four waste forms studied is summarized in the following sections. A detailed description is presented in Sects. 3, 4, and 5 for the various wastes.

### 2.1.1 General Description

We have included a general discussion of our philosophy or approach to modeling the behavior of these wastes in the SWSA-6 site at this point in the report to help put the work in perspective. We considered a total of six release barriers (Table 2.1) and attempted to evaluate the importance of each of these for the respective wastes. The six items as shown in the table are:

1. The radionuclide inventory at the time of release. We first considered the available radionuclide inventory data, but found it to be of uncertain accuracy or completeness and used it only as a general guide to identify the more important wastes. We chose to recalculate the quantity of radionuclides that have half-lives great enough to be of environmental significance in the emplaced wastes. This calculation was based on an estimation of the quantity of the radionuclides formed during the exposure of the metal parts in the HFIR. Some simplifying assumptions as to neutron flux and exposure time were required, and the values obtained may be considered conservative. Data from post-irradiation examination of parts were also utilized. These

Table 2.1. Approach to modeling near-field radionuclide release rates for HFIR wastes in SWSA-6

Sequential release barrier	Release process	Parameters evaluated
1. Radionuclide inventory at time of release	<ul style="list-style-type: none"> <li>• Source term for calculations</li> </ul>	<ul style="list-style-type: none"> <li>• Inventory discharged from reactor</li> <li>• Radionuclide half-life</li> </ul>
2. Groundwater flux	<ul style="list-style-type: none"> <li>• Volume/flow rate of groundwater available for leaching waste form</li> </ul>	<ul style="list-style-type: none"> <li>• Infiltration rate of groundwater to waste form</li> </ul>
3. Waste form leach rate	<ul style="list-style-type: none"> <li>• Rate of dissolution of radionuclide from waste form</li> <li>• Saturated solution concentration of radionuclide in leachate</li> </ul>	<ul style="list-style-type: none"> <li>• Geochemical conditions of groundwater (pH, etc.)</li> <li>• Chemical form of radionuclide solid phase and solution species</li> <li>• Equilibrium solubility of radionuclide species</li> <li>• Radiolysis effects</li> </ul>
4. Waste cladding (if present)	<ul style="list-style-type: none"> <li>• Diffusion of solubilized radionuclide through cladding breach</li> </ul>	<ul style="list-style-type: none"> <li>• Time of significant cladding breach</li> <li>• Rate of diffusion of solubilized radionuclide through breach</li> <li>• Radiolysis effects</li> </ul>
5. Auger-hole backfill	<ul style="list-style-type: none"> <li>• Reduced leachage mobility</li> </ul>	<ul style="list-style-type: none"> <li>• Rate of diffusion of solubilized radionuclide through backfill material</li> </ul>
6. Auger-hole liner (if present)	<ul style="list-style-type: none"> <li>• Diffusion of radionuclide through auger-hole liner</li> </ul>	<ul style="list-style-type: none"> <li>• Time of significant liner breach</li> <li>• Rate of diffusion of solubilized radionuclide through breach</li> </ul>

estimated radionuclide quantities were then corrected for radioactive decay during the time out of reactor until the assumed release event to give the waste radionuclide inventory at the time of release.

2. The groundwater flux. The groundwater flux is an important parameter both in evaluating infiltration and corrosion of the auger-hole engineered features, waste cladding, and waste form, as well as leaching and release of the radionuclides from the wastes. Detailed hydrologic information is not available for SWSA-6; therefore, we assumed that only infiltrating rainwater would contact the wastes. This assumption was based on the reported location of the auger holes above the water table. Expert judgment was employed to estimate a rainwater infiltration rate for the auger hole region of SWSA-6.
3. The waste form leach rate. If the radionuclides already exist within the waste in a water-soluble form, the release rates depend on the solubility limit (saturated solution concentration) for the soluble species, the rates at which the matrices are removed by chemical reactions or corrosion, and the rates of diffusion of the soluble species away from the host matrices. If the radionuclides are not present in a water-soluble form, their release rates then will depend upon (1) the rate at which reactants in the groundwater diffuse to the exposed waste surfaces, (2) the rates of reaction of the reactants at the surfaces, and (3) the rates at which the soluble reaction products diffuse into the surrounding soil/groundwater system.
4. Isolation of the radionuclide-containing matrix by cladding. When the radionuclide-containing waste forms are confined within a cladding material, the corrosion or failure of the cladding would be an important modeling aspect. We have assumed that no radioactivity could be released before the cladding is breached. The radioactive material is isolated from contact by groundwater by an external cladding material only in the case of the europium-containing HFIR control plates. Unfortunately, we

found little data that would support calculation of the corrosion rate of the aluminum control plate cladding in stagnant groundwater after neutron and thermal exposure in the reactor. We were able to take only minimal credit for this potentially important release barrier in the modeling.

5. Reduced groundwater flux and radionuclide diffusion rate due to auger-hole backfill. The auger holes are backfilled with soil or sand after the waste containers are emplaced. In the modeling of unlined auger holes, we assumed that the auger-hole backfill promptly became saturated with infiltrating rainwater and performed as a typical SWSA-6 soil/groundwater system. In the case of lined holes (see below), we assumed that the backfill remained dry until after failure of the hole liner.
6. Isolation of the emplaced waste by an auger-hole liner. In the case of some of the highly radioactive HFIR control cylinders and plates, added environmental isolation is provided by the galvanized pipe used to line the auger hole for worker radiation protection during disposal. We assumed values for the lifetime of galvanized pipe in soil/groundwater systems and assumed that no groundwater contacted the emplaced waste until after the failure of the liner. No credit could be taken for a hole liner in the case of the other waste forms since these wastes were placed in unlined auger holes.

Rarely would the overall reaction rates for the process and parameters described above be equally dependent upon all the steps in the release reaction sequences. In almost all cases of heterogeneous chemical reactions, one step in the sequence is slower than the others and becomes the rate-limiting step. Our approach has been to try and identify the most likely rate-limiting step for each of the different radionuclides in the different HFIR wastes in SWSA-6, and to calculate the radionuclide release rates based on those rate-limiting steps. Where we have been able to identify actual data that quantify the presumed rate-limiting

reaction, we have used that data. In cases where we were unable to locate actual data, we hypothesized a plausible rate-limiting step that could be modeled.

### 2.1.2 Stainless Steel and Cobalt Alloy Parts

The major long-lived radionuclides of environmental importance which are produced in the stainless steel and cobalt alloy (Haynes 25) parts during use in the HFIR are  $^{55}\text{Fe}$  (half-life 2.3 years),  $^{60}\text{Co}$  (half-life 5.27 years),  $^{59}\text{Ni}$  (half-life  $7.6 \times 10^4$  years), and  $^{63}\text{Ni}$  (half-life 100 years). The quantities of each radionuclide in the emplaced waste were estimated by assuming the following: (1) each disposed part was exposed to a spatially uniform neutron flux equal to the maximum flux that exists in the region of the reactor core where that part resides, and (2) the duration of the exposure was for the time that part was in the reactor. This calculation yields an upper limit or conservative estimate of the radionuclide production, and the actual value would be less than this conservative number. The radionuclide inventory for each part was then reduced for radioactive decay during the out-of-reactor time until the time of the release event after disposal in SWSA-6. Radioactivity release was assumed to begin promptly after disposal because these wastes are typically emplaced in unlined auger holes and contact with infiltrating rainwater would occur soon after disposal. These radionuclides were assumed (1) to be equally distributed throughout the waste form matrix, and (2) to be released at a rate that is limited by the corrosion rate of the stainless steel or cobalt alloy material in the soil/groundwater system. Release of the soluble cobalt, nickel, and iron species to groundwater was assumed not to be limited by the solubility of these elements in water, due to the low corrosion rates, or by diffusion of the soluble species from the waste surface. Data on corrosion of buried stainless steel components over the range of pH conditions which may exist at SWSA-6 (pH 4.4 to 7.7) were retrieved from the literature and used in calculating the release rates, as discussed in Sect. 3. Expert

judgment was used to estimate corrosion rates for the Haynes 25 alloy parts in the soil/groundwater system and to estimate the flux of intruding rainwater.

### 2.1.3 Control Cylinder and Plates

The radionuclides of environmental concern in the HFIR control plates are activation-induced isotopes of europium. The tantalum radionuclides formed have short half-lives and promptly decay, but only small quantities of gadolinium radionuclides are formed during irradiation. The long-lived isotopes of importance are  $^{152}\text{Eu}$  (half-life 13.4 years),  $^{154}\text{Eu}$  (half-life 8.5 years), and  $^{155}\text{Eu}$  (half-life 4.73 years). The quantities of europium isotopes in the control plates and cylinders were estimated from quantities measured in control plate No. 3 in a post-irradiation examination (Knight and Richt 1972). It was assumed that this cylinder was examined shortly after removal from the HFIR and that the most short-lived isotope,  $^{155}\text{Eu}$ , had not decayed appreciably prior to examination. Quantities for other control plates and cylinders were scaled in proportion to total irradiation in terms of Mwd. Then, this radionuclide inventory was corrected for radioactive decay until the time of the assumed release event. Some control plates are in lined auger holes; other plates and one cylinder are in unlined holes. When an auger-hole liner is present, we assume no release will occur until after the failure of the liner. The liner is galvanized steel road culvert pipe. Minimal credit was taken for the aluminum cladding on the control plates because data on corrosion after irradiation are lacking, and aluminum corrosion typically is relatively rapid in stagnant water. The release rates after auger-hole liner and cladding failure were estimated by assuming that  $\text{Eu}(\text{OH})_3$  is the chemical form of the europium oxide-aluminum cermet waste after breach of containment and reaction with intruding rainwater, and either (1) that the release rate of the soluble radionuclide species ( $\text{Eu}^{3+}$ ) from the corroded auger-hole liner can be described by a diffusion-limiting model similar to the waste performance model of Pigford and Chambré 1985, or that (2) the release is solubility limited. The release rates were calculated, as discussed in Sect. 4.

The release rates were very dependent on the pH assumed for the SWSA-6 soil/groundwater system since the  $\text{Eu}^{3+}$  solubility is very sensitive to the solution pH.

#### 2.1.4 Reflectors

The HFIR reflector components emplaced in SWSA-6 contain activation-induced  $^{10}\text{Be}$  (half-life  $1.6 \times 10^6$  years) formed from natural  $^9\text{Be}$ . Although the reflectors are manufactured from 99.99% purity beryllium, impurities which may be present in the metal may lead to the formation of  $^{55}\text{Fe}$  (half-life 2.3 years) and  $^{41}\text{Ca}$  (half-life  $1.0 \times 10^5$  years). A conservative calculation of neutron flux and exposure time was used to estimate the radionuclide inventory after discharge from the reactor. The radionuclide inventory was reduced for radioactive decay during out-of-reactor time until shipment of the components to SWSA-6. Release to infiltrating rainwater was assumed to occur promptly after emplacement because the reflector components are emplaced in unlined auger holes. The radionuclides were assumed to be evenly dispersed throughout the beryllium and to be released to groundwater at the corrosion rate of the beryllium. At low groundwater pH (pH 4.4), we assumed that the beryllium corrosion rate was limited by the diffusion to the metal surface of dissolved oxygen in the groundwater flowing past the waste. The dissolved oxygen content was estimated from data on Henry's law constants from standard references, assuming saturation at the partial pressure of atmospheric oxygen. At high pH (pH 7.7), the corrosion rate of beryllium was assumed to be limited by diffusion of  $\text{Be}(\text{OH})^+$  and  $\text{Be}(\text{OH})_2(\text{solution})$  from the solid surfaces through the boundary layer. Diffusion of oxygen to the metal surface and diffusion of dissolved beryllium from the metal surface was estimated using boundary-layer approximations similar to those used for estimating europium diffusion rates.

## 2.2 CONTRIBUTION OF HFIR WASTES TO THE RADIOACTIVITY INVENTORY AT SWSA-6

The SWSA-6 site is the current active low-level waste disposal facility for radioactive wastes generated at ORNL. A radionuclide inventory of wastes placed in SWSA-6 from 1977 through 1984 is given in

Table A.2 of Boegly et al. 1985. Of the total of 211,000 Ci of radioactivity emplaced during this period, 193,000 Ci (or 91%) of the radioactivity was placed in auger holes. (Auger holes are vertically bored holes of 18 ft or less in depth which are used for the disposal of the more radioactive wastes.) The following three radionuclide groups dominate the auger-hole inventory:

1. 400 Ci of  $^{10}\text{Be}$ , which is primarily contained in neutron reflectors discharged from the HFIR;
2. 22,200 Ci of  $^{60}\text{Co}$ , which is primarily contained in used stainless steel parts, cobalt alloy bearings, and spent ion-exchange resins discharged from the HFIR; and
3. 154,800 Ci of  $^{152,154,155}\text{Eu}$ , which is primarily contained in control cylinders and plates discharged from the HFIR.

Thus, about 84% of the total radioactivity emplaced in SWSA-6, or 92% of the activity emplaced in the auger holes, is accounted for by wastes discharged from the HFIR. The curie inventory values given in Boegly et al. 1985 have not been corrected for radioactive decay after shipment to SWSA-6; therefore, the current emplaced inventory for these radionuclides would be lower, depending on the half-life of the respective radionuclides and the accuracy of these initial inventory values.

This published radionuclide inventory information proved to be of value only as a general guide to the amount and identity of the major radionuclides in the wastes. Radiochemical analyses are not performed on the wastes prior to shipment to SWSA-6. Thus, the inventory curie values are only estimates. Also, only some of the major radionuclides believed to be present in the wastes are listed on the shipping invoice. We attempted to develop more accurate radionuclide inventory data for each of the wastes studied, as discussed in Sect. 2.1.

### 2.3 DESCRIPTION OF HFIR WASTES AND EMLACEMENT TECHNIQUE AT SWSA-6

The following general description of the major high activity low-level wastes shipped from the HFIR to SWSA-6 was developed through discussions with staff involved in HFIR operations (Farrar 1986). The main sources of radioactivity are contained in a few types of waste

materials: control cylinders and plates, stainless steel parts, cobalt alloy bearings, used ion-exchange resins, and reflector components. The mode of shipment and emplacement is similar for all these wastes and, when convenient, more than one waste material may be contained in a single shipment. The waste materials are stored under water in the HFIR pool after discharge from the reactor. For shipment to SWSA-6, the waste is placed in a mild-steel shipping basket or can under water and raised into a transport shield. The transportation shield is a drum waste cask constructed of 4 in. of mild steel and 1 to 2 in. of lead. Many of the waste parts are too large to be placed directly in the can, and these parts are broken and compacted into smaller pieces as necessary to fit in the shipping can. The steel can contains holes in the top and bottom so that pool water will drain from the basket when it is raised.

A radiochemical analysis of the wastes is not performed prior to shipment to SWSA-6. The curie values on the UCN-2822 ticket which accompanies each shipment to SWSA-6 are approximations based on reading the level of radiation at some distance from the transportation shield and extrapolating that reading to estimate the curie contents of the waste in the shipping can. Only the major radioisotopes believed to be present in a shipment usually are identified on the UCN-2822 ticket. Since the neutron flux exposure of the HFIR parts was variable and uneven during use, depending on the position of the respective part relative to the core and the HFIR operating history, the radionuclides are unevenly dispersed throughout the waste bulk. This uneven radionuclide distribution precludes an accurate measurement of the total radionuclide content of a waste shipment without extensive sampling and analysis. The strong gamma emissions from  $^{60}\text{Co}$  would also make detection of some radionuclides difficult for the stainless steel or cobalt alloy wastes. The waste can may be unevenly filled and may have an unknown void space, so neither the volume nor weight of the radioactive waste may be accurately known for a given shipment. The weight of the individual HFIR parts sent to SWSA-6 are known from the construction records, but the weight of waste material in a given shipping can may not be well known. Also, assorted wastes may be placed in a given shipping can as convenient. Considering all these

factors, both the identity of radionuclides as well as the quantity of radionuclides listed in the SWSA-6 inventory (Boegly et al. 1985) probably should be viewed with caution.

On arrival at SWSA-6, the transport shield is positioned over a prepared auger hole. The hole may be lined with a galvanized steel pipe in the case of some of the more radioactive shipments. The shipping can is lowered by a steel cable out of the transportation shield to the bottom of the auger hole. The steel cable is discarded along with the shipping can. Soil or sand is placed on top of the shipping can for radiation shielding, and then additional shipping cans may be placed into the hole. When the hole is filled to within 3 ft of the surface, a concrete plug is placed in the auger hole to act as an intruder seal. (A description of current auger-hole waste disposal practices is published in Boegly et al. 1985 and in Bates 1983.) Discussions were also held with Operations Division staff (Bolinsky 1986).

A more detailed description of the disposal method for four of the HFIR wastes is given in Sects. 3 through 5, and auger-hole construction is described in Appendix A.

#### 2.4 NEAR-FIELD GEOCHEMICAL CONDITIONS AT SWSA-6

Among the parameters that control the mobility of contaminants at geologic disposal sites, the geochemical conditions (pH, Eh, mineralogy, water composition, etc.) play an important role in the corrosion, dissolution, and solubility reactions involving the waste forms and contaminants (Lutton et al. 1982, Olsen et al. 1983). Thus, knowledge of the geochemical conditions is a prerequisite to both the successful modeling of the waste and site performance and the calculation of contaminant release rates.

Detailed geochemical information is not available for the SWSA-6 site, and a plan has been developed to collect needed data (Boegly et al. 1985). Some information was obtained for a planned field demonstration facility (Engineered Test Facility) within the SWSA-6 site boundaries (Davis et al. 1984), and this information has been provisionally used

as descriptive of SWSA-6 (Boegly 1984). The available geochemical information for the Engineered Test Facility (ETF) site which is relevant to this release rate study is discussed in the following paragraphs.

#### 2.4.1 Soil/Groundwater System Acidity

The acidity of the soil/groundwater system may play a dominant role in establishing the bulk waste dissolution rate, radionuclide dissolution rate, and radionuclide solubility (saturated solution concentration). Two very different acidity values are reported in Boegly 1984 and in Davis et al. 1984. Table C-3 of Boegly 1984 gives a pH of  $7.3 \pm 0.6$  (mean  $\pm$  standard deviation) for 19 samples of well water from well ETF-1 at the Engineered Test Facility site. Similarly, Davis et al. 1984 in Tables F.3 through F.14 give pH values ranging from 7.3 to 7.7 for well water samples from 12 different wells (ETF-1 through ETF-12) at the Engineered Test Facility site. However, much more acidic values are reported in Table 11 of Davis et al. 1984 for soil/distilled water pastes. A pH of  $4.4 \pm 0.4$  (mean  $\pm$  standard deviation) was given for mixtures of a total of 24 measurements with soil from three different trenches at the Engineered Test Facility site. There is a three order-of-magnitude difference in the  $H^+$  activity between these two pH values (4.4 and 7.3-7.7).

In considering the pH value(s) to be used in the calculation of the bulk waste dissolution rate or radionuclide solubility, there seems to be no obvious choice between these pH values. Layers of limestone have been observed at the SWSA-6 site, and the Engineered Test Facility site actually is in the Maryville Limestone member of the Conasauga Group (Boegly 1984). It seems possible that the groundwater samples from the ETF wells may have been in contact with the limestone. Thus, the slightly alkaline groundwater pH of  $\sim 7.3$  may be representative of standing groundwater, or the water table, at SWSA-6. Conversely, infiltrating rainwater, which may surround waste placed in an auger hole, may be more like the soil/distilled water paste, since the waste may be in a soil-leached-zone environment that is not dominated by limestone. Thus, it is possible that the soil/water environment around the emplaced waste could be better

represented by the pH of 4.4 in some cases. Acidic shale in the Oak Ridge Reservation typically weathers to yield soil/groundwater systems with a pH of 5 or less (Olsen et al. 1983).

For the modeling studies conducted to estimate release rates, we decided to use both a pH of 4.4 and 7.7, since these values may describe the range or extremes of acidity conditions which may exist at SWSA-6.

#### 2.4.2 Redox Condition

The soil/groundwater redox condition may play a significant role in establishing the bulk waste dissolution rate, radionuclide dissolution rate, and radionuclide solubility (Dayal et al. 1986b). No well water Eh measurements are reported in Davis et al. 1984 or Boegly 1984. It seems reasonable that these shallow groundwaters would be generally oxidizing; thus, for the release rate modeling studies, oxidizing redox conditions were presumed to exist at SWSA-6. An exception to this condition could be a situation where the bulk waste contained reactive reducing chemicals which could alter the microenvironment around the emplaced waste. While such a situation frequently exists in waste disposal trenches due to biological degradation of paper, wood, etc. (Dayal et al. 1986a and Dayal et al. 1986b), the metallic HFIR wastes in auger holes might not be reactive enough to generate reducing conditions. Conversely, readily corrodible material such as the mild steel shipping can could lead to reducing conditions immediately adjacent to the emplaced waste. In the absence of any information on the specific geochemical condition of typical closed auger holes at SWSA-6, we took no credit for the decreased solubility often associated with reducing redox conditions.

For the release rate calculations, the normal oxidized valence of all contaminant elements was assumed to prevail at SWSA-6 because there is no evidence at this time to support use of reducing conditions.

#### 2.4.3 Groundwater Chemistry

The composition of the groundwater in contact with the waste may influence the contaminant behavior in addition to pH and Eh. The information in Davis et al. 1984, or Boegly 1984, shows that the Engineered

Test Facility well waters were essentially very dilute  $\text{Ca}^{2+}$ ,  $\text{Mg}^{2+}$ ,  $\text{SO}_4^{2-}$ , and  $\text{Cl}^-$  solutions. Silica was a major solution component. For the contaminant release rate modeling work, no unusual effects due to groundwater composition were assumed to occur. The data are insufficient to indicate any possible presence of complexing ions or compounds that might increase the radionuclide solubility values.

#### 2.4.4 Soil Mineralogy

The soil mineralogy primarily influences the sorption of radionuclides. Since sorption was not evaluated in this near-field study, soil mineralogy information was not considered further. Data in Davis et al. 1984 describe the soils from three trenches at the Engineered Test Facility as highly leached solum from weathered acid shale. The minerals identified (Davis et al. 1984, Table 17) were illite, chlorite, and vermiculite/smectite. A detailed survey of SWSA-6 soil has recently been published (Lietzke and Lee 1986).

#### 2.4.5 Groundwater Flux

The groundwater flux is taken as the portion of annual rainfall which infiltrates the ground. The annual rainfall measured at the Oak Ridge station between 1948 and 1976 is 55 in./year, and the fraction that infiltrates is approximately 20 to 25% of this amount. We assumed a fraction of 25% for the calculations in this report, or about 13.75 in./year (Davis 1986). Since the auger holes are all well above the water table, the only water to which these holes are exposed is infiltrated rainwater. This flux is assumed to be vertical and constant. The value of 13.75 in./year is the darcy water velocity through the soil or the value that would obtain in the hypothetical absence of soil. The interstitial velocity of water is the darcy velocity divided by the soil porosity, a measure of the true area available for flow compared with the hypothetical situation where the presence of the soil is neglected. The value of the soil porosity in SWSA-6 is reported to be 0.5 (Davis 1986). Thus, the interstitial velocity used in the calculations is 27.5 in./year.

## 2.5 RADIOLYSIS

Radiolysis reactions involving groundwater components in the near field could change the geochemical parameters of the soil/groundwater system surrounding the emplaced waste and alter the waste form corrosion rate and/or radionuclide solubility. In particular, the field associated with the highly radioactive control plates and cylinders might be expected to influence the performance of these wastes. In general, the stainless steel parts and the beryllium reflectors are less radioactive and, therefore, radiolysis reactions could be of less importance in understanding the performance of these wastes.

A literature search revealed little quantitative information that could be used to estimate the effects of radiolysis reactions on the emplaced wastes. Considerable research has been done in the past on the radiolysis of pure water (much of this work was done at ORNL). Free radicals such as  $H^*$  and  $OH^*$ , as well as chemicals such as  $H_2$ ,  $O_2$ ,  $H_2O_2$ , and  $HNO_3$  may be formed. Carbonate ions in solution may also be polymerized to various organic compounds including carboxylic acids. The various reactions are complex, and the reaction products formed are easily influenced by the system components. Recent publications concerning high-level waste sites have reported the following: (1) the effects of radiolysis reaction products on container corrosion mechanisms and kinetics (Glass 1985; Taylor et al. 1984; Furuya et al. 1983), (2) changes in the geochemical and chemical processes in the geologic system (Reed 1985), (3) changes in the oxidation potential of the rock/groundwater system (Jantzen and Bibler 1985), (4) the formation of organic polymers (Gray 1984), (5) increases in acidity of the waste package environment (Bates and Oversby 1984; Couture and Seitz 1983), and (6) increases in the solubility of radionuclides (Wisbey 1986).

Most of the literature information was qualitative in nature, or related to specific high-level waste systems, and could not be applied to the calculation of changes in radioactivity release rates for the waste materials emplaced in SWSA-6. Therefore, we did not take radiolysis effects into account in the calculations. However, it should be born in mind that such effects are generally deleterious (increased acidity,

higher corrosion rates, increased radionuclide solubility, etc.) and failure to treat these effects in the calculations represents a potential nonconservatism in the results.

### 3. STAINLESS STEEL AND COBALT ALLOY PARTS

#### 3.1 DESCRIPTION OF PARTS EMPLACED IN SWSA-6

The following description of the disposal of stainless steel and cobalt alloy parts was developed through discussions with HFIR operations staff (Farrar 1986). Some of the structural parts of the HFIR are constructed of 304 or 347 series stainless steels. These parts include ducting for control of coolant flow and various support and assembly units. The parts closest to the core accumulate neutron and thermal exposure and are periodically replaced. After discharge from the reactor, the used parts are stored in the HFIR pool. The parts are placed in a sheet metal shipping can and transported to SWSA-6 in a lead and steel transportation shield. Many of the parts are too large to be placed directly in the shipping can and are cut into pieces that will fit into the can. The shipping can has holes in the top and bottom so pool water will drain from the can when it is raised from the pool into the transportation shield. At SWSA-6, the transportation shield is positioned over an auger hole, and the sheet metal can containing the stainless steel waste is lowered into the auger hole. The steel lowering cable is discarded with the can. (A description of auger hole emplacement methodology is given in Appendix A.)

Both 304 and 347 series stainless steels are a mixture of many alloying elements. The base element, of course, is iron with additions of 16 to 20% chromium and 8 to 14% nickel. Manganese, molybdenum, and silicon are also added to the alloys. In addition, cobalt is present as a tramp element in the chromium and nickel at a fractional percentage level in the stainless steel alloys. Neutron activation isotopes of several of these elements are formed during reactor operation. The most important radionuclide present in HFIR stainless steel wastes, in terms

of personnel exposure, is  $^{60}\text{Co}$  (half-life 5.27 years.) due to the high-energy gammas emitted. All half-life values are from Walker et al. 1984. Some of the  $^{60}\text{Co}$  is formed from the tramp cobalt in the alloy, but some also might be surface contamination of  $^{60}\text{Co}$  transported from the journal bearings (see below). In pressurized water reactors (PWRs), much of the  $^{60}\text{Co}$  on stainless steel parts has been transported from high-cobalt alloy parts. The shipments from HFIR to SWSA-6 have listed only  $^{60}\text{Co}$  as the radioactive element on the UCN-2822 form, but other radionuclides must also be present in the stainless steel. For stainless steel parts from PWRs,  $^{59}\text{Ni}$  and  $^{63}\text{Ni}$  are considered to be important radionuclides in studying repository performance of spent fuel (Kerrisk 1985). This importance is primarily due to the long half-life ( $7.6 \times 10^4$  years for  $^{59}\text{Ni}$  and 100 years for  $^{63}\text{Ni}$ ) and the solubility of nickel in groundwater. Some  $^{59}\text{Ni}$  and  $^{63}\text{Ni}$  must also be present in the HFIR stainless steel wastes from neutron activation of the nickel content. Also, some  $^{55}\text{Fe}$  (half-life of 2.3 years) must be present in the HFIR wastes from neutron activation of the iron content of the alloys. Chromium has no long-lived isotopes. It is not clear if either molybdenum or manganese, which have at least one isotope with a half-life of  $>1$  year ( $^{93}\text{Mo}$ ,  $^{53}\text{Mn}$ , and  $^{54}\text{Mn}$ ), could contribute significantly to the radioactivity in HFIR wastes; they were not considered further.

Journal bearings from the HFIR are also routinely discharged and shipped to SWSA-6 for disposal. Since these bearings are small, they are stored in the HFIR pool after discharge and then mixed in with shipments of other wastes as convenient. Therefore, there may be no inventory numbers for the amount of radioactivity associated solely with the journal bearings. The bearings are constructed of Haynes 25 alloy; 50% Co, 20% Cr, 10% Ni, 3% and 0.5% W. Neutron activation produces appreciable amounts of  $^{60}\text{Co}$  in these bearings during reactor operation. It seems reasonable to assume that some  $^{59}\text{Ni}$  and  $^{63}\text{Ni}$  also are present in the journal bearings.

During the period 1977 through 1984, the inventory (Table A.2 of Boegly et al. 1985) shows that a total of 22,200 Ci of  $^{60}\text{Co}$  were placed in auger holes in SWSA-6. Most of these curies of  $^{60}\text{Co}$  can probably be accounted for by the stainless steel parts and journal bearings from

HFIR, although some also must be due to emplacement of used ion-exchange resin from HFIR as well as disposal of cobalt sources from Isotope Distribution. The inventory (Table A.2 of Boegly et al. 1985) shows only 10 Ci of  $^{55}\text{Fe}$  and no value for  $^{59}\text{Ni}$  or  $^{63}\text{Ni}$ ; it seems probable that the  $^{55}\text{Fe}$ ,  $^{59}\text{Ni}$ , and  $^{63}\text{Ni}$  content of these stainless steel parts and journal bearings were not included in the inventory.

The inventory of  $^{55}\text{Fe}$ ,  $^{60}\text{Co}$ ,  $^{59}\text{Ni}$ , and  $^{63}\text{Ni}$  in each of the stainless steel components was estimated for this study using the following equation:

$$A_{i,c} = 1.627 \times 10^{-8} \frac{f_{i,c} m_c}{MW_i} \phi \sigma_i (1 - e^{-\lambda_i t_R}) \quad (3.1)$$

where

- $A_{i,c}$  = inventory of radioisotope i in the stainless steel component c under consideration, Ci;
- $f_i$  = mass fraction of the precursor isotope for i in the stainless steel component, kg precursor/kg stainless steel;
- $MW_i$  = atomic weight of precursor, kg/kg-mol;
- $m_c$  = mass of stainless steel component, kg;
- $\phi$  = neutron flux to which the stainless steel component is exposed, neutrons/cm<sup>2</sup>·s;
- $\sigma_i$  = capture cross section of precursor to i, b;
- $t_R$  = time of exposure to neutron flux in reactor, year;
- $\lambda_i = 0.693/t_{1/2,i}$ ;
- $t_{1/2,i}$  = half-life of isotope i.

The values for the input to this calculation are discussed in the paragraphs below.

The HFIR stainless steel components were fabricated from 347 stainless steel and 304 stainless steel. The nominal compositions for these alloys are given in standard references (e.g., Perry et al. 1963). The components of these alloys, which are precursors to long-lived radioactive isotopes, are respective stable isotopes of cobalt, iron, and nickel. The important precursor isotopes are  $^{59}\text{Co}$  (~100% relative abundance in natural cobalt),  $^{54}\text{Fe}$  (5.84% relative abundance in natural iron),  $^{58}\text{Ni}$  (67.88% relative

abundance in natural nickel), and  $^{62}\text{Ni}$  (relative abundance of 3.7% in natural nickel). Table 3.1 shows the percentage of the naturally occurring metals in the stainless steel alloys. These compositions were used in estimating the inventory of the radioactive isotopes in the buried metal parts.

The inventory of stainless steel parts emplaced in SWSA-6 (Farrar 1986) is given in Table 3.2 along with material of construction of each component, emplaced mass, specific area (as calculated in Sect. 3.2.5), maximum neutron flux to which the part was exposed (for use in Eq. 3.1), and the time of exposure in the reactor. The induced activities of  $^{55}\text{Fe}$ ,  $^{59}\text{Ni}$ ,  $^{60}\text{Co}$ , and  $^{63}\text{Ni}$ , as calculated using Eq. (3.1), are given also. The neutron capture cross sections for  $^{54}\text{Fe}$ ,  $^{58}\text{Ni}$ ,  $^{59}\text{Co}$ , and  $^{63}\text{Ni}$  were taken from Walker et al. 1984; the values used were 2.3, 4.6, 37, and 14.5 b, respectively.

## 3.2 CALCULATION OF RADIOACTIVITY RELEASE RATES

### 3.2.1 Waste Leachate Chemistry

The waste leachate was assumed to be infiltrating rainwater. As discussed in Sect. 2.4.1, the most important SWSA-6 groundwater aspects are the extreme pH values observed for SWSA-6 soil/groundwater systems (pH 4.4 and 7.7) in the modeling calculations.

Table 3.1. Cobalt, nickel, and iron contents of HFIR components

Alloy	(wt %)		
	Co	Fe	Ni
347 SS	0.2	71.5	10.0
304 SS	0.2	71.5	9.0
Haynes 25	53.65	0	10.0

Table 3.2. Inventory of HFIR stainless steel and cobalt alloy components emplaced in SWSA-6, as of June 1, 1986

Component	Material	Weight buried (kg)	Maximum flux (neutrons/cm <sup>2</sup> s)	Time in reactor (years)	Activity (Ci)			
					<sup>60</sup> Co	<sup>59</sup> Ni	<sup>55</sup> Fe	<sup>63</sup> Ni
Filings	304 SS	2.3	1.0E+12	0.5	0.986	0.000815	1.43	0.0916
Upper tracks	347 SS	502.0	1.0E+12	5.0	1540	1.62	1730	181
Lower tracks	347 SS	476.0	1.0E+12	5.0	1460	1.53	1640	172
Shroud flange	304 SS	374.0	1.0E+08	5.0	0.0363	0.000013	0.0792	0.000016
Bearings—6 months	Haynes 25	36.7	1.0E+12	0.5	0.425	0.000001	0	0.000162
Bearings—3 years	Haynes 25	6.1	1.0E+12	3.0	0.319	0.000001	0	0.000159
				Totals	3002	3.15	3372	353

### 3.2.2 Time of Radioactivity Release

We assumed that the release of radioactivity would begin immediately after emplacement of the waste in the auger hole [i.e., the time of initial radioactivity release used in the release rate calculations (Sect. 3.2.6) was 0 year.] This assumption was reached because no engineered aspects exist to isolate the waste from infiltrating rainwater. The auger holes are not lined, and the mild steel shipping can containing the waste has holes in the top and bottom. The concrete plug poured in the top of the hole for intruder protection would not provide significant hydrologic isolation. Also, the wastes are not clad or enclosed in sealed containers.

### 3.2.3 Corrosion of Metal Parts

3.2.3.1 Stainless Steel. Mechanisms of corrosion of stainless steels include general corrosion, pitting, crevice corrosion, intergranular corrosion, and stress corrosion cracking. General corrosion refers to the uniform loss of metal over the entire exposed surface. In this corrosion mode, the thickness of material is uniformly reduced. The other forms of corrosion are special cases of localized corrosion. A pit is a small cavity in the surface caused by localized corrosion. Crevice corrosion is a form of accelerated localized corrosion that occurs at locations where easy access to the bulk environment is prevented, such as the mating surfaces of metal assemblies. Intergranular (or intercrystalline) corrosion is preferential corrosion at grain boundaries in a metal or alloy. Stress corrosion cracking is the cracking of a metal produced by the combined action of corrosion and tensile stress.

The corrosion behavior of buried stainless steel waste tanks on the Hanford reservation has been assessed (PNL 1984). This work showed that the uniform corrosion rate of electrically isolated passivated stainless steel in relatively noncorrosive soil (>1000 ohm-cm resistivity) was negligible, and the pitting penetration rates <5 mil/year.

Both pitting and crevice corrosion can be caused by differences in the oxygen concentration between an occluded area and an area that is freely exposed to the bulk environment. In brief, oxygen reduction

occurs on the freely exposed surface (cathodic reaction) and metal dissolution occurs in the occluded region (anodic reaction). Because the electrical currents created by the cathodic and anodic reactions must be equal, a high ratio of the area of the freely exposed surface to the area of the occluded region (e.g., crevice or pit) can cause relatively high corrosion rates in the occluded region. A corroding crevice (or pit) becomes increasingly acidic over time due to the hydrolysis of corrosion products. Pit growth kinetics are generally governed by a cubic rate law. In the absence of chlorides, the pitting of stainless steels is relatively unaffected by the pH of the bulk environment in the range of pH 2.6 to 10.

In addition to pitting, intergranular corrosion and stress corrosion cracking occur in stainless steels that are sensitized. These corrosion modes cause the loss of structural strength of the material with relatively little weight loss.

No studies have been conducted on the corrosion of underground stainless steel in the SWSA-6 area at ORNL. The National Bureau of Standards (NBS), however, released the major study concerning the long-term underground corrosion of metals (Romanoff 1957), and their findings provided the source of corrosion rates used in this report to estimate release rates of radioactive cobalt, iron, and nickel. In the NBS study, 347 stainless steel was not considered. The NBS conducted corrosion tests in many different soil conditions around the country, but none in the east Tennessee area. Based on consultation (Lee 1986), we selected five soils described in the NBS document which resembled the known chloride and sulfate characteristics of the SWSA-6 site and spanned the known pH range of 4.4 to 7.7 at SWSA-6. The conditions selected were: (1) acidic conditions (pH of 4.5 to 5.5, low chloride and low-to-moderate sulfate), and (2) slightly alkaline conditions (pH of 7.5 to 8.0, low chloride and low sulfate). Of the soils that were listed in Table 8 of the PNL 1985 report and were also studied in the corrosion tests described in Table 7 of PNL 1985, we selected the following as representative of the acidic and slightly alkaline conditions which might exist at SWSA-6:

**Acidic Condition:**

Soil No. 58 - Muck, New Orleans, Louisiana

Soil No. 59 - Carlisle Muck, Kalamazoo, Michigan

**Slightly Alkaline Condition:**

Soil No. 65 - China silt loam, Wilmington, California

Soil No. 66 - Mohave fine gravelly loam, Phoenix, Arizona

Soil No. 67 - Cinders, Milwaukee, Wisconsin

The range of corrosion rates for all of the 300 series of stainless steels examined in these soils (Table 7 of PNL 1985) was 0.0007 to 0.01 oz/ft<sup>2</sup> per 14 years ( $1.5 \times 10^{-9}$  to  $2.2 \times 10^{-8}$  kg<sup>-1</sup>cm<sup>-2</sup>year<sup>-1</sup>). These values include the sum of all corrosion mechanisms occurring. These extremes of reported stainless steel corrosion rates were used in calculating the release rates of <sup>55</sup>Fe, <sup>59</sup>Ni, <sup>60</sup>Co, and <sup>63</sup>Ni (Sect. 3.2.6).

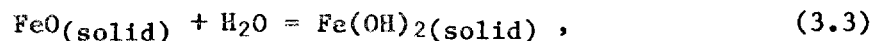
3.2.3.2 Cobalt Alloy. Based upon expert judgment (Griess 1986), we assumed that the corrosion rate of the cobalt alloy parts was the same as for stainless steel. This likely is a conservative assumption.

**3.2.4 Radionuclide Solubility**

The environmentally important radionuclides are present in the emplaced stainless steel parts as either neutron-activated alloy constituents distributed throughout the metal or as neutron-activated atoms of the iron base metal. In considering the solubility of these radionuclides, we have assumed that the solubility of Fe<sup>0</sup> metal atoms is insignificant and that the release of <sup>55</sup>Fe from the emplaced waste into groundwater would occur only after the corrosion reactions of oxidation,

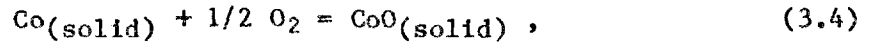


and hydrolysis,

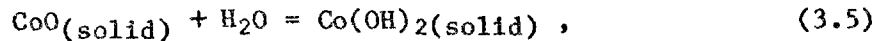


had proceeded to form ferrous hydroxide as the saturating solid phase.

Since the  $^{60}\text{Co}$ ,  $^{59}\text{Ni}$ , and  $^{63}\text{Ni}$  are dispersed throughout the iron matrix, it seems likely that the release of these radionuclides would also be controlled by the bulk metal corrosion rate. In the case of the cobalt alloy bearings, we have similarly assumed that the cobalt and nickel metal atoms have insignificant solubility in groundwater and the release of  $^{60}\text{Co}$  from the waste into groundwater would occur only after oxidation,

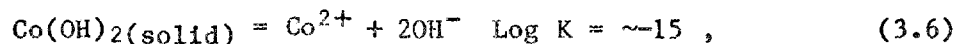


and hydrolysis reactions,

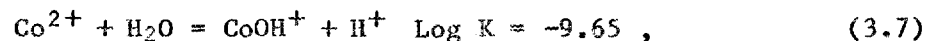


formed cobalt hydroxide as the saturating solid phase. We have also assumed that the nickel component of the journal bearings undergoes similar reactions.

Based on the assumption that the respective hydroxides would be the saturating solid phase, we have calculated the solubility of cobalt, nickel, and iron that might be achieved in the SWSA-6 soil/groundwater system at the measured extreme pH levels of 4.4 and 7.7. Considerable information is available in the literature for these compounds. The following discussion is based on the summary of thermodynamic data given in Baes and Mesmer 1976 for the respective systems,  $\text{M}(\text{OH})_2\text{-H}_2\text{O}$ . At pH 4.4, the oxidation state expected for cobalt in soil/groundwater systems would be Co(II). The dominant Co(II) solution species would be  $\text{Co}^{2+}$ , and the solubility would be high ( $>1$  mol/L). At pH 7.7, the solubility of  $\text{Co}^{2+}$  can be calculated from the solubility product,



and the equation for the first hydrolysis product,  $\text{CoOH}^+$ ,



to get the total concentration of cobalt in solution. (In these calculations, we have assumed that the equilibrium constant,  $K$ , is equivalent to the equilibrium quotient,  $Q$ , because the groundwater solutions have a low ionic strength.) From Eq. (3.6) the  $[\text{Co}^{2+}]$  is calculated to be  $\sim 4 \times 10^{-3}$  mol/L and from Eq. (3.7) the  $[\text{CoOH}^+]$  is calculated to be  $1.1 \times 10^{-5}$  mol/L at pH 7.7; thus, the hydrolyzed species is unimportant. The concentration of  $\text{Co}^{2+}$  is given as  $\sim 4 \times 10^{-3}$  mol/L because  $\text{Co}(\text{OH})_2$  has a number of different physical forms that have different solubility products. Since the form of cobalt hydroxide which might form in the SWSA-6 soil/groundwater system is unknown, we used a median value of the data in Baes and Mesmer 1976 for the log  $K$  of Eq. (3.5). Thus, the cobalt solubility value of  $4 \times 10^{-3}$  mol/L at pH 7.7 may be accurate only to within one or two orders of magnitude. It has been already established that cobalt forms many stable soluble complexes, and the cobalt solubility could be much higher than this value if such complexing ions are present in the SWSA-6 soil/groundwater system.

The solubilization reaction for nickel hydroxide is given in Baes and Mesmer 1976 as



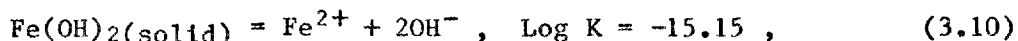
and for the first hydrolysis reaction as



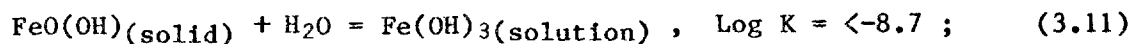
Thus, as with cobalt, the hydrolyzed species is unimportant. At pH 4.4, the solubility of  $\text{Ni}^{2+}$  would be high ( $>1$  mol/L). At pH 7.7, a solubility of  $2.5 \times 10^{-5}$  mol/L is calculated from Eq. (3.8). As with cobalt, nickel can form stable soluble complexes. In an assessment of important radio-nuclides in high-level waste (Kerrisk 1985), the saturating solid phase for Ni(II) was assumed to be  $\text{NiCO}_3$ , and a much higher solubility value of  $1 \times 10^{-2}$  mol/L was calculated at pH 7.2. This three order-of-magnitude difference in calculated nickel solubility illustrates the need to better

establish the composition and geochemical parameters of the groundwater in contact with the waste in SWSA-6 and to determine the saturating solid phase in order to calculate accurate solubility values.

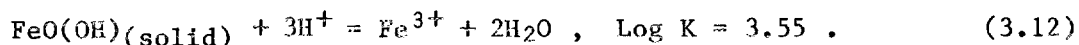
The calculation of iron solubility is more complicated than for cobalt or nickel because either Fe(II) or Fe(III) may be stable in soil/groundwater systems, depending on the redox condition. No Eh measurements had been reported for SWSA-6 groundwater (see Sect. 4.2.2); therefore, the redox condition is unknown. Since Fe(II) compounds are much more soluble than Fe(III) compounds in soil/groundwater systems, we chose a conservative approach to the calculation of iron solubility and assumed that the system was sufficiently reducing to form Fe(II), although we think it is more likely to be oxidizing. This might be a realistic condition at depth in SWSA-6 because the soil is derived from the weathering of shale strata that might contain some pyrite. Near the surface, however, the soil would be less likely to be reducing due to oxidation of the pyrite (if present) during weathering. Baes and Mesmer 1976 give the equation



for the solubility product of ferrous hydroxide. Thus, as for the other transition elements, the solubility would be high (>1 mol/L) at pH 4.4, while at pH 7.7 a lower solubility of  $2.8 \times 10^{-3}$  mol/L was calculated. In an analysis of the planned Central Waste Disposal Facility on West Chestnut Ridge (Pin et al. 1984), a much lower solubility limit of  $1 \times 10^{-13}$  mol/L was given for  $\text{Fe}^{2+}$  as the soluble species. It seems likely that much lower value was calculated, not for Fe(II) but for Fe(III), because Pin et al. 1984 gives the saturating solid phase as  $\text{Fe}_2\text{O}_3$ . If iron is assumed to be present as Fe(III), then data in Baes and Mesmer 1976 indicate the neutral species  $\text{Fe(OH)}_3$  is the dominant solution form of Fe(III) but give only limiting information on the solubilization reaction,



and they estimated the solubility from pH 6.5 to 8.5 at  $\sim 10^{-11.5}$  mol/L. At pH 4.4, an  $\text{Fe}^{3+}$  solubility of  $2.2 \times 10^{-10}$  mol/L can be calculated from the following equation:



Such large calculational differences can easily result from the initial assumptions as to the site geochemistry and only serve as a dramatic illustration of the need to better establish the SWSA-6 geochemical parameters, including groundwater composition, in order to support defensible migration modeling calculations.

These simplified calculations suggest the following conclusion considering the solubility of  $^{55}\text{Fe}$ ,  $^{59}\text{Ni}$ ,  $^{60}\text{Co}$ , or  $^{63}\text{Ni}$  in the SWSA-6 soil/groundwater system: The concentrations of cobalt, nickel, and iron in solution may be controlled by the rate of the corrosion reactions between the groundwater and the metal parts. It seems possible that the oxidation and hydrolysis reactions could proceed so slowly that insufficient  $\text{Co(OH)}_2$ ,  $\text{Ni(OH)}_2$ , or  $\text{Fe(OH)}_2$  could be formed to saturate the groundwater. (Corrosion is discussed in Sect. 3.2.3.) This situation was used in the calculation of release rates.

### 3.2.5 Geometry/Surface Area of Parts

Because of the different geometries of the parts sent to SWSA-6 (Table 3.2), plus the fact that some of these were cut or crushed to fit into the shipping can, we were forced to make simplifying assumptions about the geometries of the emplaced stainless steel and cobalt alloy material in the SWSA-6 auger holes. We assumed that each part was composed of a collection of standard engineering shapes for which the surface area per unit weight is readily calculable. We then estimated the fraction of the total weight of the reactor component which was approximated by each standard shape, and the total specific surface area was determined as the weighted sum of the contributions of each shape. The upper tracks are assumed to be composed of 20% 1/8-in. plates, 50% 1/4-in. plates, and 30% 1/2-in. plates with a weighted specific area of

412 cm<sup>2</sup>/kg. The lower tracks are assumed to be composed of 75% 1/4-in. plates and 25% 1/2-in. plates with a specific area of 343 cm<sup>2</sup>/kg. The bearings were assumed to be right circular cylinders, 3/8 in. tall by 1.19 in. in diameter, with a specific area of 429 cm<sup>2</sup>/kg. The filings were modeled as spherical particles with an arbitrarily assumed size distribution: 30% with 3-mm diam, 40% with 0.3-mm diam, 20% with 0.03-mm diam, and 10% with 0.003-mm diam. The resulting specific surface area for this combination is 284,000 cm<sup>2</sup>/kg. Obviously, the release of radionuclides from corrosion of the filings is a major component of the total release even though the weight of the filings is extremely small.

### 3.2.6 Radionuclide Release Rates

The release rates of the four radionuclides under consideration in the stainless steel and cobalt alloy components were based on the corrosion rate of stainless steel as given by the following equation:

$$R_{i,c} = C_s S_c A_{i,c} e^{-\lambda_i t_c} , \quad (3.13)$$

where

- $R_{i,c}$  = rate of release of isotope i from component c, Ci/year;
- $C_s$  = corrosion rate of stainless steel, kg<sup>-1</sup>cm<sup>-2</sup>year<sup>-1</sup>;
- $S_c$  = specific surface area of the stainless steel component c (from Sect. 3.2.5), cm<sup>2</sup>/kg;
- $A_{i,c}$  = activity of isotope i in component c [from Eq. (3.1)], Ci;
- $\lambda_i$  = 0.693/ $t_{1/2,i}$ ;
- $t_{1/2,i}$  = half-life of isotope i, years;
- $t_c$  = time out of reactor for component c, year.

The total release rate of isotope i is then given by

$$R_i = C_s \sum_c S_c A_{i,c} e^{-\lambda_i t_c} . \quad (3.14)$$

The results of these calculations for the highest, or most conservative, corrosion rate are shown in Fig. 3.1 for the maximum rate of release of the three radioactive isotopes for the next 100 years, beginning June 1, 1986. For lower corrosion rates, the release rates would be proportionally decreased. These calculations are only for the components that are currently emplaced in SWSA-6 as shown in Table 3.2. The components that have been removed from the reactor but have not yet (as of 9/1/86) been sent to burial are not included. Since SWSA-6 is an active LLW disposal site, these calculated release rates could increase as future shipments of waste from HFIR are emplaced in SWSA-6.

There are several simplifying assumptions that were made to facilitate these calculations which introduce some uncertainty into the results. These sources of uncertainty are discussed below.

The method of calculating the inventory in the stainless steel parts of the radioactive components assumed that the entire part was exposed to a uniform thermal neutron flux characteristic of the location of that part as determined by discussions with the operators of HFIR and the design basis flux maps (R. D. Cheverton, 1971). The irradiation time in the reactor of each part was provided by the HFIR operating personnel. Two off-setting errors are introduced in this manner: (1) the contribution to the inventory by the thermal flux is overestimated, since in the actual situation only a small portion of these parts sees the maximum flux; and (2) the contribution to the inventory is underestimated by neglecting the production by the fast flux. The first error is probably larger than the second error, thus this term may be conservative.

The surface area exposed to the groundwater and over which corrosion is assumed to occur was very roughly estimated by assuming that each part (for which the weight was known) was constructed primarily of simple, common engineering shapes (i.e., 1/8-, 1/4-, and 1/2-in. plates, rods, pipes, etc.) and the specific surface area ( $\text{cm}^2/\text{kg}$ ) for the assumed shapes was used. On the average, these dimensions probably underestimate the actual surface area by a small amount. The largest error probably occurs in the estimate of the surface area of the filings. An unknown error also exists in the estimate of the quantity of filings. The quantity

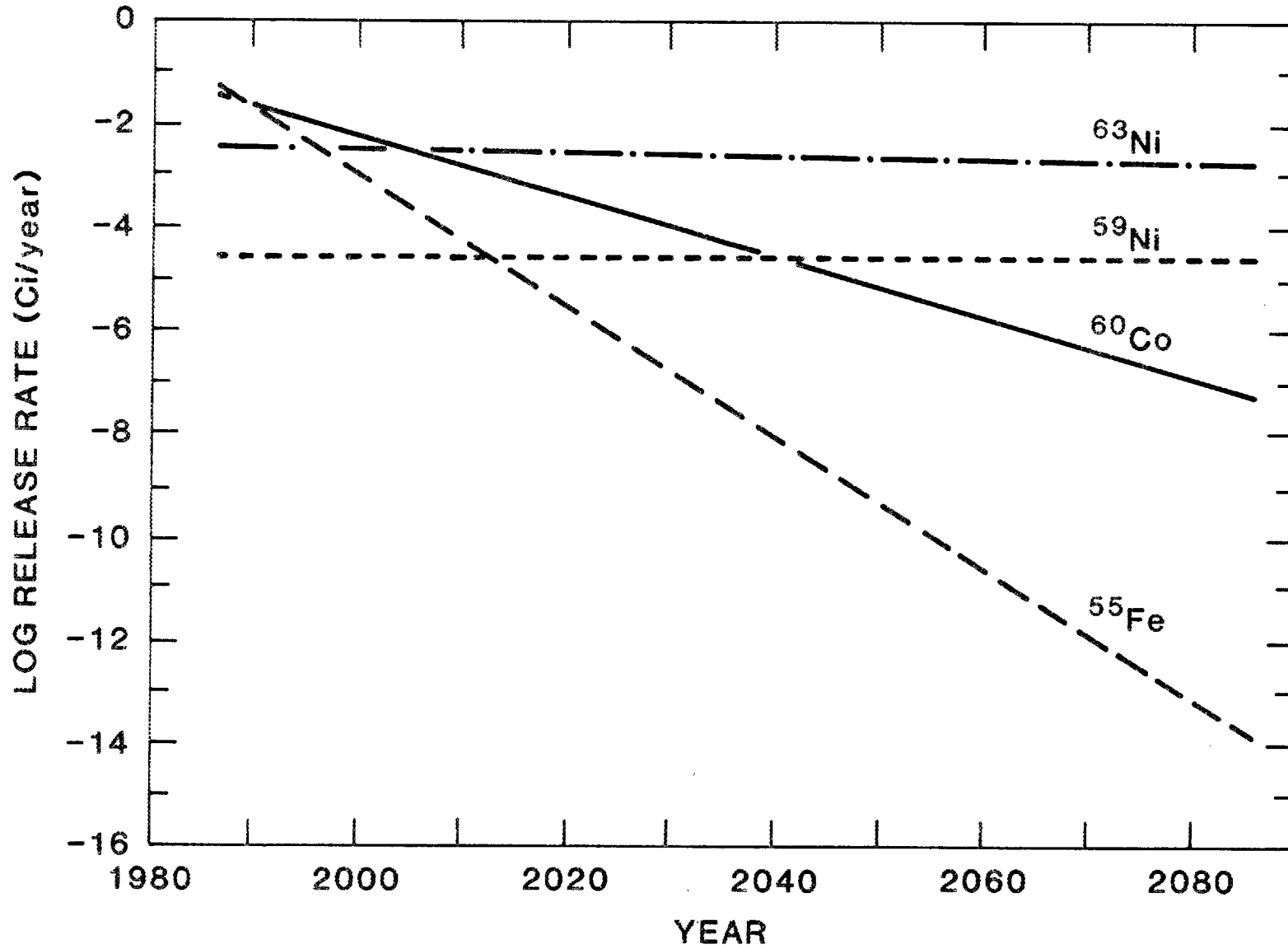


Fig. 3.1. Release rate of cobalt, nickel, and iron radionuclides from HFIR stainless steel and cobalt alloy parts emplaced in SWSA-6.

of filings was estimated from the amount of stainless steel that must be drilled to remove one of the Haynes 25 bearings and the number of bearings which have been removed.

The corrosion rate of stainless steel and cobalt alloy parts in SWSA-6 was estimated as discussed previously (Sect. 3.2.3). A range of corrosion rates was chosen which is likely to span the behavior of stainless steel in SWSA-6. This range varies by a factor of approximately 15. The rates shown in Table 3.1 are based on the maximum corrosion rate. The largest error in the release rate estimates probably resides in the corrosion rate estimate.

### 3.3 CONCLUSIONS AND RECOMMENDATIONS

#### 3.3.1 Predicted Performance of Emplaced Parts

The predicted maximum, or most conservative, near-field release rate of  $^{55}\text{Fe}$ ,  $^{59}\text{Ni}$ ,  $^{60}\text{Co}$ , and  $^{63}\text{Ni}$  from the stainless steel and cobalt alloy HFIR parts known to be emplaced in SWSA-6 is shown in Fig. 3.1 for the next 100 years, starting June 1, 1986. The rate-controlling process was assumed to be the bulk corrosion rate of these metal parts in groundwater, and Fig. 3.1 shows the release rates calculated for the maximum metal corrosion rate estimated for the geochemical conditions in the SWSA-6 soil/groundwater system ( $2.2 \times 10^{-8} \text{ kg}^{-1}\text{cm}^{-2}\text{year}^{-1}$ ). If the actual corrosion rate is different from this value, then the release rates would all be proportionally different. Corrosion and radionuclide release were assumed to be occurring at this time since these parts are directly emplaced in the soil without isolation from groundwater.

The initial release rate is about 0.07 Ci/year, primarily due to  $^{55}\text{Fe}$  and  $^{60}\text{Co}$ . The rate drops to the  $^{63}\text{Ni}$  contribution of about 0.003 Ci/year by about the year 2010 and remains nearly constant after that date. The changeover time in the release rates of the four radionuclides (Fig. 3.1) reflects the half-life of the respective radionuclides. The  $^{55}\text{Fe}$  (half-life of 2.3 years) release rate decreases by about 13 orders of magnitude over 100 years. Therefore, the release rate becomes insignificant. The  $^{60}\text{Co}$  (half-life of 5.27 years) similarly decreases by about 5 orders of

magnitude over this period. The nickel isotopes ( $^{59}\text{Ni}$ , half-life of  $7.6 \times 10^4$  years, and  $^{63}\text{Ni}$ , half-life of 100 years), however, show nearly constant release rates over this period.

The release rates in Fig. 3.1 are maximum-predicted near-field rates in the immediate vicinity of the emplaced parts and, as such, do not represent the amount of activity that could be released to the environment outside the SWSA-6 boundary. Even though values taken from Table 3.1 cannot be used directly to assess potential environmental hazards or evaluate remedial action options, some general observations are pertinent. Because of the relatively short half-lives of  $^{55}\text{Fe}$  and  $^{60}\text{Co}$ , it is possible that far-field sorption in combination with the near-field release rates might confine these radionuclides to the SWSA-6 site for times long enough for radioactive decay to essentially eliminate these radionuclides. The nickel radionuclides, however, present a different situation due to their longer half-lives, particularly  $^{59}\text{Ni}$ . These isotopes would remain radioactive for thousands of years. A more detailed assessment of the mobility of nickel isotopes in SWSA-6 would be needed to explore the long-term behavior of these radionuclides in the soil/groundwater far-field system and the associated environmental impacts.

### 3.3.2 Additional Research/Development Needs

Important uncertainties in predicting the future near-field performance of these parts in SWSA-6 and the concomitant far-field environmental impact associated with this waste are (1) the corrosion rate assumed for the parts (bulk metal corrosion was assumed to be the rate-controlling step for the near-field release rates calculated in this report), (2) the effective surface area, and (3) the subsequent far-field retardation of released radionuclides by sorption processes. The release rate calculated is directly dependent upon the corrosion rate assumed. We used literature values for similar stainless steel alloys (and assumed the Haynes 25 cobalt alloy performed like stainless steel) in similar soil/groundwater systems in the absence of specific information for these alloys in the SWSA-6 soil/groundwater system. The accuracy of the calculated release rates could be improved if more relevant corrosion rate

data were developed. Development of such information could require a long-term study of corrosion of both unirradiated and irradiated metal specimens in SWSA-6 soil/groundwater. Sorption onto site soils frequently is a very favorable site aspect. Laboratory measurement of radionuclide sorption values would be necessary as an initial step to quantify sorption retardation. Some preliminary work has been published (Friedman and Kelmers 1987). Because of the longer half-lives of  $^{59}\text{Ni}$  and  $^{63}\text{Ni}$  compared to the cobalt and iron isotopes, greater attention should possibly be given to the behavior of nickel in the SWSA-6 system than to iron or cobalt for the evaluation of site closure performance.

It also would be desirable to validate the calculated iron, cobalt, and nickel radionuclide content of the discharged wastes. This validation could easily be done by sampling some of these wastes which are currently held in the HFIR pool and obtaining a complete radiochemical analysis.

#### 4. CONTROL CYLINDERS AND PLATES

##### 4.1 CONTROL CYLINDER AND PLATES EMPLACED IN SWSA-6

###### 4.1.1 Description of Control Cylinders and Radionuclides Formed

The construction of the HFIR control cylinders is described in Bowden et al. 1984. The control cylinders occupy an annular region between the outer fuel element and the beryllium reflector in the HFIR. The radius of the outer cylinder is 9.300 in., and the radius of the inner cylinder is 8.921 in. The cylinders are 0.25 in. thick. The control plates, which are composed of a cermet of 31 vol %  $\text{Eu}_2\text{O}_3$  in aluminum metal powder, are in the upper region of the cylinder near the center. The cermet is formed by compaction and sintering at  $590^\circ\text{C}$  in vacuum. The cermet region is 22 in. long by  $3/16$  in. thick and is contained between two  $1/32$ -in. plates of 6061 aluminum. A lower section of the cylinder below the europium cermet region contains 38 vol % tantalum in aluminum. This tantalum section is 5 in. long and is also clad by 6061 aluminum plates. Each cylinder consists of four control plates containing europium and tantalum regions. The aluminum ends of the

cylinders include holes for coolant flow, and extend above and below the europium cermet and tantalum control plate regions. A pair of cylinders (inner and outer) contain 7.6 kg of  $\text{Eu}_2\text{O}_3$  and 3.6 kg of tantalum.

Both the europium cermet control plates and tantalum regions of the control cylinders act as neutron adsorbers and reflectors during HFIR operation. As a result, neutron capture by stable isotopes results in the formation of unstable nuclei. The europium radionuclides of interest after waste emplacement in SWSA-6 are:  $^{152}\text{Eu}$  (half-life, 13.4 years),  $^{154}\text{Eu}$  (half-life, 8.5 years), and  $^{155}\text{Eu}$  (half-life, 4.73 years). These values for the half-lives of these isotopes were taken from Walker et al. 1984. These europium radionuclides account for most of the radioactivity in the control plates after emplacement. A small amount of some gadolinium isotopes is also formed by the decay of the europium isotopes but was not considered in the release calculations. The longest-lived tantalum radionuclide, formed in the tantalum-containing regions of the control plates, is  $^{182}\text{Ta}$  (half-life, 112 d). We have assumed that it decays substantially prior to release events.

#### 4.1.2 Emplacement in SWSA-6

The following description of control cylinder disposal was developed through discussions with HFIR operating staff (Farrar 1986). The control cylinders are replaced after about 80,000 to 100,000 MWD of HFIR operation. The discharged cylinders are stored in the HFIR pool. For shipment to SWSA-6, the aluminum end pieces are cut off and discarded separately; aluminum has no long-lived isotopes, and the neutron-activated aluminum radionuclides decay during the pool storage period. The europium and tantalum control plates may be separated from the cylinder and placed in a sheet metal shipping can, or the intact cylinder may be shipped to SWSA-6 in a sheet metal shipping can. The sheet metal can contains holes in the top and bottom so that pool water will drain as the can is raised from the pool. The shipping can is transported to SWSA-6 in a lead and steel transportation cask. At SWSA-6, the transportation cask is positioned over a prepared auger hole, and the sheet metal can containing the

control plate waste is lowered into the hole. The steel lowering cable is discarded with the can. A description of auger hole emplacement methodology is given in Appendix A.

Eight control plates and two control cylinders — each composed of four control plate sections — were shipped from HFIR for burial from 1970 through 1981. The location of these components was determined as accurately as possible and within the limitations of the early records of the burial ground. Table 4.1 shows the best estimate of the position of each control plate and cylinder, along with date of emplacement, the cumulative irradiation in the reactor, and the date of discharge from the reactor.

All of the control plates (as opposed to the intact control cylinder) are known to be emplaced in lined auger holes Nos. 235, 236, and the unlined auger hole No. 272, located on a knoll of high ground at a point where the water table is about 25 ft below the surface. The location of the control cylinder that has been sent to SWSA-6 is not as precisely identified as the locations of the control plates. Control cylinder No. 5 apparently was emplaced in SWSA-6 on Oct. 24, 1979; however, the location is not available from the surviving records. We assume that it was placed in an unlined auger hole where it is not intercepted by the water table. Control cylinder No. 3 (not included in the SWSA-6 inventory) was sent from the HFIR to the High Radiation Level Examination Laboratory (Bldg. 3525) sometime during 1970, where it was examined to determine the amount and distribution of activation products (Knight 1972). It was sent to burial from Bldg. 3525, presumably in late 1970 or early 1971. Since SWSA-6 was not open at this date, we presume that this control cylinder was not sent to SWSA-6 but was sent to SWSA-5. Thus, we have not considered this control cylinder in our release estimates.

#### 4.2 CALCULATION OF THE RADIONUCLIDE INVENTORY

Estimated radionuclide inventories of the contents of the auger holes that contain the HFIR control plates and cylinder are available from the ORNL Solid Waste Disposal Log (Bolinsky 1986). These inventories were estimated by HFIR personnel at the time of emplacement and

Table 4.1. Discharge of control cylinders from the HFIR and disposal in SWSA-6

<u>SWSA-6 Auger hole</u> No.	<u>Construction</u>	SWSA-6 Emplacement date	Date out of reactor	Cylinder set No.	Irradiation (Mwd)
<u>Control plates<sup>a</sup></u>					
235	Lined	6/05/80	11/70	4-3A	3,764
236	Lined	6/10/80	6/77	4-4A	68,192
			2/75	6-1	54,697
			10/70	8-3	11,409
272	Unlined	2/23/81	12/76	9-1	72,660
			12/76	9-2	72,660
			2/77	9-3	67,886
			12/76	9-4	72,660
<u>Control cylinders<sup>b</sup></u>					
Unknown	Unlined <sup>c</sup>	10/24/79	3/77	5	78,185

<sup>a</sup>These control cylinders were separated into individual plates for disposal.

<sup>b</sup>These control cylinders were disposed intact.

<sup>c</sup>This cylinder was assumed to be in an unlined auger hole in SWSA-6.

represent upper-limit approximations. We reestimated these inventories such that our calculated inventory of control cylinder No. 3 coincided with the measured inventory of that control cylinder as reported by Knight and Richt (Knight and Richt 1972). We feel that our estimates are more accurate than the disposal log since they reproduce the one measured value.

Knight and Richt (1972) analyzed samples from control cylinder No. 3 for the content of  $^{152}\text{Eu}$ ,  $^{154}\text{Eu}$ , and  $^{155}\text{Eu}$  at distances of 0.5, 2, 5, 10, and 20 in. from the high flux edge of the control cylinder. We numerically integrated the reported values [given in atom percent (at. %)] over the 22-in. length of the control cylinder to calculate an average value

for each isotope. Our calculated values were: 3.38 at. %  $^{152}\text{Eu}$ , 2.34 at. %  $^{154}\text{Eu}$ , and 0.81 at. %  $^{155}\text{Eu}$  at the time of discharge from the reactor. Control cylinder No. 3 was exposed to 48,615 MWd or 1.45 full power years, assuming 33,500 MWd per full-power year (Farrar 1986). This control cylinder was discharged from the reactor in January 1970. The isotopic concentrations calculated above correspond to the following activities of the radionuclides at the time of discharge of the control cylinder from the reactor: 9520 Ci  $^{152}\text{Eu}$ , 8510 Ci  $^{154}\text{Eu}$ , and 25,100 Ci  $^{155}\text{Eu}$ .

We extrapolated the activities of the europium isotopes from this one measured value in the following way: The HFIR operating personnel supplied us with the irradiation in MWd for each control plate and cylinder that has been discharged from the reactor. The equations for production and burnup of the five europium isotopes  $^{151}\text{Eu}$  through  $^{155}\text{Eu}$  are

$$\frac{dN_i}{dt} = A_{i-1}N_{i-1} - B_iN_i \quad i = 1, 2, \dots, 5, \text{ corresponding to } ^{151}\text{Eu} \dots ^{155}\text{Eu} \quad (4.1)$$

where

$$N_i = \text{number of atoms of } \underline{i},$$

$$A_0 = 0,$$

$$A_i = \phi \sigma_i \quad i = 1, 2, \dots, 5,$$

$$B_i = A_i + \lambda_i,$$

$$\lambda_i = \ln(2)/t_{1/2,i},$$

$$t_{1/2,i} = \text{half-life of } \underline{i}, \text{ years},$$

$$\phi = \text{neutron flux, neutrons} \cdot \text{cm}^{-2} \cdot \text{s}^{-1},$$

$$\sigma_i = \text{absorption cross section, cm}^2.$$

These equations were initially solved for the conditions at 0.5, 2, 5, 10, and 20 in. from the high flux edge of each plate and cylinder using literature values of  $\sigma_i$  and of  $\lambda_i$  for each of the isotopes (Walker et al. 1984). The value of the flux at each position was adjusted until

the calculated value of the concentration of  $^{151}\text{Eu}$  matched the measured value as given by Knight and Richt 1972. Since, in general, the calculated and measured values of the other isotopes did not agree, the values of the cross sections of each isotope in the B terms were varied successively until each calculated isotope concentration matched the measured concentration at 48,615 MWd irradiation. Literature values of cross section were always used in the A terms, and these values were not varied. Since calculations were done in the time domain, this corresponded to matching calculated and measured values at 1.45 years. When the calculated europium isotope concentrations matched those of Knight and Richt 1972, Eq. (4.1) was solved for the range of irradiation of 0 to 92,000 MWd, spanning the irradiations of all control plates and cylinders to date (16 in all). For each plate and cylinder, the calculated values of the five isotopic concentrations at each location along the control surface were integrated to get an average concentration for each isotope in each plate. The values for the average isotope concentrations were empirically fitted to equations for ease in computer manipulations. These equations are:

$$f_{152} \text{ (at. fraction)} = (3.95 \times 10^{-2}) [1 - \exp(-\text{MWd}/25,000)] \quad (4.2)$$

$$f_{154} \text{ (at. fraction)} = (4.8 \times 10^{-7})(\text{MWd}) \quad (4.3)$$

$$f_{155} \text{ (at. fraction)} = (3.84 \times 10^{-7})(\text{MWd})[1 - \exp(-\text{MWd}/65,000)] \\ - (1.16 \times 10^{-2}[1 - \exp(-\text{MWd}/300,000)] \quad (4.4)$$

and are plotted in Fig. 4.1. The units on the abscissa on Fig. 4.1, however, are in atom percent (at. %) rather than atom fraction.

The calculated europium radionuclide inventory of the control cylinder and plates in SWSA-6 as of June 1, 1986, is given in Table 4.2. The totals are 19,878 Ci of  $^{152}\text{Eu}$ , 21,307 Ci of  $^{154}\text{Eu}$ , and 9,494 Ci of  $^{155}\text{Eu}$ . These values are about one-third of the corresponding values given in Table A.2 of Boegly et al. 1985 for the SWSA-6 auger hole inventory. The

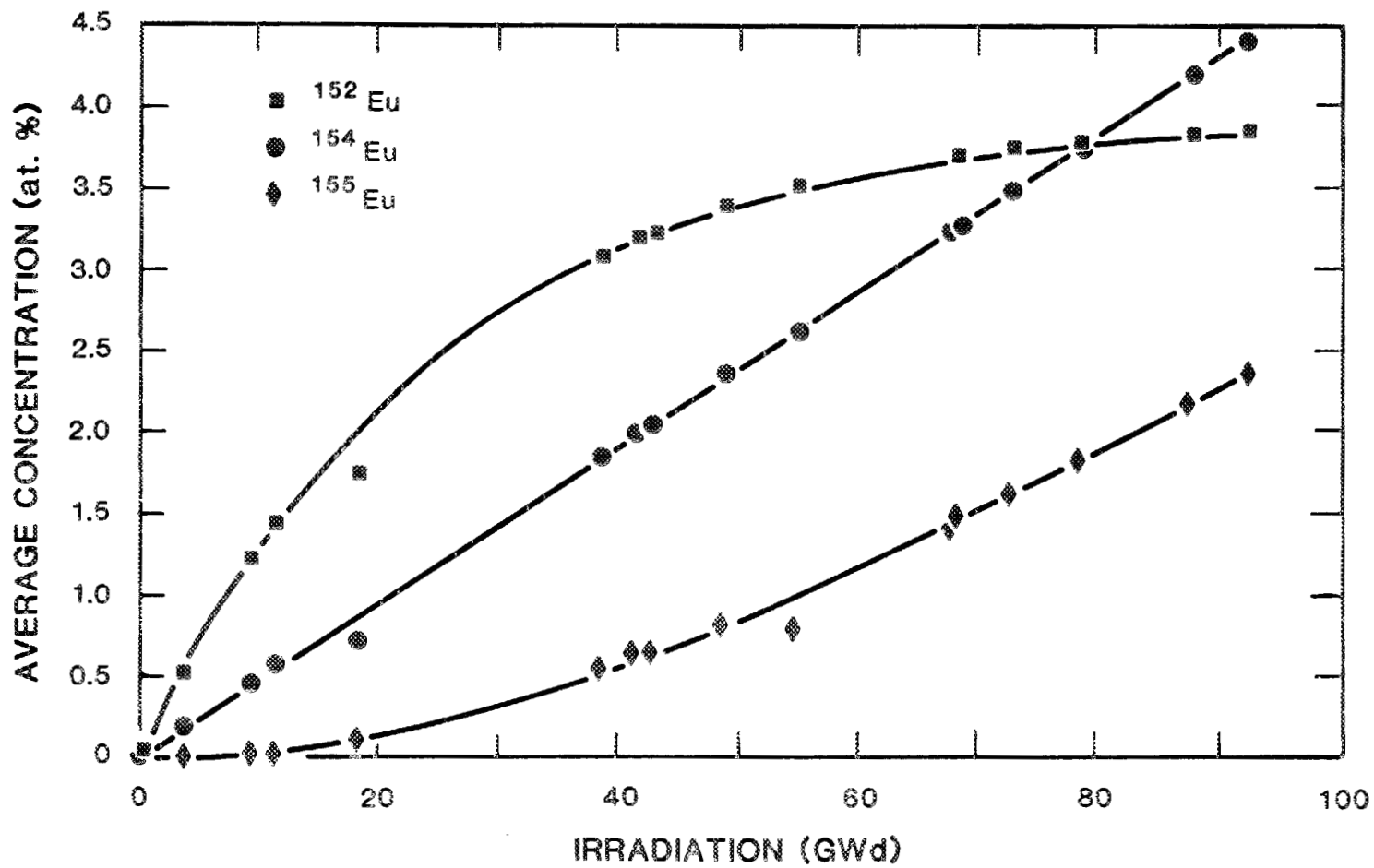


Fig. 4.1. Average europium isotope concentration in HFIR control plates as a function of irradiation.

Table 4.2. Calculated europium isotope inventory of control plates and cylinder in SWSA-6 as of June 1, 1986

Auger hole No.	Cylinder set No.	Total activity (Ci)		
		$^{152}\text{Eu}$	$^{154}\text{Eu}$	$^{155}\text{Eu}$
<u>Control plates</u>				
235	4-3A	207	66.6	2.38
236	4-4A	1,950	2,060	916
	6-1	1,640	1,370	445
	8-3	541	201	6.40
272	9-1	1,920	2,110	946
	9-2	1,920	2,110	946
	9-3	1,910	2,000	866
	9-4	1,920	2,110	946
<u>Control cylinders</u>				
Unknown	5	<u>7,870</u>	<u>9,280</u>	<u>4,420</u>
Totals		19,878	21,307.6	9,493.78

variations in our inventory estimates and the estimates of Boegly and coworkers 1985 can probably be explained by the following: (1) the waste data base that they used does not consider radioactive decay, and (2) their inventory possibly included other sources of europium radionuclides. Considering all the approximations and estimates involved in the summation of either our inventory or that of Boegly et al. 1985, we feel that the values of Boegly et al. 1985 are not inconsistent with our calculations. We feel that our values are more accurate, however, because of our inclusion of a correction for radioactive decay out of reactor.

In the release rate calculations, the inventory values were corrected from June 1, 1986, to the date under consideration. The June 1, 1986, date was selected to give a common reference point for a comparison of these wastes.

### 4.3 WASTE LEACHATE CHEMISTRY AND PARAMETERS USED IN CALCULATIONS

#### 4.3.1 Auger-Hole Liner Corrosion

Literature review revealed little information on corrosion of buried galvanized road culvert pipe. The corrosion would be highly dependent upon the soil pH and the content of chloride and sulfate ions. The records of the burial ground also did not contain information on the specifications to which the liners were purchased. Specifically, there was no information on the thickness of the zinc coating. Because of a lack of information, we arbitrarily modeled the time of failure for the auger-hole liners at 10 years and again at 20 years.

#### 4.3.2 Aluminum Cladding Corrosion

A literature search was conducted and expert opinion solicited (Griess 1986) to identify information that would help describe the rate of corrosion of the HFIR control plates emplaced in SWSA-6. The control plates consist of internal neutron-adsorbing regions formed of an  $\text{Eu}_2\text{O}_3$ -aluminum cermet and a tantalum-aluminum compact which are contained within 6061 aluminum cladding plates (see Sect. 4.1.1). The 6061 aluminum contains 0.4 to 0.8% Si, 0.15 to 0.40% Cu, 0.8 to 1.2% Mg, and 0.15 to 0.35% Cr as alloying elements. The discharged control plates are emplaced in SWSA-6 without rupturing the aluminum cladding surrounding the cermet. We have assumed that the europium radionuclides ( $^{152}\text{Eu}$ ,  $^{154}\text{Eu}$ ,  $^{155}\text{Eu}$ ) in the cermet would not become available for release to groundwater and migration through the SWSA-6 site until after the aluminum cladding plates have been breached by pit or crevice corrosion reactions. Therefore, the rate of corrosion of the aluminum plates under SWSA-6 soil/groundwater geochemical conditions is an important parameter in calculating the europium radioactivity releases that may be associated with the emplaced control plates. We have also assumed that tantalum radionuclides such as  $^{182}\text{Ta}$ , half-life of 112 d, would not be significantly released to groundwater from the tantalum-aluminum compact after aluminum cladding breach because of the chemical stability and corrosion resistance of tantalum metal and have not further considered the release of tantalum radionuclides.

A good general summary of the corrosion of aluminum in aqueous environments is given in Shrier 1977. Based on that discussion and experience at ORNL, it seems reasonable that the most likely failure mode of the aluminum cladding in contact with the wet soil would be pitting corrosion. Shrier 1977 points out that very low levels (fractional ppm) of heavy metals in water, such as copper, produce pits in aluminum alloys. The experience with aluminum in potable water (Gray et al. 1978) and in water-filled beam tubes in the Oak Ridge Linear Accelerator (Griess and Neumann 1968) illustrate the susceptibility of aluminum to pitting in stagnant water. The composition of the aluminum alloy appears to be of only minor importance with regard to pitting in water.

A few laboratory tests with small specimens were run to simulate the corrosion of defected control plates (English and Griess 1965). In 1965, a gadolinium-samarium-europium oxide mixture with aluminum was under consideration for the neutron-adsorber material, so the test results may not be directly representative of the corrosion behavior of the  $\text{Eu}_2\text{O}_3$ -aluminum regions of the current HFIR control plates. In these accelerated tests, appreciable reaction occurred between water and the rare-earth material. Severe exfoliation occurred along edges of contact between the rare-earth material and water for sheared specimens, and blisters developed in samples defected by drilling holes through the aluminum cladding. In an extreme case, an aluminum-clad, rare-earth compact split after 100 h exposure to pH 5.0 water at 100°C. It appeared that the water had reacted with the rare-earth oxides to form a larger-volume product, probably a hydrated oxide or hydroxide, which forced the cladding plates apart.

The available information describing control plate corrosion under conditions representative of the SWSA-6 soil/groundwater system is extremely limited and allows consideration of only a conjectural model of control plate corrosion after failure of the auger-hole liner and the subsequent intrusion of groundwater. The following sequential events may occur:

- Event 1 - The discharged control plates, minus the aluminum end pieces that have been removed, are placed in the auger hole in a mild steel shipping can that has holes in the lid and bottom. The auger hole is filled with sand or

soil. No release of europium radionuclides occurs as long as the aluminum cladding has not been ruptured during the disposal operations.

- Event 2 - The auger-hole liner (when present) fails, and groundwater enters the shipping can through the holes in the lid and bottom of the can. The control plates are now in a wet soil/groundwater system at a pH between 4.4 and 7.7 (the pH extremes reported for SWSA-6 soil/groundwater systems; see Sect. 2.4.1), and are in contact with the mild steel can. Corrosion of the aluminum cladding begins, but no release of europium radionuclides occurs since the cladding has not been breached.
- Event 3 - Pitting corrosion continues until small breaches occur in the aluminum cladding, and groundwater contacts a small area of the  $\text{Eu}_2\text{O}_3$ -aluminum cermet. Some of the  $\text{Eu}_2\text{O}_3$  hydrolyzes, and some soluble europium is formed. A small amount of the europium diffuses through the breaches and is available for migration with groundwater through the site.
- Event 4 - Pitting and crevice corrosion of the aluminum cladding continue. More groundwater contacts a greater volume of the europium cermet. More of the  $\text{Eu}_2\text{O}_3$  hydrolyzes to form larger-volume products [possibly  $\text{Eu}(\text{OH})_3$ ] which expand and cause extensive rupturing of the aluminum cladding. Now, extensive contact between the  $\text{Eu}_2\text{O}_3$  and groundwater occurs. More europium dissolves, and more europium becomes available for migration with groundwater through the site. The concentration of europium may be controlled by the solubility product for  $\text{Eu}_2\text{O}_3$  or  $\text{Eu}(\text{OH})_3$ . The hydrolysis and dissolution reactions continue until all the europium radionuclides have been leached from the control plate wastes and discharged to the site soil/groundwater system.

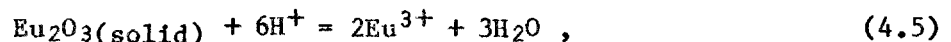
The existing information is inadequate to allow accurate prediction of times for this conjectural series of corrosion steps. The evolution of events might take a number of months or years. Laboratory research would be required to identify and to quantify the rates of the various corrosion reactions involved. Since discharged control plates have accumulated a significant neutron and thermal exposure, they could perform differently in the soil/groundwater environment than unirradiated control plates. It might be necessary to conduct corrosion experiments

with samples of irradiated control plates in order to develop defensive corrosion rate data. If so, such research would need to be conducted in hot cells for radiation shielding. Such work could represent an appreciable effort.

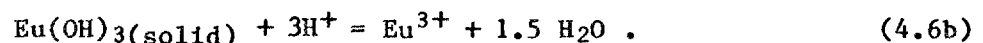
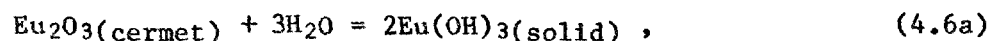
For our modeling calculations, we arbitrarily modeled the cladding failure at 2 and again at 4 years after the failure of the auger-hole liner. These values were chosen since it seemed unrealistically conservative to assume instantaneous failure of the cladding on contact with groundwater. On the other hand, there is no evidence that exists to suggest that the cladding might remain intact for periods of time as long as decades.

#### 4.3.3 Rate of Reaction of Cermet with Groundwater

The europium radionuclides are contained in a unique europium oxide-aluminum metal cermet. Apparently no studies of the reactions that may occur between this cermet and water have been performed, thus we can not predict the rate of reaction after the cement is contacted with groundwater or, with certainty, even the compounds which might be formed. In the absence of other evidence, we have assumed that the europium oxide portion of the cermet would react to yield the same products as pure europium oxide. Therefore, we were forced to assume that europium oxide ( $\text{Eu}_2\text{O}_3$ ) chemistry would describe the behavior of the control plate cermet. We considered both direct solubilization of the europium oxide



and hydrolysis of the cermet by groundwater at the time of cladding breach to form high surface area  $\text{Eu}(\text{OH})_3$  and subsequent solubilization.



Of the two, the hydrolysis reaction may be the more likely, based on the observation of English and Griess 1965 that the rare-earth oxide portion of defected control plate specimens showed swelling and exfoliation.

In the absence of any reaction rate information, we were unable to take any credit for the reaction rate of the cermet with groundwater.

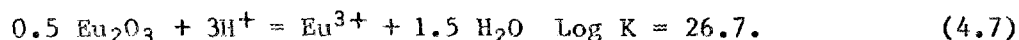
#### 4.3.4 Time of Initial Radioactivity Release

The time of initial radioactivity release depends upon (1) the length of time for the aluminum cladding in the unlined auger holes to fail, (2) the length of time for the galvanized steel pipe liners in the lined holes to fail, and (3) the length of time for the aluminum cladding in the lined holes to fail. No credit was taken for the reaction time of the cermet with groundwater. We examined two cases to show the effect of time to failure of the two types of barriers. The first case assumes a life of 10 years for the galvanized pipe and a life of 2 years for the aluminum cladding following first exposure to groundwater, or an initial release time of 12 years after emplacement. The second case assumes a life for the galvanized liners of 20 years and a life for the aluminum cladding of 4 years, resulting in an initial release time of 24 years after emplacement. It should be understood that the actual time these two barriers fail is highly uncertain in the absence of data in SWSA-6. As discussed, the time to failure of these barriers depends upon many factors including the soil pH, dissolved ions, oxidation potential, radiolysis effects, etc. Even though it would be more conservative to assume that the time of barrier failure is zero years (i.e., immediately after emplacement), we felt that such an approach would be overly conservative and fail to take credit for a reasonable life of the galvanized steel auger hole liners and the aluminum cladding. Clearly, better information on this subject would be needed to allow estimation of a more accurate time of initial release.

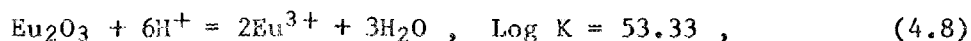
#### 4.3.5 Radionuclide Solubility

A literature search for information on the system  $\text{Eu}_2\text{O}_3\text{-H}_2\text{O}$  was conducted, but very little information relevant to europium(III) chemistry under typical groundwater geochemical parameters was identified. Under the range of soil/groundwater acidity conditions reported for SWSA-6, pH 4.4 to 7.7 (see Sect. 2.4.1), neither the equilibrium europium solid phase(s) nor the europium solution species have been characterized experimentally.

A previously published calculation of Eu(III) solubility in more alkaline carbonate groundwaters at a pH of 8 (Early et al. 1982) was based on data for the  $\text{Eu}_2\text{O}_3$  solubilization reaction:



Early et al. 1982 referenced the source of that equilibrium constant as Benson and Teague 1980, which is a compilation of thermodynamic data for many elements common to radioactive waste systems. Most of the data in Benson and Teague 1980 are referenced to the original literature source that they used. However, they state that some of the data have been obtained by estimation or extrapolation where published information was not available. The  $\text{Eu}_2\text{O}_3$  solubilization reaction given in Benson and Teague 1980,

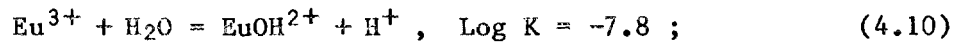


was unreferenced. Thus, it seems likely that this reaction for the solubilization of  $\text{Eu}_2\text{O}_3$  was obtained by some sort of estimation; Benson and Teague 1980 did not discuss this reaction in the text of their report.

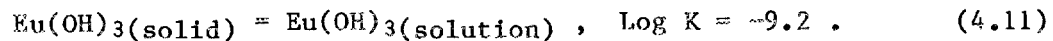
Data have been published (Baes and Mesmer 1976) for the solubilization reaction for europium hydroxide:



(In these calculations, we have assumed that the equilibrium constant,  $K$ , is equivalent to the equilibrium quotient,  $Q$ , because the groundwaters have low ionic strength.) This equilibrium constant was estimated (Baes and Mesmer 1976) by a comparison of the hydroxide crystal  $\alpha$  parameters and hydroxide solubility constants for the lanthanide-group elements. Apparently, Baes and Mesmer 1976 were unable to locate specific hydroxide solubility constant data for europium(III). Baes and Mesmer 1976 also report constants for the first hydrolysis reaction of  $\text{Eu}^{3+}$  as



and, for the solubility of the neutral hydroxide species, as



The log  $K$  value for Eq. (4.10) apparently was derived from a correlation of the formation quotients vs the quantity of the lanthanides, but the log  $K$  value for Eq. (4.11) was derived from "smoothed" data for hydrolysis reactions. All of the pertinent europium thermochemical values in Baes and Mesmer 1976 appear to have been derived through extrapolation and lanthanide group element similitude rather than experimental measurement.

Since the solubilization reactions for either the oxide,  $\text{Eu}_2\text{O}_3$  [Eq. (4.5)], or the hydroxide,  $\text{Eu}(\text{OH})_3$  [Eq. (4.6b)], are dependent upon the third power of the hydrogen ion concentration,

$$\frac{[\text{Eu}^{3+}]}{[\text{H}^+]^3} = 10^{17.5} \text{ or } 10^{26.7} , \quad (4.12)$$

the  $\text{Eu}^{3+}$ -saturated solution concentration calculated from these reactions is very sensitive to the solution pH used in the calculation. Thus, using the log  $K$  value for either of these reactions, europium is calculated to be very soluble at pH 4.4. In fact, the values obtained for  $[\text{Eu}^{3+}]$  are so large as to be meaningless. It is possible that neither  $\text{Eu}_2\text{O}_3$  or  $\text{Eu}(\text{OH})_3$  are the the correct equilibrium solid phase under pH 4.4

geochemical conditions. A hydrated oxide, or possibly a silicate or some other compound might be the appropriate stable solid phase. At pH 4.4, the  $[\text{EuOH}^{2+}]$  concentration would be insignificant. From Eq. (4.10), the  $[\text{EuOH}^{2+}]$  would be only  $10^{-3.4}$  of the  $[\text{Eu}^{3+}]$  concentration (i.e., hydrolysis is not important at low pH). Since Eq. (4.11) is independent of pH, the concentration of the neutral species  $\text{Eu}(\text{OH})_3(\text{solution})$  would be only  $10^{-9.2}$  M, and this value would be meaningful only if the hydroxide is stable at pH 4.4. It appears that only the species  $\text{Eu}^{3+}$  is important in considering europium solubility at pH 4.4, and that the saturated solution concentration of this species could be high, but an accurate value cannot be calculated because of the inadequacy of the supporting thermochemical data.

Much lower europium solubilities are calculated at pH 7.7 using Eqs. (4.7) and (4.9) and their equilibrium constants. For  $\text{Eu}_2\text{O}_3$ , the calculated  $[\text{Eu}^{3+}]$  is  $10^{3.6}$  M at pH 7.7. However, this solubility value is still much too large to be meaningful or acceptable. It is not consistent with qualitative observations of low europium solubility in neutral or slightly alkaline groundwater solutions (Meyer 1986). Hydrolysis and precipitation of acidic solutions of europium salts usually can be observed to begin at about pH 5 to 6, and solubility decreases further at higher pHs. For  $\text{Eu}(\text{OH})_3$ , the calculated  $[\text{Eu}^{3+}]$  is  $10^{-5.6}$  M at pH 7.7. The ratio of  $[\text{EuOH}^{2+}]/[\text{Eu}^{3+}]$  calculated from Eq. (4.10) is  $10^{-0.1}$ . An additional europium solubility of  $10^{-9.2}$  M is contributed by  $\text{Eu}(\text{OH})_3(\text{solution})$ . Thus, at pH 7.7 the total europium saturated solution concentration calculated from the available data for the species  $\text{Eu}^{3+} + \text{EuOH}^{2+} + \text{Eu}(\text{OH})_3(\text{solution})$  is about  $5 \times 10^{-6}$  M. This value, at least, is not inconsistent with qualitative observations of low europium solubility in neutral or slightly alkaline solutions. Considering the very poor quality of the supporting thermochemical data, however, the value of  $5 \times 10^{-6}$  M could easily be in error by several orders of magnitude.

One experimental measurement of europium solubility was identified (Ral and Serne 1978). Their plot of europium activity vs pH (Fig. 4.2) shows a strong dependence on pH. We have assumed that activity may be taken as equivalent to concentration for the low europium concentrations

ORNL DWG 86-015

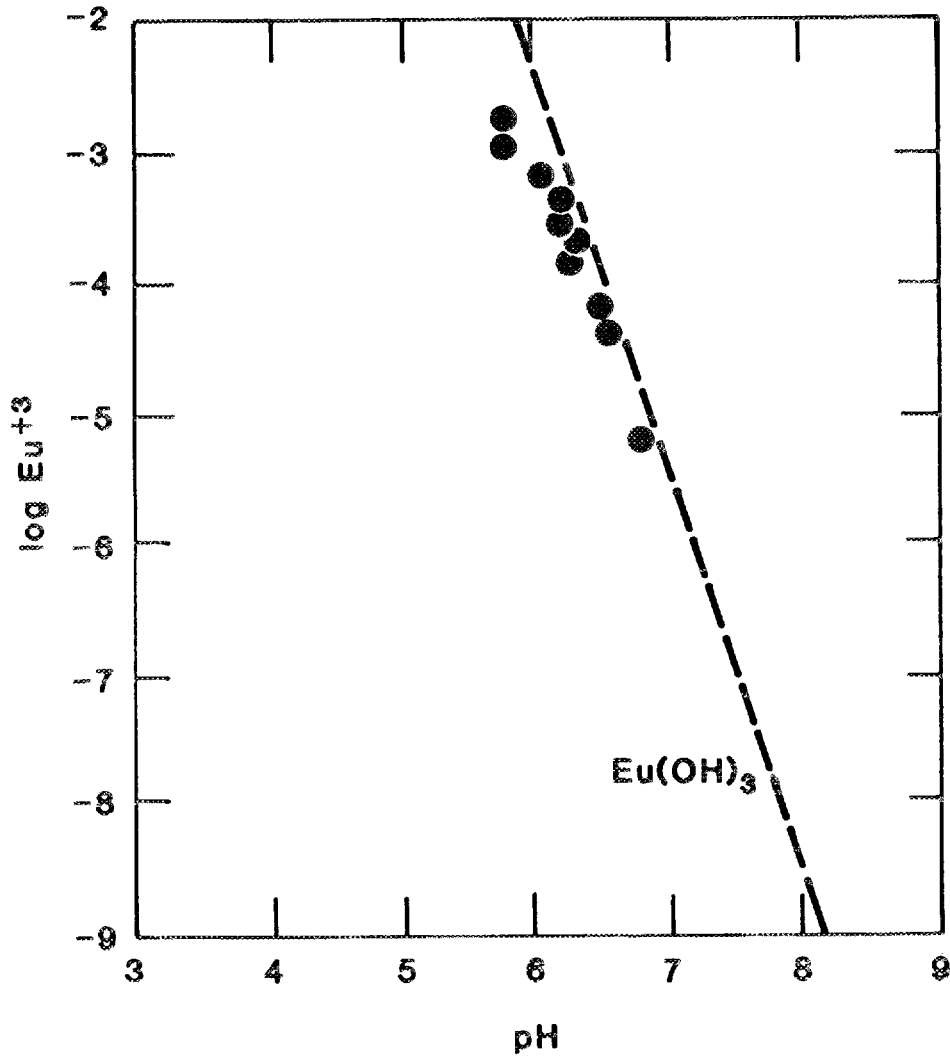


Fig. 4.2. The influence of pH on the activity of europium in solution (Fig. 14 of Serne and Rai 1976).

and low ionic strength of the supporting solution. Thus, by extrapolating the data in the figure to pH 7.7, the solubility of  $\text{Eu}^{3+}$  would be between  $10^{-7}$  and  $10^{-8}$  mol/L. At lower pHs the solubility increases rapidly and at the lowest pH experimentally measured, pH 5.5, the plotted solubility is between  $10^{-2}$  and  $10^{-3}$  mol/L. At pH 4.4 the extrapolated saturated solution line would be off the top of the graph.

We then compared these literature europium solubility values with practical laboratory experience at ORNL. Generally, europium solubility is known to decrease with increasing pH. In one brief qualitative experiment, a europium nitrate solution was added to SWSA-6 well water at pH 7.3 (Friedman 1986). At an  $\text{Eu}^{3+}$  concentration of  $10^{-3}$  mol/L, a visible precipitate formed immediately. At  $10^{-5}$  mol/L or lower concentrations, no precipitate formed. In ongoing work in the ORNL Chemistry Division to study europium chemistry in groundwater relevant to a candidate high-level waste repository at Yucca Mountain, Nevada (Meyer 1986), the chemistry of europium at near-neutral pH has proven to be complex. When this groundwater was brought to a concentration of  $10^{-4}$  mol/L  $\text{Eu}^{3+}$ , no precipitate was seen. However, slow reactions occurred over a period of months which gradually decreased the apparent solution concentration of europium to less than  $10^{-4}$  mol/L without the appearance of a visible precipitate. The nature of these reactions is currently unknown.

For the calculation of the release of europium radionuclides from the planned Central Waste Disposal Facility at West Chestnut Ridge, Pin et al. 1984 used a value of  $1 \times 10^{-4}$  mol/L for the solubility of  $\text{Eu}^{3+}$  at pH 6.9. That value was obtained from a calculation of the solubility limit using the computer code PHREEQE assuming  $\text{Eu}(\text{OH})_3$  to be the saturating solid phase. Computer codes such as PHREEQE require thermodynamic data as input information, and it seems likely that the calculation used estimated or extrapolated values for  $\text{Eu}(\text{OH})_3$  (possibly the estimated data for  $\text{Eu}(\text{OH})_3$  from Baes and Mesmer 1976) since no other thermodynamic data seem to be available.

Even though the europium solubility information available is very limited in scope and of uncertain accuracy, it does suggest the following for consideration in estimating europium solubility in SWSA-6 groundwater:

1. The calculated europium saturated solution concentration will be very sensitive to the solution pH used in the calculation, regardless of the specific thermodynamic value employed. Similarly, measured europium solubility values were highly dependent upon the experimental pH. Therefore, knowledge of the near-field groundwater pH in the immediate vicinity of the disposed control plates is essential for a defensible calculation of europium solubility and, then, release rates. At the present time, the groundwater pH at SWSA-6 is not well known (see Sect. 2.4.1) and can only be bracketed by the range of measured values of pH 4.4 to 7.7. Better characterization of pH of SWSA-6 soil/groundwater system(s) will be needed to improve the accuracy of europium solubility and release rate calculations for SWSA-6.
2. If the near-field SWSA-6 groundwater is as acidic as pH 4 to 5 (values typical of shale-derived soils), then europium released from the control plates could be relatively soluble. The available thermodynamic data (or experimental information) are insufficient to allow quantification of the term "relatively soluble." Laboratory research would be required to characterize the  $\text{Eu}_2\text{O}_3\text{-H}_2\text{O}$  system in this pH range and measure appropriate thermodynamic constants. Such an investigation could represent an appreciable effort.
3. If the near-field SWSA-6 groundwater system is neutral to slightly alkaline (pH of 7 to 8), then europium released from the control plates could be relatively insoluble. Again, the the available thermodynamic data (or experimental information) are inadequate to allow accurate quantification of "relatively insoluble". In order to better quantify the europium solubility and release rates, an appreciable laboratory research effort would be required to characterize the system  $\text{Eu}_2\text{O}_3\text{-H}_2\text{O}$  in this pH range and measure appropriate thermodynamic constants.

After considering the uncertainty associated with the sparse information available for the selection of europium solubility values for use in the release rate calculations, we elected to use  $10^{-4}$  and  $10^{-6}$  mol/L because it seemed possible that the europium solubility under conditions which may exist in the SWSA-6 auger holes might be bracketed by these solubility values. The higher solubility value could typically result from low pH, radiolysis effects, and/or presence of complexing anions (such as  $F^-$ ) or complexing organics (such as EDTA). The lower solubility value could be indicative of (1) higher pH conditions, and (2) the absence of radiolysis effects or complexing reagents.

#### 4.3.6 Radionuclide Diffusivity

A search of Chemical Abstracts identified only one reference that gave values for the diffusion coefficient of the  $Eu^{3+}$  ion in aqueous solutions. Horowitz and Bloomquist 1972 reported values for the self-diffusion coefficient of Eu(III) in dilute nitric acid solutions at various temperatures. The self-diffusion coefficient is equivalent to the diffusion coefficient at infinite dilution, so we accepted the reported value of the self-diffusion coefficient at infinite dilution at 25°C for use in the calculation of europium diffusion through the boundary layer. The value in that reference was given as  $(1.24 \pm 4) \times 10^{-5}$  cm<sup>2</sup>/s. Since the reported error was larger than the first significant figure of the value, we chose to round it to  $1 \times 10^{-5}$  cm<sup>2</sup>/s. This reported value is consistent with other tabulated values of the diffusion coefficients for strong electrolytes at dilute concentrations (Table F-62 of CRC 1976-1977), which range from 1.3 to  $1.9 \times 10^{-5}$  cm<sup>2</sup>/s at 25°C. The diffusivity of  $Eu^{3+}$  in the boundary layer was taken as  $1 \times 10^{-5}$  cm<sup>2</sup>/s in the calculations.

#### 4.4 MODELS FOR ESTIMATING RELEASE OF EUROPIUM RADIONUCLIDES

HFIR control plates and a cylinder were placed in both lined and unlined holes in SWSA-6. The wastes in the unlined auger holes were assumed to be directly in contact with infiltrating rainwater because the shipping can has holes in the top and bottom. The wastes were

assumed to be contacted with a volume of water equivalent to the net infiltration rate (13.75 in./year) times the cross-sectional area of the auger hole (1735 in.<sup>2</sup>), and the release rate-limiting step was assumed to be the saturation of this volume of groundwater by europium. We envisioned two possible release modes for the wastes in the lined auger holes. In one case, we assumed that the concrete end plugs, and possibly also the steel liner, underwent massive failure. Thus, for this case, the wastes in the lined auger holes would experience a groundwater-contact situation similar to the wastes in unlined auger holes, and the release of radionuclides was similarly modeled by assuming saturation as the rate-limiting step. We also envisioned a situation where the auger-hole end plugs would remain intact, but the liner would corrode and develop a limited number of small breaches which would allow groundwater to enter and saturate or flood the interior of the liner. For this case, we assumed the wastes were standing in stagnant groundwater and that diffusion of radionuclides into the boundary layer would be the release rate-limiting step. The calculation of the release of europium radionuclides from these two modes of groundwater contact will require separate models. The following sections describe the models utilized to estimate release from each type of emplacement.

#### 4.4.1 Diffusion-Limited Release Model

As discussed in the previous sections, we assume that the europium radionuclides are not released into the soil/groundwater system until the galvanized steel liner in the disposal well and the aluminum cladding on the control plates and cylinders both fail due to corrosion. We assume that when the galvanized pipe fails, water will fill the pipe. This influx of water will cause (1) the aluminum cladding to fail, and (2) the europium to dissolve and saturate the water inside the pipe. We assume that the pipe does not completely disintegrate, but maintains its shape and prevents europium transport by convection. That is, we assume that the water enters the pipe upon failure; however, because the water flux is vertical and parallel to the pipe walls and is prevented from intersecting the pipe contents by the concrete plug on top and bottom of the

pipe, the dissolved europium species saturating the water inside the pipe are transported only by molecular diffusion in the direction perpendicular to the pipe and are convected away by the vertical water flux once the europium species diffuse from the vicinity of the pipe wall. The situation is diagrammed in Fig. 4.3.

An approximate solution for the molar flux of europium diffusing from the perforated pipe into the downward flow of water around the pipe is given in the following equation:

$$N_i = \pi R_o^2 U C_i f_i \left(\frac{\zeta}{\zeta-1}\right)^2 \left(\zeta^4/2 - 4\zeta^3/3 + \zeta^2 - 1/6\right), \quad (4.13a)$$

$$\zeta = 1.55 \left(\frac{\epsilon \mathcal{D} L}{R_o^2 U}\right)^{0.4} + 1, \quad (4.13b)$$

where

$N_i$  = molar rate of diffusion of europium isotope i from the pipe wall into the water flowing through the soil, g-mol/s;

$\mathcal{D}$  = the molecular diffusivity of europium, cm<sup>2</sup>/s;

$\epsilon$  = porosity of the soil, dimensionless;

$C_i$  = saturation concentration of europium inside the pipe, g-mol/cm<sup>3</sup>;

$R_o$  = radius of the pipe, cm;

$L$  = length of the pipe, cm;

$U$  = darcy velocity of water in vertical direction, numerically equal to that portion of rainfall which penetrates the ground, cm/s;

$f_i$  = relative abundance of europium isotope i (dimensionless fraction).

This equation is derived in Appendix B. Table 4.3 shows values for relative abundance,  $f_i$ , in each hole in SWSA-6 as of June 1, 1986. These values were calculated from information found in Sect. 4.2.

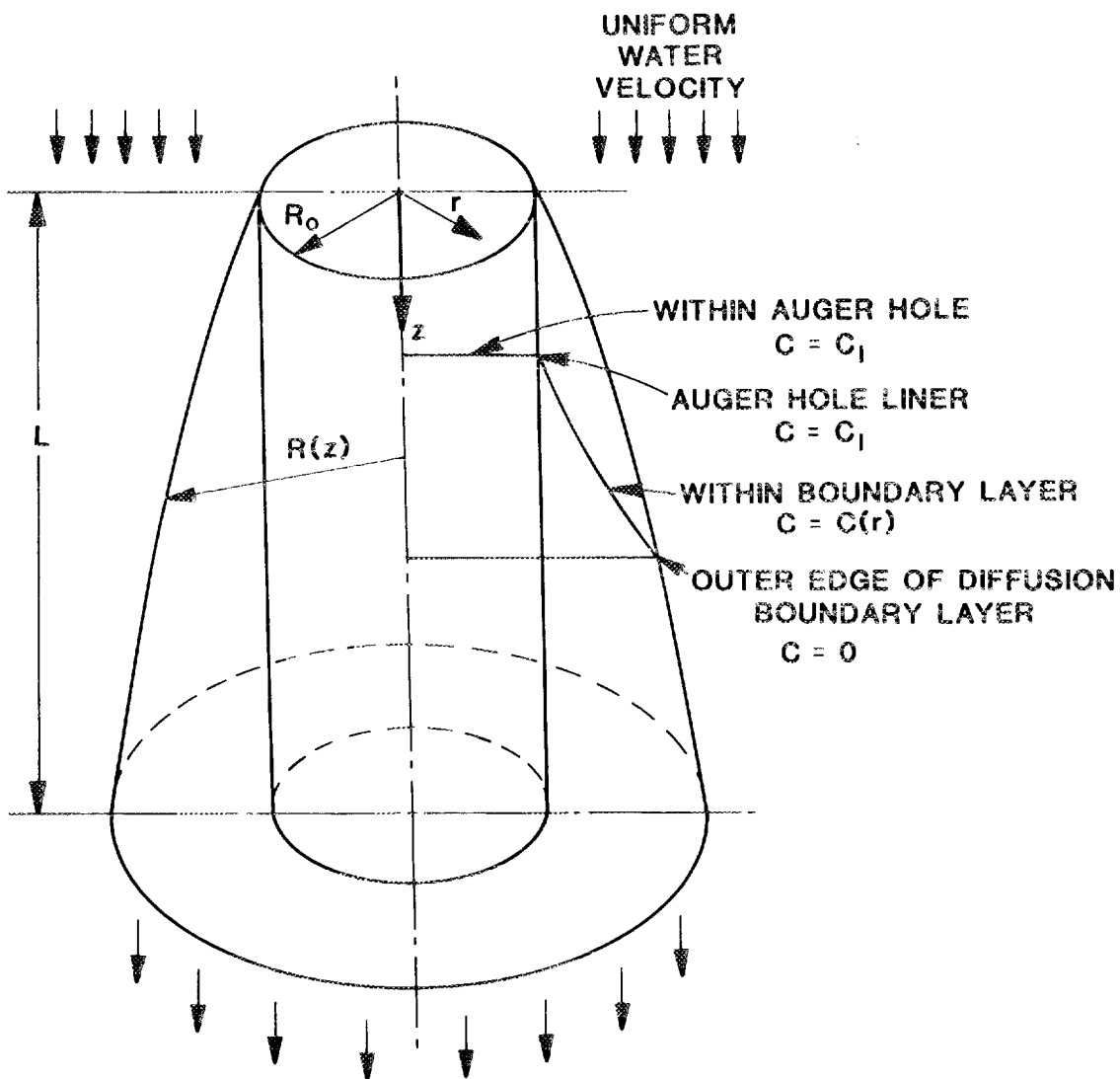


Fig. 4.3. Conceptual model for diffusion of europium from lined auger holes.

Table 4.3. Average europium isotope concentrations  
in SWSA-6 auger holes as of June 1, 1986

Auger hole No.	Average concentration (at. %)		
	<sup>152</sup> Eu	<sup>154</sup> Eu	<sup>155</sup> Eu
235	0.25	0.05	1.02E-03
236	1.64	0.93	1.95E-01
272	2.29	1.59	3.97E-01
Unknown	2.34	1.77	4.73E-01

#### 4.4.2 Saturation-Limited Release Model

For modeling the release from the unlined auger holes or from lined auger holes after massive liner failure, we assume that europium radionuclides are not released until the aluminum cladding on the control plates and cylinders fail. This event is assumed to be 2 or 4 years after emplacement. After failure of the cladding, the rate of release of each isotope is assumed to be given by the product of the europium solubility in the groundwater, the relative abundance of the isotope under consideration, the flux of water, and the cross section of the hole in which the plates have been buried. The diameter of the unlined holes is assumed to be 47 in. The equation for the release rate is

$$N_i = \pi R_o^2 U C_{I_i} f_i, \quad (4.14)$$

where the definition of the variables are the same as for Eq. [4.13(a)(b)]

### 4.5 RELEASE RATES OF EUROPIUM RADIONUCLIDES

#### 4.5.1 Mixed Release Rate-Limiting Modes

The more conservative europium release situation involves a mixture of release rate-limiting modes, and we chose to model that situation first. For this case, the release of radioactivity from wastes in the unlined auger hole (see Table 4.3) was assumed to be controlled by the solubility (saturated solution concentration) of  $\text{Eu}^{3+}$  ions in the

infiltrating groundwater, and the release rates were calculated as described in Sect. 4.4.2. The release of radioactivity from the wastes in the lined auger holes was assumed to be controlled by the diffusion of  $\text{Eu}^{3+}$  ions through the boundary layer, and the release rates were calculated as described in Sect. 4.4.1. A base-case situation was selected, and then the sensitivity of the calculated release rates to changes in some of the input values was explored. The base case assumed the following: the liner (when present) fails 10 years after emplacement, the aluminum cladding fails after 2 years of exposure to groundwater (thus, 12 years after emplacement for the lined auger holes), and the europium solubility is  $10^{-6}$  mol/L. The release rates of europium radio-nuclides for 50 years after emplacement are shown in Fig. 4.4. The wastes in the unlined hole begin to release activity in 1982, while release from the wastes in the lined holes is delayed until 1992. The peak release occurs about 1995 and is about 5.3 Ci/year total for  $^{152,154,155}\text{Eu}$ . Because the calculated release rates are directly proportional to the value used for the  $\text{Eu}^{3+}$  solubility, the rates are 2 orders-of-magnitude greater (Fig. 4.5) if the solubility is assumed to be  $10^{-4}$  mol/L. Thus, for this case, the maximum release rate in about 1992 is ~420 Ci/year for  $^{152,154,155}\text{Eu}$ . If, on the other hand, the time of release is delayed by assuming that the liner remains intact for 20 years and the aluminum cladding failure is at 4 years (total of 24 years for the lined holes), then much lower release rates are calculated because of the continuing decay of the radioactive isotopes during the isolation (prerelease) period. As shown in Fig. 4.6, now the two release-rate peaks are delayed to about 1987 and 2006, and the total release rates are only 2.2 and 1.8 Ci/year, respectively.

#### 4.5.2 Single Release Rate-Limiting Mode

It is possible that the release of radioactivity from wastes in both the unlined and lined auger holes could be controlled by the solubility of europium in the intruding groundwater, as discussed in Sect. 4.4, and we have also modeled this situation as described in Sect. 4.4.2. It also was of interest to model this situation as a check on the release rates

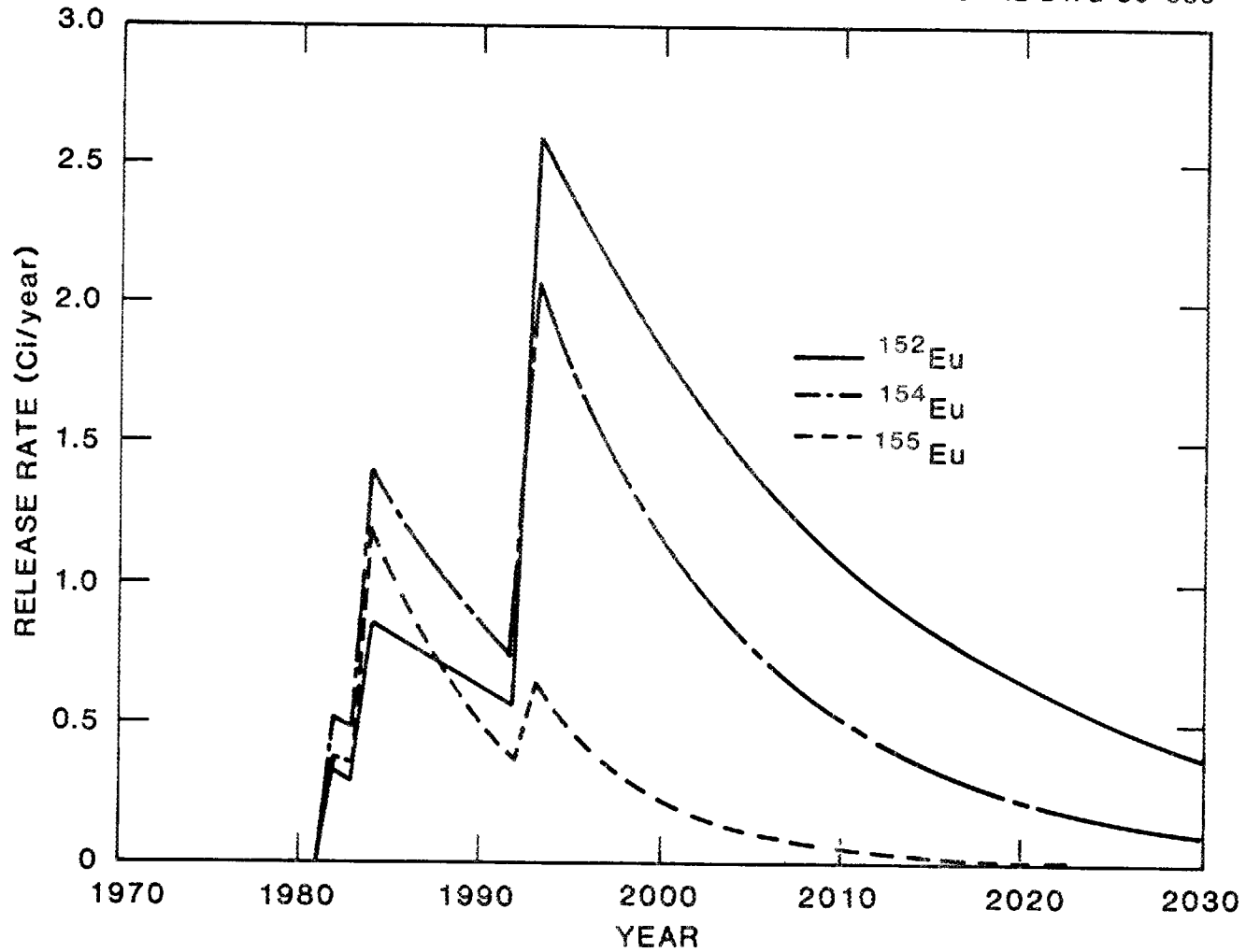


Fig. 4.4. Mixed-mode release of europium isotopes for the parameters:  
Eu solubility of  $10^{-6}$  mol/L; liner failure at 10 years; cladding failure at 2 years.

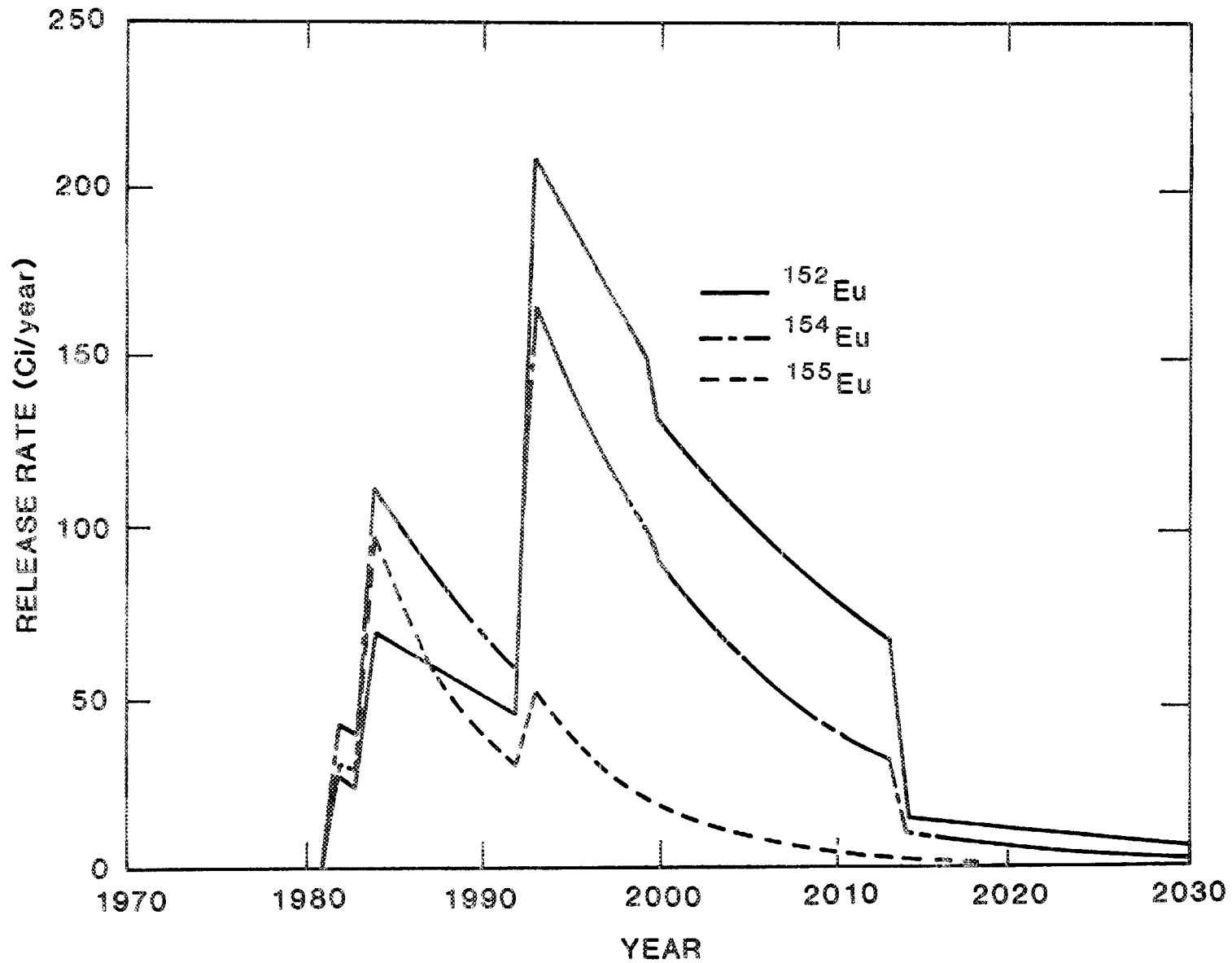


Fig. 4.5. Mixed-mode release rates of europium isotopes for the parameters: Eu solubility of  $10^{-4}$  mol/L; liner failure at 10 years; cladding failure at 2 years.

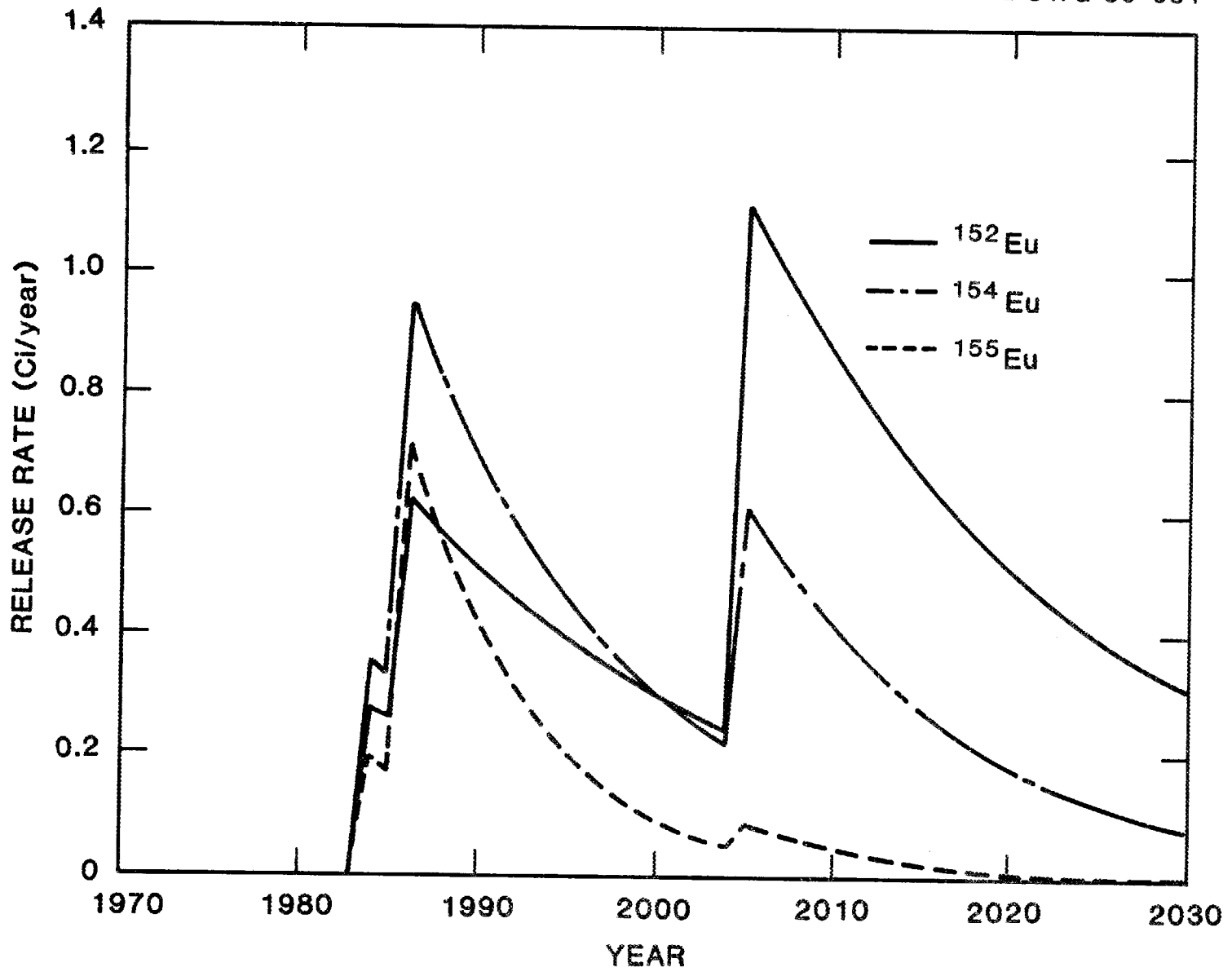


Fig. 4.6. Mixed-mode release rates of europium isotopes for the parameters: Eu solubility of  $10^{-6}$  mol/L; liner failure at 20 years; cladding failure at 4 years.

calculated by the diffusion model (Sect. 4.5.1). The same range of input values was used in the calculations: time-to-failure of the liner (when present) of 10 and 20 years; time-to-failure of the cladding of 2 and 4 years; and,  $\text{Eu}^{3+}$  solubility of  $10^{-4}$  and  $10^{-6}$  mol/L. The calculated release rates for the base case are shown in Fig. 4.7. For the base case, the wastes in the unlined holes dominate the release rates; releases begin about 1982 and peak at about 1.6 Ci/year in 1985. If the europium solubility is assumed to be  $10^{-4}$  mol/L instead of  $10^{-6}$  mol/L, then the calculated release rates are 2 orders-of-magnitude greater (Fig. 4.8). If the liner and cladding are assumed to remain intact for 20 and 4 years, respectively, then (Fig. 4.9) the release rates are slightly reduced relative to the base case in Fig. 4.7.

In comparing these calculated single-mode release rates (Figs. 4.7--4.9) with those calculated for the mixed mode (Figs. 4.4--4.6), it can be seen that the calculated releases from the wastes in the lined auger holes are substantially lower. These lower values result from the underlying assumptions used to construct the release models. When the rate-limiting step is assumed to be saturation of the infiltrating groundwater, the only area for release is that of the auger-hole cross section because no allowance is made for axial mixing. When the rate-limiting step is assumed to be diffusion from the entire cylindrical surface of the auger hole, however, a much greater area for release is present which results in larger calculated release rates. The actual situation in SWSA-6 probably is somewhere between these two modeling limits -- an interesting case where release calculations based on the saturation of the volume of infiltrating groundwater is not necessarily the most conservative or maximum limiting rate.

## 4.6 CONCLUSIONS AND RECOMMENDATIONS

### 4.6.1 Predicted Performance of Emplaced Cylinder and Plates

Within the limitations of the caveats in the following paragraphs, we believe that the europium release-rate calculations described in Sect. 4.5 may bound the actual situation for the control cylinder and plates emplaced in SWSA-6. The release-rate plots for the bounding

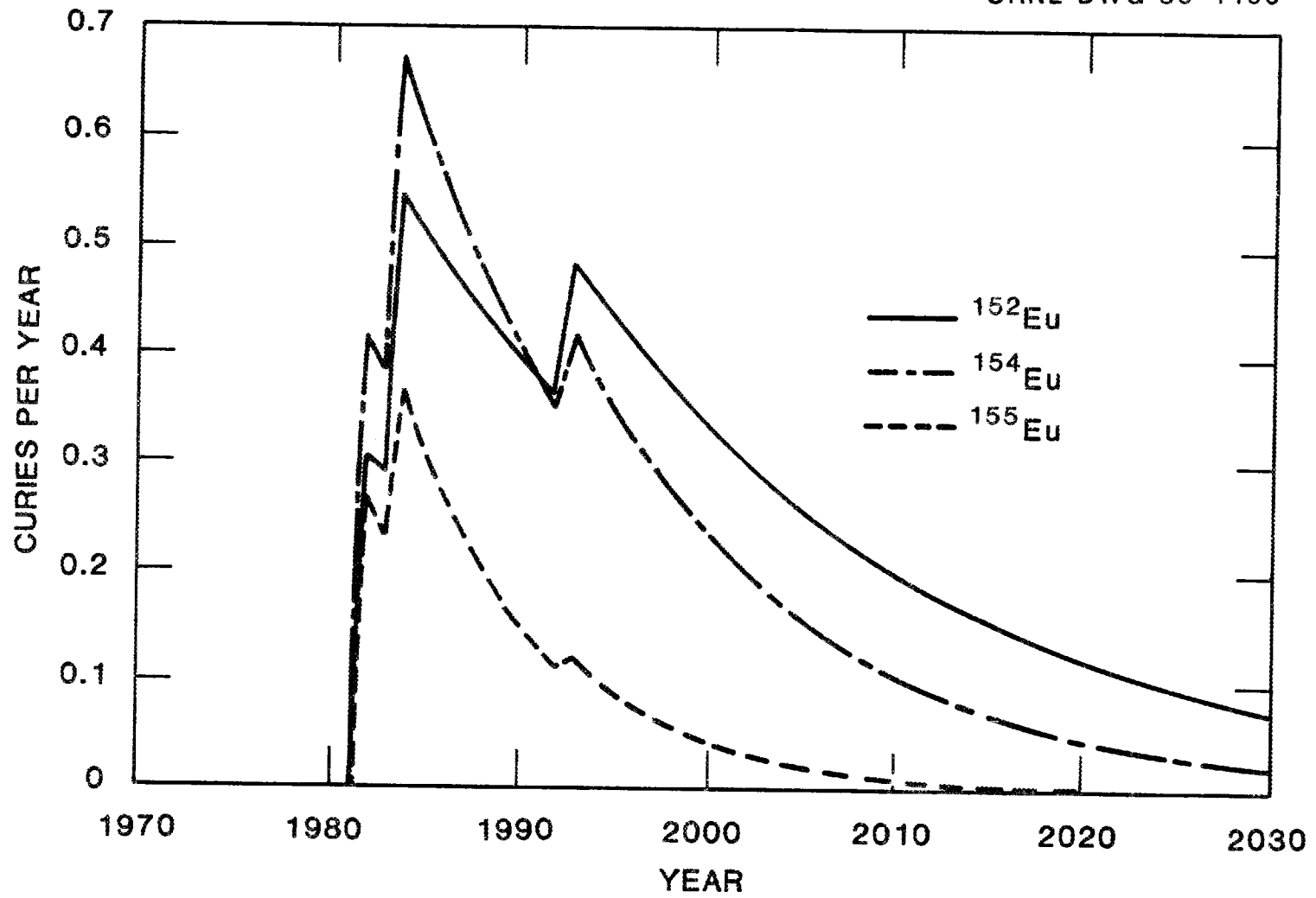


Fig. 4.7. Single-mode release rates of europium isotopes for the parameters: Eu solubility of  $10^{-6}$  mol/L; liner failure at 10 years; cladding failure at 2 years.

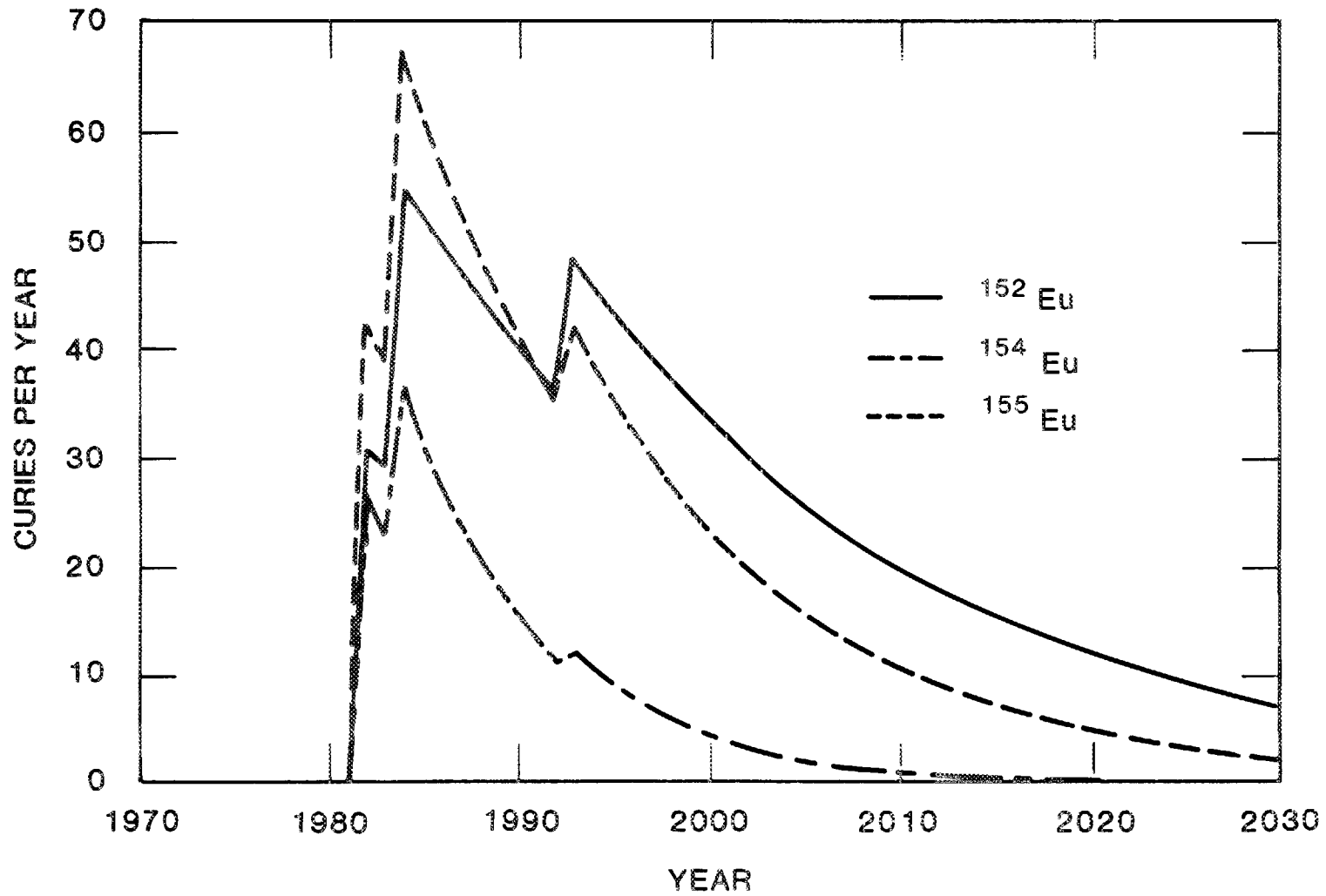


Fig. 4.8. Single-mode release rates of europium isotopes for the parameters: Eu solubility of  $10^{-4}$  mol/L; liner failure at 10 years; cladding failure at 2 years.

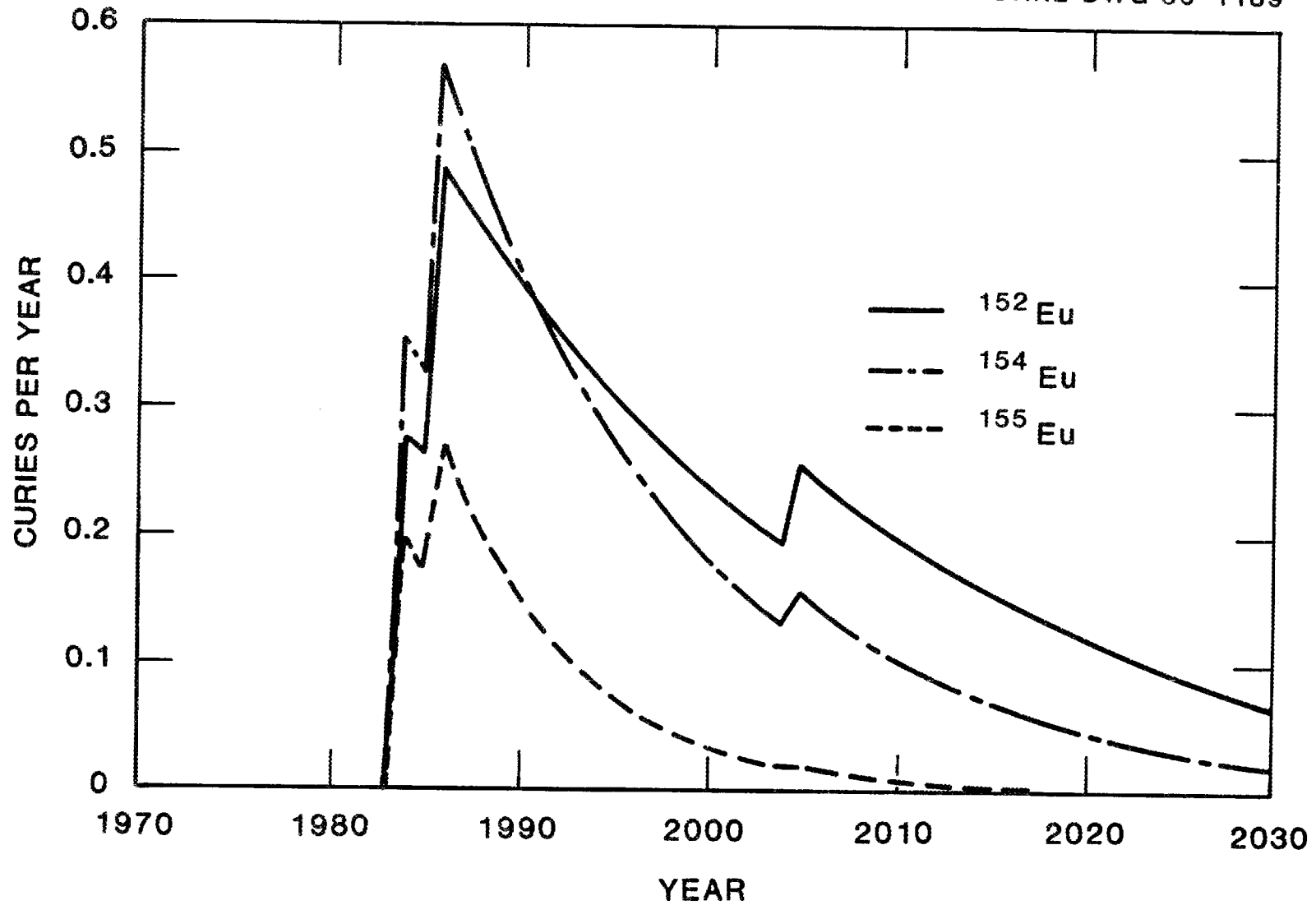


Fig. 4.9. Single-mode release rates of europium isotopes for the parameters: Eu solubility of  $10^{-6}$  mol/L; liner failure at 20 years; cladding failure at 4 years.

situations are repeated in Fig. 4.10 for easy comparison. The lower bound (least conservative, or lowest release rates) occurs with the single-mode release model where the near-field release from wastes in both lined and unlined auger holes are assumed to be limited by the  $\text{Eu}^{3+}$  solubility in the volume of infiltrating rainwater. Release begins about 1984 and peaks at a total of about 1.3 Ci/year in about 1987. After about 1987, the curves decrease due to the radioactive decay of the respective radionuclides, and the proportions between the  $^{152}\text{Eu}$ ,  $^{154}\text{Eu}$ , and  $^{155}\text{Eu}$  curves changes accordingly. The small spike in the curves at about 2006 is caused by the release from the lined auger holes. The higher bound (most conservative, or highest release rates) occurs with the mixed-mode release model, where release from wastes (1) in unlined auger holes is assumed to be solubility limited, and (2) in lined auger holes is assumed to be limited by diffusion of  $\text{Eu}^{3+}$  through the boundary layer. The wastes in the unlined auger holes begin to release activity about 1982 and peak at about 290 Ci/year about 1984. A greater release peak of about 420 Ci/year occurs about 1992 due to releases from the wastes in lined auger holes. The release rate drops abruptly at about 2015 because all of the europium has been leached from the wastes in the lined holes. As discussed in the following paragraphs, better input data would be necessary to reduce the range between these bounding calculations or to increase the certainty that these two calculations do actually bound the SWSA-6 system.

The predicted near-field radioactivity release rates for the control cylinder and plates emplaced in SWSA-6 is much more uncertain than for the stainless steel and cobalt alloy parts or for the beryllium reflectors. This uncertainty results from a lack of information for a number of the important parameters used in the calculations, which include (1) time of failure for the auger-hole liner (in the cases of lined auger holes), (2) time of failure of the aluminum cladding, (3) rate of the reaction of the europium cermet with groundwater, (4) the solubility or saturated solution concentration of europium in groundwater, and (5) the pH of the near-field groundwater (which has a major effect on the solubility value). Conservative, limiting, or reasonable assumptions were made to

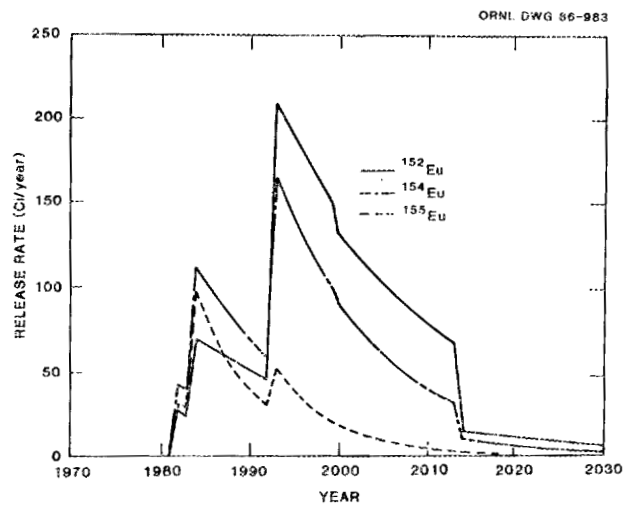
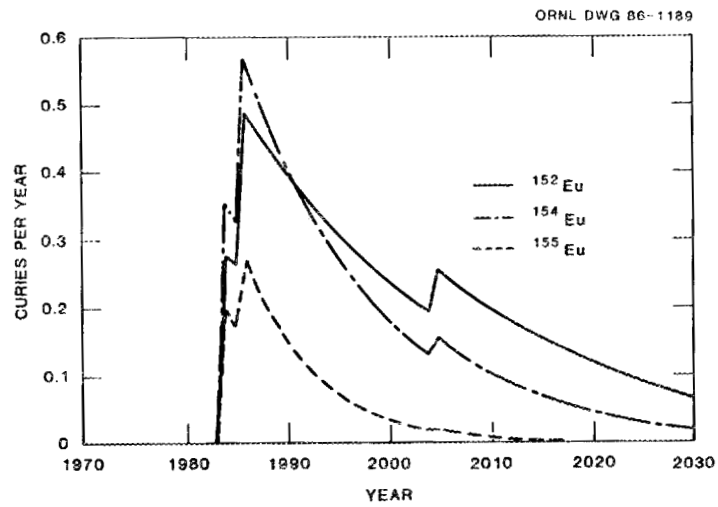


Fig. 4.10. Bounding europium release rates: (a) lower bound — single-mode release model; liner fails after 20 years; cladding 4 years;  $\text{Eu}^{3+}$  solubility is  $10^{-6}$  mol/L; (b) higher bound — mixed-mode release model; liner fails at 10 years; cladding fails at 2 years; Eu solubility is  $10^{-4}$  mol/L.

supply the missing accurate or site-specific data for the calculations. In some cases, several values were used in the calculations to explore the sensitivity of the release rate to specific parameters. In light of the uncertainty in the data used, it seems reasonable to suggest caution in considering environmental impacts, remedial action options, or future disposal options based on these calculated release rates.

The europium release rates are directly proportional to the solubility value used in the calculations. We employed values of  $1 \times 10^{-6}$  mol/L and  $1 \times 10^{-4}$  mol/L for the europium(III) solubility. There is considerable uncertainty in the validity of these values for the near-field system (see Sect. 4.2.6), which results both from the lack of experimental or thermodynamic data as well as the strong dependence of the europium solubility on the groundwater pH. The pH of the SWSA-6 near-field system also is poorly known (see Sect. 2.4.1). Better information for both the groundwater pH and the solubility of europium are needed to improve this aspect of the calculations. The times for failure of the auger-hole liners (10 and 20 years) and the aluminum cladding (2 and 4 years) are simply estimates because of the absence of any applicable data. The europium isotopes have relatively short half-lives (decay rapidly), thus if these barriers lasted longer than assumed for these calculations, the radioactivity release rates would be substantially reduced. Better information on the corrosion rates for these materials is needed to improve these aspects of the calculations. Improved corrosion rate data could be particularly useful in the consideration of remedial action options.

Since no information is available descriptive of the reactions of the europium cermet with groundwater, we assumed instant reaction and dissolution until the saturated solution concentration of europium is reached. This may be an unrealistically conservative assumption. Better data on the reactivity of the europium cermet could result in substantially delayed radioactivity releases. Due to the relatively short half-lives of the europium radionuclides, inclusion of this release barrier would significantly reduce the release rate values as releases are postponed to later dates.

The limited evidence available to date from SWSA-6 monitoring well samples (ORNL 1985) does not indicate that europium isotopes have already been released from the HFIR sources as predicted by this model. One possible explanation for this negative finding is that the aluminum plates have not yet failed, and thus the barriers to release have a substantially longer life than was assumed in this study. Another possible explanation is that the solubility of europium in the groundwater in SWSA-6 is indeed very low ( $<10^{-6}$  mol/L), and the release rates of europium are small enough so that the  $\text{Eu}^{3+}$  concentration in monitoring well samples has not been detected at this time. Since sorption of europium on waste materials or soil has not been considered in these near-field calculations, it also is possible that europium released from the control plates or cylinders has been sorbed by adjacent solids and thus is not available for migration to the SWSA-6 monitoring wells.

#### 4.6.2 Additional Research/Development Needed

Considerable additional R&D work would be needed to substantially decrease the uncertainties in the calculated europium near-field release rates. Corrosion information to pin-point the time of failure of the auger-hole liner and aluminum cladding is needed under site-specific geochemical conditions. The reactivity of the europium-aluminum cermet with groundwater should be investigated. Also, the solubility or saturated solution concentration of europium(III) under the near-field and far-field groundwater geochemical conditions should be experimentally explored. Finally, quantification of the releases of europium predicted from the SWSA-6 site to the environment would also require values for the far-field sorption processes. Measurement of all these parameters would certainly be a significant laboratory experimental project extending over several years. An alternative approach to improving the release calculations is suggested below.

Since isolation of the control plates from groundwater for >134 years would allow nearly complete decay of all the europium radionuclides, an alternative approach would be to study only isolation features — a plan that would be effective either for remedial action or future disposal

options. Utilization of a hole liner of sufficient integrity to assure isolation for >134 years would resolve environmental concerns (since the europium radionuclides would have decayed) and negate the need for an extensive R&D program to quantify all the release-rate parameters discussed above. Such a liner might be made of thick steel, advanced metals such as titanium, or bulk materials such as concrete. The liner might be employed in below-grade or above-grade tumulus configurations. Therefore, we suggest giving priority to the consideration of an improved liner for potential use in future disposal of control plates from the HFIR.

## 5. REFLECTORS

### 5.1 DESCRIPTION OF REFLECTORS EMPLACED IN SWSA-6

The core and control cylinders of the HFIR are surrounded by a massive neutron reflector (Fig. 1 of Bowden et al. 1984). The following discussion of reflector disposal was developed through discussions with HFIR operations staff (Farrar 1986). The reflector is highly purified beryllium (99.99% Be) and is not clad or covered with other material. When the reflector is replaced, the various segments are removed from around the reactor and stored in the HFIR pool. For shipment to SWSA-6, the reflector segments are broken up and placed in a shipping can constructed of 16-gauge mild steel. The can has holes in the top and bottom so that pool water will drain when the can is raised from the pool. The shipping can is enclosed in a transportation shield for shipment to SWSA-6. At SWSA-6, the transportation shield is positioned over an auger hole, and the shipping can containing the reflector parts is lowered into the hole. The steel-lowering cable is discarded with the can.

Operation of the HFIR results in neutron capture reactions that form some  $^{10}\text{Be}$  (half-life  $1.6 \times 10^6$  years) in the reflector. All half-lives are from Walker et al. 1984. Although the reflectors are manufactured from 99.99% beryllium, impurities in the beryllium could lead to the formation of other radionuclides. Based on literature information of

contaminants in reactor-grade beryllium (Cukr 1978), we have included  $^{55}\text{Fe}$  (half-life 2.3 years) and  $^{41}\text{Ca}$  (half-life  $1.0 \times 10^5$  years) in our calculations. For the period 1977 through 1984, the data base shows that 400 Ci of  $^{10}\text{Be}$  were placed in auger holes at SWSA-6 (Table A.2 of Boegly et al. 1985). Apparently, the curie content of neutron-activated contaminants in the beryllium was not reported. During this period, nine sets of HFIR reflector assemblies, or about 1200 kg of Be, were shipped to SWSA-6 (Farrar 1986).

## 5.2 CALCULATION OF RADIOACTIVITY RELEASE RATES

### 5.2.1 Inventory of Reflector Components in SWSA-6

The list of beryllium reflector components that are buried in SWSA-6 were supplied to us by the operating staff of HFIR (Farrar 1986) from their operating records. These components are listed in Table 5.1 along with component weights, accumulated irradiation in the reactor, the maximum flux to which the components were exposed, and the date of removal from the reactor. From this information we estimated (using the equations in Sect. 3.1) the specific activity (Ci/kg) and total activity (Ci) of  $^{41}\text{Ca}$ ,  $^{55}\text{Fe}$ , and  $^{10}\text{Be}$ . These values are also shown in Table 5.1. This table shows that the total activity of these three radionuclides in the reflector components are not major contributors to the radioactive contents of SWSA-6. Our calculated  $^{10}\text{Be}$  inventory value of 0.0721 Ci is in very poor agreement with the data-base inventory given in Table A.2 of Boegly et al. 1985, which shows 400 Ci of  $^{10}\text{Be}$  in the auger holes. We believe that our calculated value cannot possibly be in error by such a large margin but have no good explanation for the difference in the two numbers. It is possible that the data base contains a significant misestimation for this radionuclide.

### 5.2.2 Waste Leachate Chemistry

The waste leachate was assumed to be infiltrating rainwater. As discussed in Sect. 2.4.1, the most important SWSA-6 groundwater aspect for corrosion and solubility estimates is the acidity. We used the extreme pH values observed for the SWSA-6 soil/groundwater system (pH 4.4

Table 5.1. Discharge from HFIR and inventory of beryllium reflectors emplaced in SWSA-6

	Irradiation (MWd)	Time in reactor (years)	Flux (neutrons/cm <sup>2</sup> .s)	Discharge date	Emplaced (kg)	Total activity as of June 1, 1986 (Ci)		
						<sup>41</sup> Ca	<sup>55</sup> Fe	<sup>10</sup> Be
Permanent reflector								
No. 1	278254	8.31	1.5E+15	6/75	547.3	3.95E-03	1.67E+00	4.81E-02
Semiperm. reflector								
No. 1	190009	5.67	1.5E+15	10/72	50.9	2.51E-04	6.77E-02	3.05E-03
No. 2	122616	3.66	1.5E+15	8/76	50.9	1.62E-04	1.45E-01	1.97E-03
No. 3	171791	5.13	1.5E+15	10/81	50.9	2.27E-04	6.64E-01	2.76E-03
Removable reflector								
No. 1	48226	1.44	1.7E+15	6/68	126.8	1.80E-04	2.52E-02	2.19E-03
No. 2	76570	2.29	1.7E+15	10/70	126.8	2.85E-04	6.61E-02	3.48E-03
No. 3	82769	2.47	1.7E+15	4/73	126.8	3.08E-04	1.33E-01	3.76E-03
No. 4	105060	3.14	1.7E+15	8/76	126.8	3.92E-04	3.72E-01	4.77E-03
C. R. access plugs								
No. 1	235292	7.02	1.5E+15	6/75	<u>27.3</u>	<u>1.66E-04</u>	<u>7.87E-02</u>	<u>2.03E-03</u>
				TOTALS	1234.5	5.92E-03	3.22E+00	7.21E-02

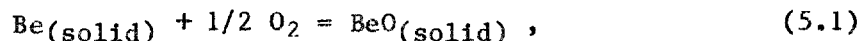
and 7.7) in the modeling calculations. Because of the slow corrosion rates (low chemical reactivity) of the beryllium metal (Sect. 5.2.5), it seemed unlikely that the waste form would substantially alter the in situ near-field geochemical parameters.

### 5.2.3 Time of Radioactivity Release

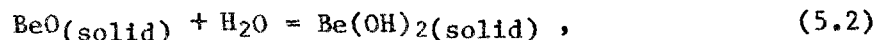
We assumed that radioactivity release would begin immediately on the emplacement of the waste in the auger hole [i.e., the time of initial radioactivity release used in the release rate calculations (Sect. 5.2.8) was 0 years]. This assumption was reached because no engineered aspects exist to isolate the waste from infiltrating rainwater. The auger holes typically are not lined, and the mild-steel shipping can containing the waste has holes in the top and bottom. The concrete plug poured in the top of the hole for intruder protection would not provide significant hydrologic isolation.

### 5.2.4 Radionuclide Solubility

The reflectors emplaced in SWSA-6 are composed of pure beryllium metal. The solubility of beryllium metal atoms ( $\text{Be}^0$ ) in groundwater would be negligibly small, and we have assumed that significant beryllium solubility and concomitant release of  $^{10}\text{Be}$  from the reflectors would occur only after oxidation,



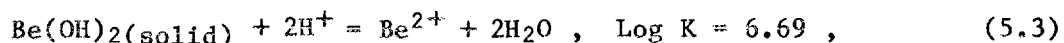
and hydrolysis,



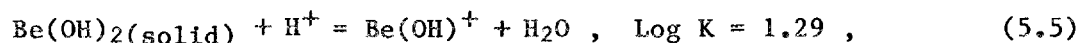
reactions proceed to form beryllium hydroxide on the surface of the reflector parts in contact with the soil/groundwater system. We have assumed that beryllium hydroxide would be the saturating solid phase that would control the solubility of beryllium in groundwater.

Considerable information is available in the literature on the solubility of beryllium hydroxide in aqueous solutions. A good summary of the thermodynamic data for  $\text{Be}(\text{OH})_2$  is given in Baes and Mesmer 1976, and the following discussion of beryllium solubility in groundwater at SWSA-6 is based on data in that reference. Since pH extremes of 4.4 and 7.7 have been measured for SWSA-6 soil/groundwater systems (see Sect. 2.4.1), the beryllium solubility (saturated solution concentration) was considered at both pH 4.4 and pH 7.7 in order to explore the range of beryllium concentrations that could be encountered in groundwater at SWSA-6.

The beryllium solubility at pH 7.7 was calculated from data for the dissolution of solid beryllium hydroxide,

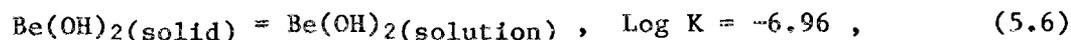


and for the hydrolysis of the  $\text{Be}^{2+}$  ion,



to get an equilibrium constant for the dissolution of beryllium hydroxide to form the  $\text{Be}(\text{OH})^+$  species. (In these calculations, we have assumed that the equilibrium constant, K, is equivalent to the equilibrium quotient, Q, since groundwater has a low ionic strength.)

$\text{Be}(\text{OH})^+$  is the dominant ionic form of beryllium at pH 7.7. In addition, undissociated beryllium hydroxide has an appreciable solubility



and contributes to the concentration of beryllium in solution. The total beryllium solubility was obtained by summing the solubilities of  $\text{Be}(\text{OH})^+$

and  $\text{Be}(\text{OH})_2$

$$\text{Be}(\text{OH})^+ \text{ from Eq. (5.5)} \quad 3.9 \times 10^{-7} \text{ M}$$

$$\text{Be}(\text{OH})_2 \text{ from Eq. (5.6)} \quad \underline{1.1 \times 10^{-7} \text{ M}}$$

$$5.0 \times 10^{-7} \text{ M}$$

which gave a value of  $\sim 5 \times 10^{-7} \text{ M}$  for the beryllium concentration at pH 7.7. Since the chemistry of beryllium is fairly well understood in aqueous solutions, this solubility value may be relatively accurate as long as complexing ions, such as  $\text{F}^-$ , are absent. Because of its small ionic radius and high surface charge,  $\text{Be}(\text{II})$  ions readily form stable complexes with a number of anions and soluble species such as  $\text{BeF}_4^{2-}$  are well known. Additional information on the groundwater composition in contact with the reflectors in the auger holes would be needed to understand the possible contribution of complexing ions to beryllium solubility at pH 7.7 at SWSA-6.

At pH 4.4, beryllium hydroxide would be expected to be very soluble. According to Baes and Mesmer 1976, the solution species is  $\text{Be}_6(\text{OH})_8^{4+}$  and the solubility would be greater than 1 M (as Be). Such a high concentration of beryllium in groundwater likely never would be observed since the rate of solubilization of beryllium probably would be limited by the rate of the oxidation and hydrolysis reactions [Eqs. (5.1) and (5.2)]. Also, in soil/groundwater systems, other low-solubility solids such as beryllium silicates may form. For example, the natural mineral bertrandite,  $\text{Be}_4\text{Si}_2\text{O}_7(\text{OH})_2$ , is insoluble in acid solutions (CRC 1976-1977). Boegly 1984 or Davis et al. 1984 reported soluble silica concentrations of 7 to 14 mg/L of  $\text{SiO}_2$  in the ETF well water samples. Thus, it is conceivable that the formation of an insoluble beryllium silicate could result in a beryllium concentration at pH 4.4, which is much lower than that calculated from the data in Baes and Mesmer 1976 for the system  $\text{Be}(\text{OH})_2\text{-H}_2\text{O}$ .

The following observations can be drawn from this consideration of beryllium solubility in SWSA-6 groundwater:

1. The concentration of beryllium in solution may be controlled by the reactions between groundwater and the massive beryllium metal parts. It is possible that the oxidation and hydrolysis reactions could proceed so slowly that insufficient  $\text{Be}(\text{OH})_2$  would be formed to allow saturation of the groundwater. An experimental activity would be required to study the rates of these reactions.
2. If it is assumed that the oxidation and hydrolysis reactions can proceed rapidly enough to generate  $\text{Be}(\text{OH})_2$  in sufficient quantity to saturate the soil/groundwater system, then the pH of the soil/groundwater system is an important variable that will strongly affect the beryllium solubility. Additional data are needed for the SWSA-6 site to better characterize the soil/groundwater pH in the vicinity of the waste and along the release pathway. The present data define extreme values of pH 4.4 and 7.7; beryllium solubility would be quite different at these pH levels.
3. If the groundwater pH is 7.7 and complexing ions such as  $\text{F}^-$  are not present in sufficient quantity to react and form soluble complexes, the beryllium solubility (saturated solution concentration) can be calculated from thermodynamic data in the literature. A value of  $\sim 5 \times 10^{-7} \text{ M}$  is obtained for the total solubility of  $\text{Be}(\text{OH})^+$  plus  $\text{Be}(\text{OH})_2$ . This value may be fairly accurate unless complexing ions are present. Better data are needed for the SWSA-6 groundwater composition to confirm the absence of complexing ions.
4. If the groundwater pH is as low as 4.4, as seems possible for shale-derived soil systems, then the literature information indicates a high solubility of beryllium as the species  $\text{Be}_6(\text{OH})_8^{4+}$ . However, insoluble beryllium compounds such as silicates could possibly form in groundwater at SWSA-6. The present information does not appear to be sufficient to allow an estimation of the beryllium saturated solution concentration to be expected in SWSA-6 if the pH is as low as 4.4. An

experimental effort would be required to identify the saturating solid phase and the beryllium solubility in solutions representative of SWSA-6 groundwater.

The other radionuclides of environmental concern,  $^{41}\text{Ca}$  and  $^{55}\text{Fe}$ , probably would be present in the pure beryllium at such low molar concentrations that the quantities released could never approach their solubility limits. We did not consider solubility constraints for these radionuclides.

#### 5.2.5 Radionuclide Diffusivity

A search of Chemical Abstracts references established that the paper of Heukeshoven and Winkel 1933 is the primary reference for values of the diffusion coefficient of beryllium in aqueous solutions. They measured the diffusivity of beryllium in potassium chloride solution at  $10^\circ\text{C}$  as a function of pH from pH 0 to 5.8. The diffusion coefficient changed only slightly (from  $0.45 \times 10^{-5}$  to  $0.34 \times 10^{-5}$   $\text{cm}^2/\text{s}$ ) over this pH range. According to Baes and Mesmer 1976, the species in solution over this pH range would be  $\text{BeOH}^+$ . We chose the diffusion coefficient value at pH 4.4 given by Heukeshoven and Winkel 1933 ( $0.43 \times 10^{-5}$   $\text{cm}^2/\text{s}$ ) for the calculation of beryllium transport through the boundary layer of the reflectors at the lower pH environment of SWSA-6. No beryllium diffusion data apparently exist for the higher pH environment of SWSA-6 (pH 7.7). Hydrolysis reactions would result in the formation of some  $\text{Be}(\text{OH})_2$  species in solution at this pH, and the diffusivity value for  $\text{BeOH}^+$  would not be strictly accurate for this species. Since the diffusion coefficient is dependent upon the species size and shape, but not charge, the data for  $\text{BeOH}^+$  may be adequate to describe  $\text{Be}(\text{OH})_2$  diffusivity. The diffusion coefficient data of Heukeshoven and Winkel 1933 show a gradual decrease with increasing pH, which is consistent with increasing species size due to hydrolysis, so we graphically extrapolated their data to pH 7.7 to obtain a value for use in boundary layer calculations at the higher pH environment of SWSA-6; this value is  $0.3 \times 10^{-5}$   $\text{cm}^2/\text{s}$ .

### 5.2.6 Corrosion of Beryllium Metal

We located no published information on the corrosion rates of beryllium metal in soil/groundwater systems. As discussed in the previous section, we have assumed that beryllium corrosion occurs from reaction with dissolved oxygen in the groundwater to form  $\text{BeO}$ , which in turn, hydrolyzes to give soluble  $\text{Be}(\text{OH})_2$ . We assumed that beryllium corrosion rates were diffusion controlled. For corrosion in water of pH 7.7, we assumed that in the immediate vicinity of the metal/water interface the water becomes saturated with corrosion product  $\text{Be}(\text{OH})_2$ , and the rate of diffusion of  $\text{Be}(\text{OH})_2$  away from the metal surface limited the corrosion rate. For corrosion in water of pH 4.4, we assumed that the rate of diffusion of dissolved oxygen to the metal surface limited the corrosion rate, and the  $\text{Be}(\text{OH})_2$  never saturated the water.

The rate of diffusion of dissolved oxygen from the groundwater to the metal surface and the rate of diffusion of  $\text{Be}(\text{OH})_2$  from the metal surface to the bulk groundwater were calculated assuming flat-plate geometry, with the groundwater flowing parallel to the flat plate and oxygen or  $\text{Be}(\text{OH})_2$  diffusing normal to the water flux. The expression for this diffusion rate is derived in the Appendix C and is given below:

$$J = \frac{2\sqrt{3}}{3} \frac{\epsilon \mathcal{D} (C_B - C_I)}{\left( \frac{\epsilon \mathcal{D} L}{U} \right)^{1/2}}, \quad (5.7)$$

where

- $J$  = molar flux of  $\text{O}_2$  or  $\text{Be}(\text{OH})_2$ ,  $\text{g-mol/cm}^2\text{s}$ ;
- $C_B$  = concentration of  $\text{O}_2$  or  $\text{Be}(\text{OH})_2$  in bulk groundwater,  $\text{g-mol/cm}^3$ ;
- $C_I$  = concentration of  $\text{O}_2$  or  $\text{Be}(\text{OH})_2$  at metal/water interface,  $\text{g-mol/cm}^3$ ;
- $\epsilon$  = porosity of soil (see Sect. 4.2.8), dimensionless;
- $\mathcal{D}$  = diffusivity of  $\text{O}_2$  or  $\text{Be}(\text{OH})_2$  in water,  $\text{cm}^2/\text{s}$ ;
- $U$  = darcy groundwater velocity parallel to reflector component (see Sect. 4.2.8),  $\text{cm/s}$ ;
- $L$  = characteristic length of reflector component,  $\text{cm}$ .

At pH 7.7 where the corrosion rate is controlled by the diffusion of the corrosion product  $\text{Be}(\text{OH})_2$  from the surface, the corrosion rate is given by:

$$C_{\text{Be}} = 3.16 \times 10^4 \text{ MW}_{\text{Be}} J, \quad (5.8)$$

where

$C_{\text{Be}}$  = corrosion rate of Be,  $\text{kg}/\text{cm}^2 \cdot \text{year}$ ;

$\text{MW}_{\text{Be}}$  = atomic weight of Be,  $\text{kg}/\text{kg-mol}$ ;

$3.16 \times 10^4$  = factor to convert from g to kg and from s to years.

At pH = 4.4 where the corrosion rate was assumed to be limited by the rate of dissolved oxygen to the metal surface from the bulk of the groundwater, the corrosion rate is given by:

$$C_{\text{Be}} = 6.32 \times 10^4 \text{ MW}_{\text{Be}} J, \quad (5.9)$$

where

$C_{\text{Be}}$  = corrosion rate of Be,  $\text{kg}/\text{cm}^2 \cdot \text{year}$ ;

$\text{MW}_{\text{Be}}$  = atomic weight of Be,  $\text{kg}/\text{kg-mol}$ ;

$6.32 \times 10^4$  = factor converting g to kg and s to y. (Includes a factor of 2 since 2  $\text{kg-mol}$  of Be reacts with 1  $\text{kg-mol}$  of  $\text{O}_2$ .)

To calculate the corrosion rate at pH 7.7 from Eqs. (5.7) and (5.8), we used a value of  $5 \times 10^{-7} \text{ M}$  ( $5 \times 10^{-10} \text{ mol}/\text{cm}^3$ ) for the solubility of  $\text{Be}(\text{OH})_2$ ; a value of  $0.3 \times 10^{-5} \text{ cm}^2/\text{s}$  for the diffusivity of beryllium ions; a value of 13.75 in./year for the groundwater velocity; a value of 0.5 was used for the soil porosity as discussed in the section on europium release; and a value of 24 in. for the characteristic length of a reflector component. The bulk value of  $\text{Be}(\text{OH})_2$  concentration is assumed to be zero. Substituting these values into Eqs. (5.7) and (5.8) gives a value for the beryllium corrosion rate at pH 7.7 of  $0.62 \times 10^{-10} \text{ kg}/\text{cm}^2 \cdot \text{year}$ .

To calculate the corrosion rate at pH 4.4 from Eqs. (5.7) and (5.9) we used a value of  $5.6 \times 10^{-2} \text{ mol}/\text{cm}^3$  for the solubility of dissolved oxygen in the bulk groundwater. This value assumes saturation with air at 1 atm and  $25^\circ\text{C}$ , using a value for the Henry's Law constant for oxygen of  $4.01 \times 10^4 \text{ atm/unit mol fraction}$  (Perry et al. 1963). The concentration of  $\text{O}_2$  at the metal surface was assumed to be zero. A value of

$2.41 \times 10^{-5}$  cm<sup>2</sup>/s was used for the diffusivity of dissolved oxygen (Vivian and King 1964). The same values for porosity and characteristic length were used in this calculation as in the previous calculation. Substituting these values into Eqs. (5.7) and (5.9) results in a value for the beryllium corrosion rate at pH 4.4 of  $0.18 \times 10^{-6}$  kg/cm<sup>2</sup>·year.

### 5.2.7 Geometry/Surface Area of Emplaced Reflectors

The beryllium reflectors in HFIR are massive blocks of beryllium with regular geometric shapes whose surface areas are readily calculated from the engineering drawings. The surface areas per unit weight reported in Table 5.1 were determined in this manner: the surface area for each component was calculated from engineering drawings of each component, and this result was divided by the weight of the component. When each component is buried, however, it is broken up and deformed into undefinable fragments. Since it was impossible to estimate surface area of these fragments, we simply used the estimate determined for undeformed components.

### 5.2.8 Radionuclide Release Rates

The release rates of the three radionuclides considered in the beryllium reflectors were calculated from the corrosion rates determined in Sect. 5.2.6 in a manner similar to the calculation of release rates of radionuclides from the stainless steel components. The release rates are given by the following equation:

$$R_{i,c} = C_{Be} S_c A_{i,c} e^{-\lambda_i t} \quad (5.10)$$

where

- $R_{i,c}$  = rate of release of isotope i from component c, Ci/year;
- $C_{Be}$  = corrosion rate of beryllium given by Eqs. (5.8) and (5.9), kg<sup>-1</sup>cm<sup>-2</sup>year<sup>-1</sup>;
- $S_c$  = specific surface area of beryllium component c, cm<sup>2</sup>/kg;
- $A_{i,c}$  = activity of isotope i in component c [from Eq. (3.1) and Table 5.1], Ci;
- $\lambda_i$  =  $0.693/t_{1/2,i}$ ;

$t_{1/2,i}$  = half-life of isotope  $i$ , year;  
 $t_c$  = time out of reactor for component  $c$ , years;  
 and the total release of radionuclide  $i$  is given by

$$R_i = C_{Be} \sum_c S_{c,i,c} e^{-\lambda_i t_c} . \quad (5.11)$$

The results of the calculations showing the release rates of the three radionuclides on June 1, 1986, at pH 4.4 and pH 7.7, are given in Table 5.2. The time-dependent behavior of the release rates for the conditions at pH 4.4 (the higher values of release rates) is shown in Fig. 5.1. These results indicate that the most significant releases are likely to be from radionuclides introduced as very minor contaminants in the beryllium. The release rates of all radionuclides from the beryllium reflectors are estimated to be extremely low.

Table 5.2. Radionuclide release rates from beryllium reflectors as of June 1, 1986

pH of groundwater	Radionuclide release rate (Ci/year)		
	$^{41}\text{Ca}$	$^{55}\text{Fe}$	$^{10}\text{Be}$
4.4	1.4E-05	1.07E-04	1.76E-06
7.7	5.00E-09	3.70E-08	6.06E-10

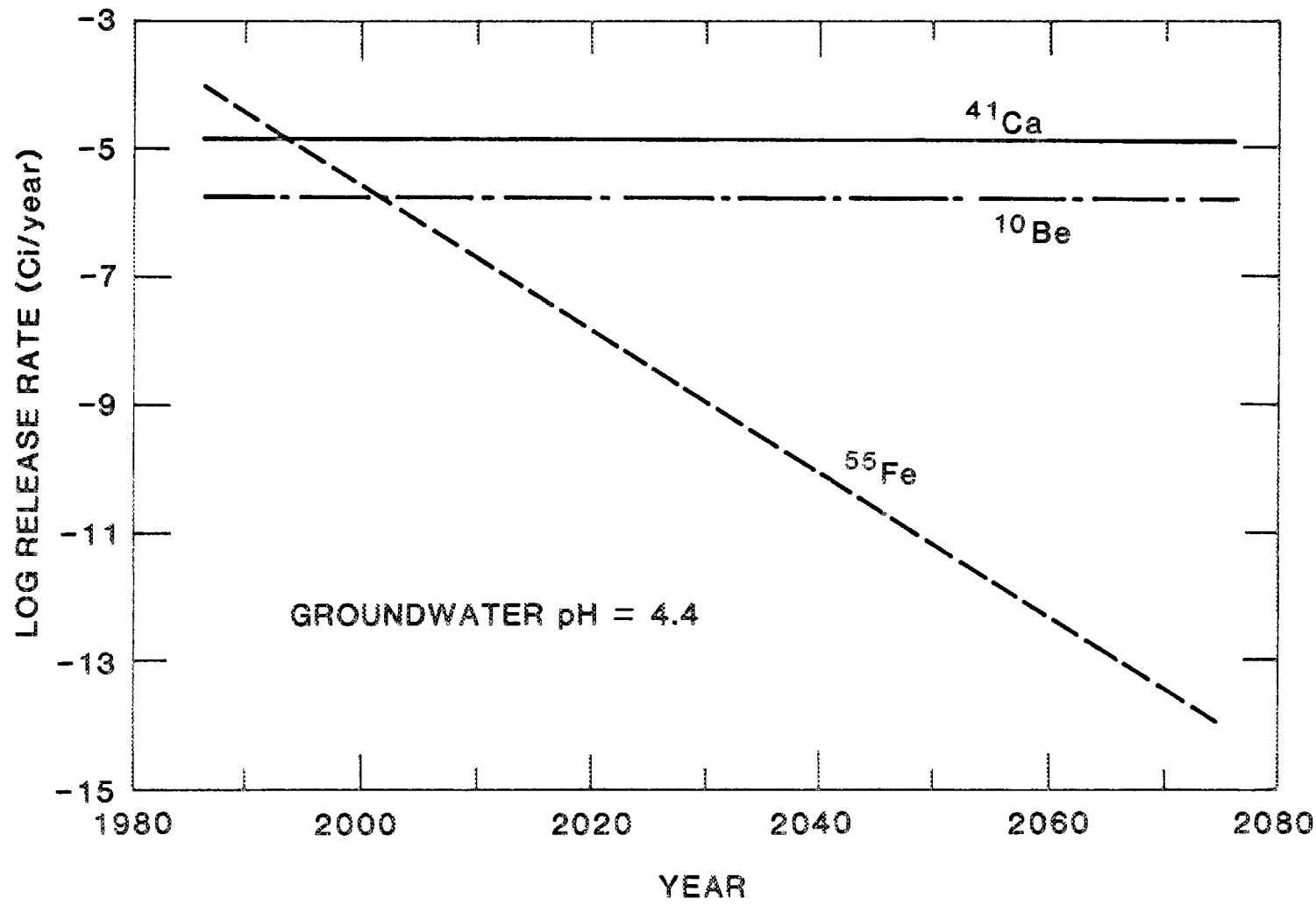


Fig. 5.1. Release rates of  $^{41}\text{Ca}$ ,  $^{55}\text{Fe}$ , and  $^{10}\text{Be}$  from reflectors at pH 4.4.

### 5.3 CONCLUSIONS AND RECOMMENDATIONS

#### 5.3.1 Predicted Performance of Emplaced Reflectors

The near-field release rates for  $^{41}\text{Cs}$ ,  $^{55}\text{Fe}$ , and  $^{10}\text{Be}$  for the next 100 years are shown in Fig. 5.1 for the most conservative (highest release rate) situation, which assumes acidic groundwater at pH 4.4. Under this situation, the rate controlling step was assumed to be diffusion of oxygen to the reflectors. Initially,  $^{55}\text{Fe}$  establishes the release rate at about  $1.2 \times 10^{-4}$  Ci/year. The  $^{55}\text{Fe}$  decays rapidly, however, and after about 1994 the release rate is established at about  $1.5 \times 10^{-5}$  Ci/year by the  $^{41}\text{Ca}$  content of the reflectors. This release rate stays nearly constant with time due to the long half-life of  $^{41}\text{Ca}$ . The release rate of the  $^{10}\text{Be}$  component of the reflectors is still lower; nearly  $1.8 \times 10^{-6}$  Ci/year. If the soil/groundwater system is at a pH as high as 7.7, then the calculated release rates are all about 3 to 4 orders of magnitude lower. At this higher pH, the rate-controlling step was assumed to be diffusion of  $\text{Be}(\text{OH})_2$  from the reflectors.

As with the calculations for the stainless steel or control plate wastes, many assumptions were necessary in order to calculate these release rates. Perhaps the most uncertain is the assumed calcium and iron contaminant concentration in the highly purified beryllium used to construct the reflectors. Errors in the assumed composition would be directly reflected in the calculated release rates for  $^{41}\text{Ca}$  and  $^{55}\text{Fe}$ .

#### 5.3.2 Additional Research/Development Needed

Because the radioactivity associated with the release of beryllium contaminants, rather than beryllium isotopes, dominates the calculated release rates, it would be desirable to confirm the assumed contaminant concentrations. Analysis of the trace contaminants in the beryllium used to construct the reflectors and radiochemical analysis of samples of reflectors discharged from the HFIR should be performed to confirm the importance of  $^{55}\text{Fe}$  and  $^{41}\text{Ca}$  to the radioactivity releases from emplaced reflectors. If the contaminant concentration varies from lot to lot of beryllium, then the calculated release rates would vary correspondingly. Analysis of the  $^{10}\text{Be}$  content of discharged reflector parts also is

desirable to validate our calculated low  $^{10}\text{Be}$  inventory value and the presence of  $^{41}\text{Ca}$  and  $^{55}\text{Fe}$ , relative to the data base (see Sect. 5.2.1). Resolution of this difference in  $^{10}\text{Be}$  values could allow the removal of spurious Ci values from the data base.

## 6. ACKNOWLEDGMENTS

The authors wish to acknowledge the cooperation of J. Bolinsky, M. Farrar, and G. R. Hicks (Operations Division) in helping compile the information of parts discharged from the HFIR and emplaced in SWSA-6. They also wish to thank Janice Shannon and Carol Johnson for typing the many drafts of this report and Catherine H. Shappert for editorial assistance in preparation of the final report.

## 7. REFERENCES

- Baes and Mesmer 1976. C. F. Baes, Jr. and R. E. Mesmer, The Hydrolysis of Cations, Wiley-Interscience, New York, 1976.
- Bates and Oversby 1984. J. K. Bates and V. M. Oversby, Gamma Irradiation in a Saturated Tuff Environment, CONF-841157, Argonne National Laboratory, Chicago, Ill., 1984.
- Bates 1983. L. D. Bates, Radioactive Solid Waste Storage and Disposal at Oak Ridge National Laboratory - Description and Safety Analysis, ORNL/TM-8201, Oak Ridge National Laboratory, Oak Ridge, Tenn., October 1983.
- Benson and Teague 1980. L. V. Benson and L. S. Teague, A Tabulation of Thermodynamic Data for Chemical Reactions Involving 58 Elements Common to Radioactive Waste Package Systems, LBL-11448, Lawrence Berkeley Laboratory, Berkeley, Calif., 1980.
- Boegly et al. 1985. W. J. Boegly, Jr., R. B. Drier, D. D. Huff, A. D. Kelmers, D. C. Kocher, S. Y. Lee, F. R. O'Donnell, F. G. Pin, and E. D. Smith, Characterization Plan for Solid Waste Storage Area 6, ORNL/TM-9877, Oak Ridge National Laboratory, Oak Ridge, Tenn., December 1985.
- Boegly 1984. W. J. Boegly, Jr., Site Characterization Data for Solid Waste Storage Area 6, ORNL/TM-9442, Oak Ridge National Laboratory, Oak Ridge, Tenn., December 1984.
- Bowden et al. 1984. G. A. Bowden, G. R. Hicks, and R. W. Knight, Fabrication Procedures for HFIR Control Plates, ORNL/TM-9365, Oak Ridge National Laboratory, Oak Ridge, Tenn., October 1984.
- Cheverton 1971. R. D. Cheverton and T. M. Sims, HFIR Core Nuclear Design, ORNL-4621, Oak Ridge National Laboratory, Oak Ridge, Tenn., July 1971.
- Couture and Seitz 1983. R. A. Couture and M. G. Seitz, Physical Response of Backfill Materials to Mineralogical Changes in a Basalt Environment, CONF-8308126, Argonne National Laboratory, Chicago, Ill., 1983.
- CRC 1976-1977. Handbook of Chemistry and Physics, CRC Press, Cleveland, Ohio, 1976.
- Cukr 1978. B. Cukr, Chap. VIII., "Beryllium and Its Alloys," in Corrosion Resistance of Reactor Materials, pp. 268-78, INIS-mf-5019, 1978.

- Davis et al. 1984. E. C. Davis, W. J. Boegly, Jr., E. R. Rothschild, B. P. Spalding, N. D. Vaughen, C. S. Haase, D. D. Huff, S. Y. Lee, E. C. Walls, J. D. Newbold, and E. D. Smith, Site Characterization Techniques Used at a Low-Level Waste Shallow Land Burial Field Demonstration Facility, ORNL/TM-9146, Oak Ridge National Laboratory, Oak Ridge, Tenn., July 1984.
- Dayal et al. 1986a. R. Dayal, R. F. Pietrzak, and J. H. Clinton, "Source Term Characterization for the Maxey Flats Low-Level Radioactive Waste Disposal Site," Nucl. Technol. 72, 158-77 (1986).
- Dayal et al. 1986b. R. Dayal, R. F. Pietrzak, and J. H. Clinton, "Oxidation-Induced Geochemical Changes in Trench Leachates from the Maxey Flats Low-Level Radioactive Waste Disposal Site," Nucl. Technol. 72, 184-93 (1986).
- Denn 1980. M. M. Denn, Chap. 15 in Process Fluid Mechanics, p. 285, Prentice-Hall, Englewood Cliffs, N.J., 1980.
- Early et al. 1982. T. O. Early, D. R. Drews, G. K. Jacobs, and R. C. Rouston, Geochemical Controls on Radionuclide Releases from a Nuclear Waste Repository in Basalt: Estimated Solubilities for Selected Elements, RHO-BW-ST-39P, Rockwell Hanford Operations, Richland, Wash., September 1982.
- English and Griess 1965. J. L. English and J. C. Griess, Laboratory Corrosion Studies for the High Flux Isotope Reactor, ORNL/TM-1029, Oak Ridge National Laboratory, Oak Ridge, Tenn., June 1965.
- Farrar 1986. Personal communication, M. B. Farrar, Operations Division, Oak Ridge National Laboratory, Oak Ridge, Tenn., March 1986.
- Friedman 1986. Personal communication, H. A. Friedman, Chemical Technology Division, Oak Ridge National Laboratory, Oak Ridge, Tenn., March 1986.
- Friedman and Kelmers 1987. H. A. Friedman and A. D. Kelmers, Preliminary Laboratory Measurements of Radionuclide Sorption in Solid Waste Storage Area 6 Soil/Groundwater Systems, ORNL/TM-9883, Oak Ridge National Laboratory, Oak Ridge, Tenn. (in press).
- Furuya et al. 1983. T. Furuya, T. Fukuzuka, K. Fujiwara, and H. Tomari, "Gamma-Ray Irradiation Effects on Stress Corrosion Cracking of Alloys for a High Level Liquid Waste Package," Kobe Seiko Giho 33, 43-46 (1983).
- Glass 1985. R. S. Glass, Corrosion Processes of Austenitic Stainless Steels and Copper-Based Materials in Gamma-Irradiated Aqueous Environments, URCL-92941, Lawrence Livermore National Laboratory, Livermore, Calif., September 1985.

Gray 1984. W. J. Gray, "Gamma Radiolysis Effects on Grande Ronde Basalt Groundwater", pp. 147-52 in Scientific Basis for Nuclear Waste Management VII, ed. G. L. McVay, Materials Research Society Symposia Proceeding Volume 26, Elsevier Science Publishing Co. New York, 1984.

Grey et al. 1978. R. J. Grey, J. C. Griess, R. S. Crouse, and J. H. DeVan, "Examination of Aluminum Tubing Pitted in Stagnant Water", in Microstructural Science, eds. J. E. Bennett, L. R. Cornwell, and J. L. McCall, Vol. 6, 261-278, Elsevier-North Holland, 1978.

Griess and Neumann 1968. Letter, J. C. Griess and P. D. Neumann, to A. L. Boch, "Corrosion of Aluminum in Oak Ridge Electron Linear Accelerator," Oak Ridge National Laboratory, Oak Ridge, Tenn., March 1968.

Knight 1972. R. W. Knight and A. E. Richt, "Evaluation of Absorber Materials Performance in HFIR Control Cylinders," Nucl. Tech. 15, 384 (1972).

Homan 1986. Personal communication, F. J. Homan, Operations Division, Oak Ridge National Laboratory, Oak Ridge, Tenn., November 1986.

Horwitz and Bloomquist 1972. E. P. Horwitz and C. A. A. Bloomquist, "The Preparation, Performance and Factors Affecting Band Spreading of High Efficiency Extraction Chromatographic Columns for Actinide Separations," J. Inorg. Nucl. Chem. 34, 3851-71 (1972).

Lee 1986. Personal communication, S. Y. Lee, Environmental Sciences Division, Oak Ridge National Laboratory, Oak Ridge, Tenn., April 1986.

Lietzke and Lee 1986. D. A. Lietzke and S. Y. Lee, Soil Survey of Solid Waste Storage Area 6, ORNL/TM-10013, Oak Ridge National Laboratory, Oak Ridge, Tenn., June 1986.

Lutton et al. 1982. R. J. Lutton, P. G. Malone, R. B. Meade, and D. M. Patrick, Parameters for Characterizing Low-Level Radioactive Waste Sites, NUREG/CR-2700, U.S. Nuclear Regulatory Commission, Washington, D.C., May 1982.

McFadden 1980. K. M. McFadden, Organic Components of Nuclear Wastes and Their Potential for Altering Radionuclide Distribution when Released to Soil, PNL-2563, Pacific Northwest Laboratory, Richland, Wash., August 1980.

Means et al. 1978. J. L. Means, D. A. Crerar, and J. O. Duguid, "Migration of Radioactive Wastes: Radionuclide Mobilization by Complexing Agents", Science 200, 1477-81 (1978).

Olsen et al. 1983) - C. R. Olsen, P. D. Lowery, S. Y. Lee, I. L. Larsen, and N. H. Cutshall, Chemical, Geological, and Hydrological Factors Governing Radionuclide Migration from a Formerly Used Seepage Trench, ORNL/TM-8839, Oak Ridge National Laboratory, Oak Ridge, Tenn., September 1983.

ORNL-1985. Environmental Monitoring Report United States Department of Energy Oak Ridge Facilities, Calendar Year 1984, ORNL/TM-6209, Oak Ridge National Laboratory, Oak Ridge, Tenn., August 1985.

Perry et al. 1963. R. H. Perry, C. H. Chilton, S. D. Kirkpatrick, eds., Chemical Engineer's Handbook, Fourth Ed. pp. 23-36; 23-46, McGraw-Hill Book Company, New York, 1963.

Pigford and Chambré 1986. T. H. Pigford and P. L. Chambré, Closed-System Postulates for Predicting Waste-Package Performance in a Geologic Repository; addendum to Reliable Predictions of Waste Performance in a Geologic Repository, LBL-21277, Lawrence Berkeley Laboratory, Berkeley, Calif., March 1986.

Pigford and Chambré 1985. T. H. Pigford and P. L. Chambré, Reliable Predictions of Waste Performance in a Geologic Repository, LBL-20166, Lawrence Berkeley Laboratory, Berkeley, Calif., August 1985.

Pin et al. 1984. F. G. Pin, J. P. Witherspoon, D. W. Lee, J. R. Cannon, and R. H. Ketelle, Radionuclide Migration Pathways Analysis for the Oak Ridge Central Waste Disposal Facility on the West Chestnut Ridge Site, ORNL/TM-9231, Oak Ridge National Laboratory, Oak Ridge, Tenn., October 1984.

PNL 1984. Pacific Northwest Laboratory, Corrosion Assessment of Submerged Demineralizer System Vessels for Burial as High-Integrity Containers at the Hanford Commercial Waste Disposal Site, GEND-INF-057, Three Mile Island Operations Office, U.S. Department of Energy, November 1984.

Rai and Serne 1978. D. Rai and R. J. Serne, Solid Phases and Solution Species of Different Elements in Geologic Environments, PNL-2651, Pacific Northwest Laboratory, Richland, Wash., March 1978.

Reed 1985. D. T. Reed, Effect of Alpha and Gamma Radiation on the Near-Field Chemistry and Geochemistry of High-Level Waste Packages, RHO-BW-SA-406-P, Rockwell Hanford Operations, Richland, Wash., December 1985.

Romanoff 1957. M. Romanoff, Underground Corrosion, National Bureau of Standards Circular 579, Washington, D.C., 1957.

Romanoff 1957 - M. Romanoff, Underground Corrosion, National Bureau of Standards Circular 579, Washington, D.C., 1957.

Shrier 1977 - L. L. Shrier, ed., Corrosion 1, 4:14-4:28, Newnes-Butterworths, Boston, Mass., 1977.

Swanson 1985 - J. L. Swanson, Organic Complexant-Enhanced Mobility of Toxic Elements in Low-Level Wastes, PNL-4965-8, Pacific Northwest Laboratory, Richland, Wash., December 1985.

Taylor et al. 1984 - K. J. Taylor, I. D. Bland, and G. P. Marsh, Corrosion Studies on Containment Materials for Vitrified High-Level Nuclear Waste. Annual Progress Report for 1983, AERE-G-2964, UKAEA Atomic Energy Research Establishment, Harwell, England, January 1984.

Vivan and King 1964 - J. E. Vivian and C. J. King, AIChE J. 10, 220 (1964).

Walker et al. 1984 - W. F. Walker, D. G. Miller, and F. Feiner, Chart of the Nuclides, General Electric Co., 13th ed., 1984.

Wisbey 1986 - S. J. Wisbey, Preliminary Studies on the Effect of Radiolytic Oxidation on Radionuclide Solubility, AERE-R-11992, UK Atomic Energy Authority, Harwell Laboratory, Oxfordshire, Great Britain, 1986.



## APPENDIX A.

### DESCRIPTION OF AUGER-HOLE CONSTRUCTION AND PAST HFIR WASTE EMPLACEMENT PRACTICE

The following information describes the construction of the auger holes containing the high activity wastes shipped from the HFIR to SWSA-6 through June 1986 (Bolinsky 1986). The current, post-June 1986, methodology involves a more highly engineered structure (Homan 1986). Some of the HFIR control plate waste shipments were placed in lined auger holes due to the high levels of radioactivity involved. Other high activity waste shipments from HFIR, primarily the stainless steel parts, cobalt-alloy bearings, or beryllium reflectors, were placed in unlined holes.

1. All high activity waste auger holes are located on a knoll of high ground in SWSA-6. The water table is about 25 ft below the surface at this location.
2. A 47-in.-diam hole was augered to a depth of 18 to 20 ft. Thus, the bottom of the hole is about 5 to 7 ft above the water table.
3. At this point, the hole was lined with corrugated 24-in. 14-16 gauge galvanized steel culvert pipe (not asphalt coated) if desired. The liner extends the full depth of the hole. The purpose of the liner was to reduce the radiation shine from the top of the hole by limiting the top diameter and, thus, reduce personnel exposure. The decision to line with pipe, or not, was based on the total radioactivity expected in a planned shipment.
4. For lined holes, the pipe was placed in position, and the space between the 24-in. pipe and the nominal 47-in.-diam hole was backfilled with available soil.
5. An approximately 1-ft concrete plug was poured in the bottom of the pipe in the case of lined holes. No concrete was poured in the bottom of unlined holes.

6. A mild-steel waste shipping container from HFIR was then placed in the hole. The steel and lead transportation shield was positioned over the hole, and the container was lowered with a steel cable. The steel cable was discarded with the container.
7. To reduce radiation shine out the top, fill was promptly added to the hole. In the case of lined holes, river sand and/or fine shale from the area were used to cover the shipping container. A skip bucket was used to place the sand and fine shale in the hole; use of the skip bucket helped reduce personnel exposure. In the case of unlined holes, available soil was pushed into the hole.
8. From 1 to 3 mild-steel shipping containers were placed in a single auger hole, depending on the total radioactivity involved. When added, the second and third containers were placed in the hole, as described in step 7; several feet of sand or soil were added to the hole between containers.
9. After all waste containers were placed in the hole, either lined or unlined, the hole was backfilled to within about 1 ft of the surface. At least 1 ft of concrete was poured in the top of the hole for intruder protection. The plug may also provide some sealing from rain infiltration in the case of lined holes.

APPENDIX B.

DERIVATION OF RELEASE RATE FROM LINED AUGER HOLES

A schematic of the flow and concentration field surrounding a lined auger hole is given in Fig. 4.3, Sect. 4.2.8. The steady-state diffusion equation for cylindrical coordinates for this field is

$$v \frac{\partial c}{\partial z} = \mathcal{D} \left\{ \frac{1}{r} \frac{\partial}{\partial r} \left( r \frac{\partial c}{\partial r} \right) \right\}, \quad (\text{B1})$$

where

- $v$  = interstitial water velocity through the soil, cm/s;
- $\mathcal{D}$  = molecular diffusivity of europium, cm<sup>2</sup>/s;
- $c$  = concentration of europium, g-mol/cm<sup>3</sup> ( $c$  is a function of  $\underline{r}$  and  $\underline{z}$ );
- $r$  = radial coordinate measured from the pipe centerline, cm;
- $z$  = axial coordinate, measured from the concrete plug, cm.

To solve Eq. (B1) for  $c$ , we assumed the following functional relationship exists for  $c$ :

$$c = c(\eta) = c \left( \frac{r}{R(z)} \right), \quad (\text{B2})$$

where  $R(z)$  is the outer edge of the diffusion boundary layer, cm.

We further assume that

$$c(\eta_0) = c \left( \frac{R_0}{R(z)} \right) = c_I \text{ (the saturation concentration of europium),}$$

$$\left( \frac{R_0}{R(z)} \right) < 1 ;$$

$$c(1) = 0;$$

$R_0$  = radius of auger hole liner, cm.

By substituting the relations

$$\eta = \frac{r}{R} \quad [R = R(z)] ,$$

$$\frac{\partial \eta}{\partial r} = \frac{1}{R} ,$$

$$\frac{\partial \eta}{\partial R} = -\frac{r}{R^2} = -\frac{\eta}{R} ,$$

$$\frac{\partial c}{\partial r} = \frac{\partial c}{\partial \eta} \frac{\partial \eta}{\partial r} = \frac{1}{R} \frac{\partial c}{\partial \eta} , \tag{B3}$$

$$\frac{\partial^2 c}{\partial r^2} = \frac{1}{R^2} \frac{\partial^2 c}{\partial \eta^2} ,$$

$$\frac{\partial c}{\partial z} = -\frac{\eta}{R} \frac{dc}{d\eta} \frac{dR}{dz} ,$$

Eq. (B1) becomes

$$-\nu \frac{dc}{d\eta} \frac{dR}{dz} = \mathcal{D} \left\{ \frac{1}{\eta R} \frac{d^2 c}{d\eta^2} + \frac{1}{\eta^2 R} \frac{dc}{d\eta} \right\} . \tag{B4}$$

An approximate solution to Eq. (B4) is found by assuming a reasonable functional relationship for  $C(\eta)$ :

$$c(\eta) = c_I \left( \frac{\eta - 1}{\eta_0 - 1} \right)^2 , \tag{B5}$$

where

$$\eta_0 = \frac{R_0}{R} .$$

This choice of function satisfies the requirements

$$\begin{aligned}
 r = R_0 \quad c = C_I , \\
 r = R \quad c = 0 , \\
 r = R \quad \frac{dc}{dr} = 0 .
 \end{aligned}
 \tag{B6}$$

From Eq. (B5) we can evaluate relations for  $\frac{dc}{d\eta}$  and  $\frac{d^2c}{d\eta^2}$  to substitute into Eq. (B4):

$$\frac{dc}{d\eta} = \frac{2c_I}{(\eta_0 - 1)^2} (\eta - 1) ,
 \tag{B7}$$

$$\frac{d^2c}{d\eta^2} = \frac{2c_I}{(\eta_0 - 1)^2} .$$

Substituting Eqs. (B7) into (B4) yields:

$$R \frac{dR}{dz} \frac{\eta^2(1 - \eta)}{2\eta - 1} = \frac{\mathcal{D}}{v} .
 \tag{B8}$$

If the terms within the parentheses are averaged over the range  $R_0 \leq r \leq R(z)$  or  $\eta_0 \leq \eta \leq 1$ , the  $r$  dependence of concentration will be approximately accounted for, and the result will allow the approximation of the locus of the outer edge of the diffusion boundary layer.

Averaging the terms in parentheses over the range  $\eta_0 \leq \eta \leq 1$ :

$$R \frac{dR}{dz} \frac{\int_{\eta_0}^1 \left( \frac{\eta^2(1 - \eta)}{2\eta - 1} \right) d\eta}{\int_{\eta_0}^1 d\eta} = \frac{\mathcal{D}}{v} ,
 \tag{B9}$$

$$\text{or } R \frac{dR}{dz} \left\{ \frac{1/4(1 - \eta_0^2) + 1/4(1 - \eta_0) - 1/8 \ln(2\eta_0 - 1)}{1 - \eta_0} \right\} = \frac{\mathcal{D}}{v} . \quad (\text{B10})$$

From Eq. (B10) the dependence of R as a function of z (axial distance along the pipe) can be determined by letting

$$R/R_0 = \xi \text{ or } R = R_0 \xi \text{ and } dR = R_0 d\xi . \quad (\text{B11})$$

Substituting (B11) into (B10) yields:

$$\xi \left\{ \frac{1/4(1 - \xi^{-2}) + 1/4(1 - \xi^{-1}) - 1/8 \ln(2\xi^{-1} - 1)}{(1 - \xi^{-1})} \right\} d\xi = \frac{\mathcal{D}}{R_0^2 v} dz . \quad (\text{B12})$$

The desired relationship is obtained by integrating the left-hand side of Eq. (B12) from  $\xi = 1$  to  $\xi = R/R_0$  and the right-hand side of Eq. (B12) from  $z = 0$  to  $z = L$  to give

$$\int_1^{R/R_0} \xi \left( \frac{1/4(1 - \xi^{-2}) + 1/4(1 - \xi^{-1}) - 1/8 \ln(2\xi^{-1} - 1)}{(1 - \xi^{-1})} \right) d\xi = \frac{\mathcal{D}}{R_0^2 v} \int_0^L dz = \frac{\mathcal{D}L}{R_0^2 v} . \quad (\text{B13})$$

The left-hand side of Eq. (B13) was evaluated using the trapezoidal rule to perform the integration numerically for a range of values of  $R/R_0$ . The results of this series of calculations were fitted to the following empirical equation:

$$R/R_0 = 1.55 \left( \frac{\varepsilon \mathcal{D}L}{R_0^2 U} \right)^{0.8} + 1 . \quad (\text{B14})$$

Equation (B14) is used to estimate the outer radius of the diffusion boundary layer (R) at the lower end of the lined auger hole of length L.

In Eq. (B14) the following relation has been used:

$$v = \frac{U}{\epsilon} ,$$

where

- U = "superficial" water velocity (explained in Sect. 2.4.5), cm/s;  
 v = interstitial water velocity, cm/s;  
 $\epsilon$  = porosity, dimensionless.

At steady state the molar rate of release of europium from the pipe is equal to the rate of convection of europium by the flowing water through the annular region  $R_0 \leq r \leq R$  at the lower end of the auger hole liner ( $z = L$ ). This is given by the relation

$$N = \int_{R_0}^R 2\pi r U c(r) dr , \quad (\text{B15})$$

where

- N = molar rate of release of europium, g-mol/s;  
 U = "superficial" groundwater velocity, cm/s;  
 $c(r)$  = concentration of europium, g-mol/cm<sup>3</sup>;

$$= c_I \left( \frac{1 - r/R}{1 - R_0/R} \right)^2 ,$$

- r = radial coordinate, cm;  
 $R_0$  = radius of auger hole liner, cm;  
 R = radius of edge of diffusion boundary layer [determined from Eq. (B14)].

When the indicated integration is performed the result is

$$N = \pi R_0^2 U c_I \left( \frac{\xi}{\xi - 1} \right)^2 \left( \xi^4/2 - 4\xi^3/3 + \xi^2 - 1/6 \right) , \quad (\text{B16})$$

where

- $\xi = R/R_0$  [calculated from Eq. (B14)].  
 This is Eq. (4.13a) of Sect. 4.2.8.



## APPENDIX C.

### DERIVATION OF DIFFUSION RATES IN THE VICINITY OF BERYLLIUM REFLECTORS

The rate of diffusion of oxygen from the bulk groundwater to the beryllium metal surface or diffusion of  $\text{Be}(\text{OH})_2$  from the metal surface to the bulk groundwater was estimated from a simple boundary-layer diffusion model assuming flat-plate geometry. The flow and concentration fields are diagrammed in Fig. C.1. The diffusion equation for the diffusing species in this geometry is

$$v \frac{\partial c}{\partial x} = \mathcal{D} \frac{\partial^2 c}{\partial y^2} , \quad (\text{C1})$$

with the boundary conditions

$$c = c_I \text{ for } y = 0, \text{ all } x,$$

$$c = c_B \text{ for } y = \infty, \text{ all } x,$$

where

$c$  = concentration of diffusing species, g-mol/cm<sup>3</sup>;

$v$  = interstitial water velocity (assumed constant), cm/s;

$x$  = distance coordinate in direction of water flow, measured from leading edge of the beryllium surface, cm;

$y$  = distance coordinate normal to direction of water flow, measured from the beryllium metal surface, cm;

$\mathcal{D}$  = diffusivity of diffusing species in water, cm<sup>2</sup>/s.

For an approximate solution of Eq. (C1) we assume that the change in concentration between the metal surface and the bulk of the groundwater is confined to a boundary layer of thickness  $\delta$  cm. The boundary layer thickness  $\delta$  is a function of  $x$  which will be determined through well-established boundary layer analysis methods (Denn 1980).

In this analysis we assume a reasonable concentration profile within the boundary layer, substitute this into Eq. (C1), and solve for the boundary layer thickness  $\delta$ , so that Eq. (C1) is approximately satisfied.

ORNL DWG 86-901

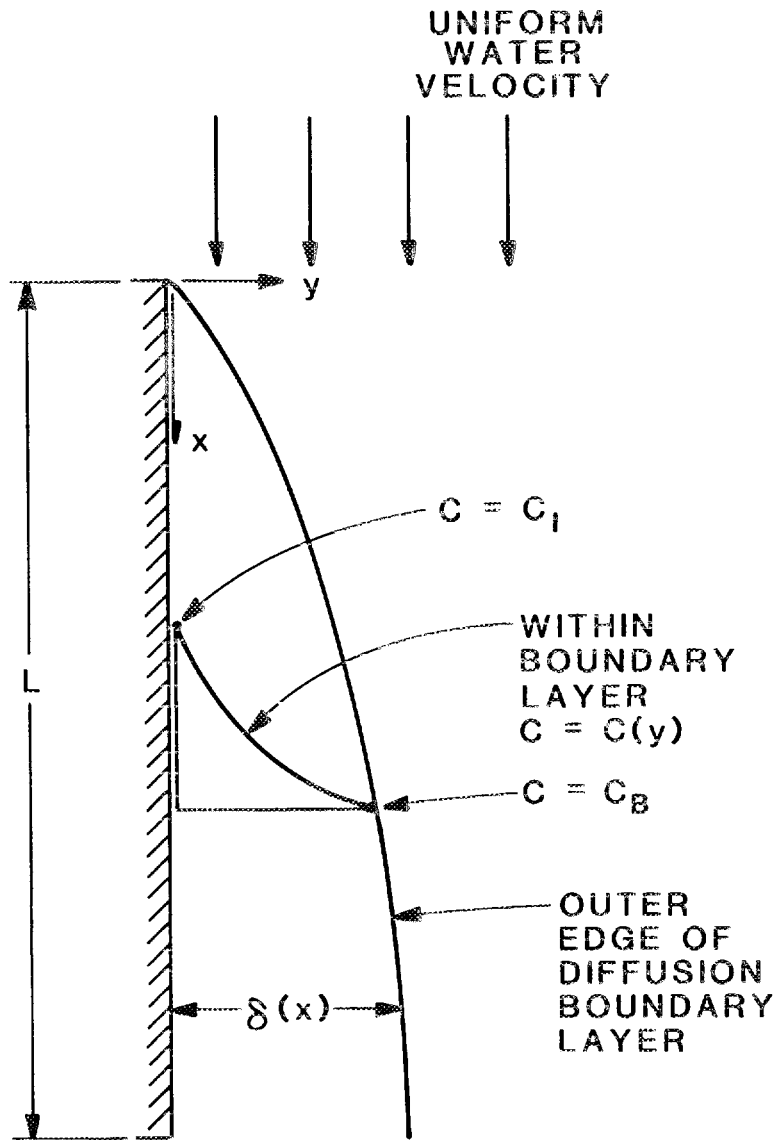


Fig. C.1. Diffusion in the vicinity of beryllium reflector components.

We make the following assumption for the concentration profile:

$$c = c_I + (c_B - c_I)(2\eta - \eta^2), \quad (C2)$$

where  $\eta = y/\delta$ .

This equation satisfies the boundary conditions

$$c = c_I \text{ at } y = 0, \text{ and}$$

$$c = c_B \text{ at } y = \delta.$$

In order to substitute Eq. (C2) into Eq. (C1) the following relations are needed:

$$\frac{\partial \eta}{\partial \delta} = -\frac{y}{\delta^2} = -\frac{\eta}{\delta},$$

$$\frac{\partial c}{\partial x} = (c_B - c_I)(2 - 2\eta)\left(-\frac{\eta}{\delta}\right) \frac{d\delta}{dx},$$

$$\frac{\partial c}{\partial y} = \frac{\partial c}{\partial \eta} \frac{\partial \eta}{\partial y} = (c_B - c_I) \frac{2}{\delta} - \frac{2y}{\delta^2},$$

$$\frac{\partial^2 c}{\partial y^2} = \frac{\partial}{\partial y} \frac{\partial c}{\partial y} = -\frac{2(c_B - c_I)}{\delta^2}.$$

When Eqs. (C3) are substituted into Eq. (C1) the following expression is obtained:

$$\delta \frac{d\delta}{dx} (1 - \eta)\eta = \frac{\mathcal{D}}{\nu} \quad (C4)$$

The terms containing  $\eta$  are averaged over the diffusion boundary layer ( $0 \leq \eta \leq 1$ ):

$$\delta \frac{d\delta}{dx} \frac{\int_0^1 (1 - \eta)\eta d\eta}{\int_0^1 d\eta} = \frac{\mathcal{D}}{\nu}, \quad (C5)$$

resulting in the following ordinary differential equation for  $\delta(x)$ :

$$\delta \frac{d\delta}{dx} = 6 \frac{D}{v} . \quad (C6)$$

Equation (C6) is solved to give the following equation for  $\delta$  as a function of  $x$ :

$$\delta(x) = \sqrt{12} \left( \frac{\epsilon D x}{U} \right)^{1/2} . \quad (C7)$$

In Eq. (C7) the following relation has been used:

$$v = \frac{U}{\epsilon}$$

where

$U$  = "superficial" water velocity (explained in Sect. 2.4.5), cm/s;

$v$  = interstitial water velocity, cm/s;

$\epsilon$  = porosity, dimensionless.

The molar flux of the diffusing species at the metal surface is given by:

$$J_{y=0} = - D \left. \frac{dc}{dy} \right|_{y=0} \quad (C8)$$

From the fourth line in Eq. (C3),

$$\left. \frac{dc}{dy} \right|_{y=0} = (c_B - c_I) \frac{2}{\delta} . \quad (C9)$$

Substituting Eq. (B7) and Eq. (B9) into Eq. (B8):

$$J_{y=0} = - \frac{\sqrt{3} D (c_B - c_I)}{3 \left( \frac{\epsilon D x}{U} \right)^{1/2}} . \quad (C10)$$

The total molar diffusion rate at the surface of the beryllium reflector component is given by

$$N = \int_0^L J_y = 0 \quad \epsilon W dx ,$$

$$= - \frac{\sqrt{3} \epsilon \mathcal{D} (c_B - c_I) W}{3 \left( \frac{\epsilon \mathcal{D}}{U} \right)} \int_0^L x^{-1/2} dx ,$$

$$\text{or } N = - \frac{2\sqrt{3} \epsilon (c_B - c_I) W L}{3 \left( \frac{\epsilon \mathcal{D}}{U} \right)^{1/2}} , \quad (\text{C11})$$

where

W = width of flat plate, cm;

L = length of flat plate, cm.

The average molar flux at the beryllium surface is given by

$$J = \frac{N}{WL} = - \frac{2\sqrt{3}}{3} \frac{\epsilon \mathcal{D} (c_B - c_I)}{\left( \frac{\epsilon \mathcal{D}}{U} \right)^{1/2}} . \quad (\text{C12})$$

This is Eq. (5.7) in Sect. 5.2.6.



INTERNAL DISTRIBUTION

- |                        |  |
|------------------------|--|
| 1. J. T. Bell          | 32. A. L. Lotts                                      |
| 2. W. J. Boegly        | 33. J. C. Mailen                                     |
| 3. J. Bolinsky         | 34. E. W. McDaniel                                   |
| 4. T. W. Burwinkle     | 35. R. B. McLean                                     |
| 5. K. E. Cook          | 36. C. E. Nix  |
| 6. K. W. Cook          | 37. P. T. Owen                                       |
| 7. A. G. Croff         | 38. R. K. Owenby                                     |
| 8. N. H. Cutshall      | 39. W. W. Pitt                                       |
| 9. E. C. Davis         | 40. M. J. Sale                                       |
| 10. M. B. Farrar       | 41. R. J. Selfridge                                  |
| 11. H. A. Friedman     | 42-44. C. H. Shappert                                |
| 12. C. W. Gehrs        | 45. D. K. Solomon                                    |
| 13. R. K. Genung       | 46. A. J. Stewart                                    |
| 14. T. M. Gilliam      | 47. J. R. Trabalka                                   |
| 15. R. M. Gove         | 48. L. D. Voorhees                                   |
| 16-20. J. R. Hightower | 49. S. K. Whatley                                    |
| 21. S. G. Hildebrand   | 50. G. T. Yeh  |
| 22. F. J. Homan        | 51-52. Laboratory Records                            |
| 23. L. D. Hyde         | 53. Laboratory Records, RC                           |
| 24-28. A. D. Kelmers   | 54. ORNL Patent Section                              |
| 29. J. R. Lawson       | 55. Central Research Library                         |
| 30. D. W. Lee          | 56. ORNL Y-12 Library,<br>Document Reference Section |
| 31. S. Y. Lee          |  |

EXTERNAL DISTRIBUTION

57. Office of Assistant Manager for Energy Research and Development,  
Department of Energy, Oak Ridge Operations Office, Post Office  
Box E, Oak Ridge, TN 37831
- 58-416. Given distribution as shown in TIC-4500 under UC-70B, Low-Level  
Radioactive Waste Management.

